

by Andy Gale<sup>1,2\*</sup>, Sietske Batenburg<sup>3</sup>, Rodolfo Coccioni<sup>4</sup>, Zofia Dubicka<sup>5</sup>, Elisabetta Erba<sup>6</sup>, Francesca Falzoni<sup>6</sup>, Jim Haggart<sup>7</sup>, Takishi Hasegawa<sup>8</sup>, Christina Ifrim<sup>9</sup>, Ian Jarvis<sup>10</sup>, Hugh Jenkyns<sup>11</sup>, Agata Jurowska<sup>12</sup>, Jim Kennedy<sup>11,13</sup>, Matteo Maron<sup>6§</sup>, Giovanni Muttoni<sup>6</sup>, Martin Pearce<sup>2</sup>, Maria Rose Petrizzo<sup>6</sup>, Isabella Premoli-Silva<sup>6</sup>, Nicolas Thibault<sup>14</sup>, Silke Voigt<sup>15</sup>, Michael Wagreich<sup>16</sup>, and Irek Walaszczyk<sup>5</sup>

## The Global Boundary Stratotype Section and Point (GSSP) of the Campanian Stage at Bottaccione (Gubbio, Italy) and its Auxiliary Sections: Seaford Head (UK), Bocieniec (Poland), Postalm (Austria), Smoky Hill, Kansas (U.S.A), Tepayac (Mexico)

<sup>1</sup> School of the Environment, Geography and Geological Sciences, University of Portsmouth, Burnaby Building, Burnaby Road, Portsmouth PO13QL UK; \*Corresponding author, *E-mail: andy.gale@port.ac.uk*

<sup>2</sup> Department of Earth Sciences, Natural History Museum, Cromwell Road, London SW75BD UK

<sup>3</sup> Departament de Dinamica de la Terra i de l'Ocea, Facultat de Ciències de la Terra, Universitat de Barcelona, 08028 Barcelona, Spain

<sup>4</sup> Dipartimento di Scienze della Terra, della Vita e dell'Ambiente, Università degli Studi di Urbino "Carlo Bo", Campus Scientifico "E. Mattei", 61029 Urbino, Italy

<sup>5</sup> Faculty of Geology, University of Warsaw, Al. Zwirki i Wigury 93, 02-089 Warszawa, Poland

<sup>6</sup> Dipartimento di Scienze della Terra "A. Desio", Università degli Studi di Milano, via Mangiagalli 34, 20133 Milano, Italy

<sup>7</sup> Geological Survey of Canada, 1500-605 Robson Street, Vancouver, BC V6B 5J3 Canada

<sup>8</sup> Department of Earth Sciences, Faculty of Science, Kanazawa University, Kakuma-machi, Kanazawa 920-1192, Japan

<sup>9</sup> SNSB Jura Museum, Eichstatt, Germany

<sup>10</sup> Department of Geography, Geology and the Environment, Kingston University London, Kingston upon Thames KT1 2EE, UK

<sup>11</sup> Department of Earth Sciences, South Parks Road, Oxford OX13AN, UK

<sup>12</sup> Faculty of Geology, Geophysics and Environmental Protection, AGH University of Science and Technology, Mickiewiczza 30, 30-059 Krakow, Poland

<sup>13</sup> Oxford University Museum of Natural History, Parks Road, Oxford OX13PW, UK

<sup>14</sup> Department of Geosciences and Natural Resource Management, University of Copenhagen, Øster Voldgade 10, 1350 Copenhagen K, Denmark

<sup>15</sup> Institute of Geosciences, Goethe-University Frankfurt, Altenhöferallee 1, 60438 Frankfurt am Main, Germany

<sup>16</sup> Department of Geology, University of Vienna, Althanstrasse 14, Vienna, A-1090, Austria

<sup>§</sup>*now at:* Dipartimento di Ingegneria e Geologia, Università degli Studi "G. D'Annunzio" di Chieti-Pescara, via dei Vestini 31, 66100 Chieti, Italy

\*co-ordinator

Additional Working Group members are: Elise Chenot (University of Bourgogne, Dijon, France) and Mario Sprovieri (Istituto per l'Ambiente, Capo Granitola, Italy).

(Received: October 12, 2022; Revised accepted: December 27, 2022)

<https://doi.org/10.18814/epiiugs/2022/022048>

Following the unanimous vote of the Executive Committee of International Union of Geological Sciences in October 2022, the Global boundary Stratotype Section and Point for the base of the Campanian Stage is confirmed as the magnetic polarity reversal from Chron 34n (top of the Long Cretaceous Normal Polarity-Chron) to Chron C33r at the 221.53 m level in the Bottaccione Gorge section at Gubbio, Umbria-Marche Basin, Italy. This event has been widely identified in oceanic settings and in wide-spread onshore outcrops. Sedimentation across the Santonian-Campanian boundary interval in the proposed

GSSP appears to be continuous, supported by evidence from the carbon isotope record and complete micro- and nanofossil biostratigraphy. The succession comprises deep-water cherty limestones (mudstones and foraminiferal wackestones) which provide a detailed record of calcareous nanofossils and planktonic foraminifera and yields an excellent palaeomagnetic record. The high-resolution carbon isotope record, derived from bulk sediment, provides an important additional means of correlation to other regions.

## Introduction

A reconstruction of the Campanian world is provided (Fig. 1) which shows the position of localities mentioned in the text.

## Historical Background

The étage Campanien was introduced by Henri Coquand in 1857 in his *Position des Ostrea columba et bauriculata dans le groupe de la craie inférieure* (1857, p. 749) as the third division of the former étage Sénonien, introduced by d'Orbigny in 1843 (p. 403).

“Troisième étage. – Campanien Craie tendre (*Ostrea vesicularis*, Lam., *O. larva*, Lam., *Sphaerulites hoeninghausi*, des Moul., *Anachytes ovata*, Lam.). Cet étage correspond au septième étage des rudistes.”

Coquand (1857) revised his former 1856 subdivision of his Craie Supérieure, and defined the Coniacien, Santonien, Campanien and Dordonnien as the 1<sup>st</sup>, 2<sup>nd</sup>, 3<sup>rd</sup> and 4<sup>th</sup> étages of the Craie supérieure, respectively. The named localities for the Campanien, formerly named *Deuxième étage* by Coquand in 1856 (pp. 88–92) included Grande-Champagne, the escarpments that dominate the banks of the Dronne, at the southern end of the department, the surroundings of Aubeterre, the village of Archiac, and the cliffs that extend from Mortagne to Royan. Subsequent research on the Campanian in northern Aquitaine is reviewed in detail by Seronivivien (1972), Kennedy (1986) and Platel (1989), who document the progressive refinements of knowledge of the sequence.

For Coquand (1856, 1857), the Campanian Stage was characterised by a diverse assemblage of bivalves (including rudists), and echinoids. Coquand (1858, 1859, 1860) cited various ammonites as characteristic of the Campanian, discussed by Kennedy (1986) who concluded that many were inappropriately used names referring mostly to what are now regarded as Maastrichtian species. Arnaud (1878) subsequently subdivided the Campanian of the Aquitaine Basin into three units (P1, lower; P2, middle; P3, upper), and suggested a correlation with the chalks of northern France. De Grossouvre (1894) revised the ammonite faunas of the ‘Craie Supérieure’ of France, and in 1901 (pp. 810, 830) established a three-fold ammonite zonation for the Campanian as now conceived, based on records from Aquitaine (Table 1; his fourth zone of *Pachydiscus neubergicus* is now regarded as Lower Maastrichtian).

Kennedy (1986), in a revision of the ammonite faunas of the Campanian of Aquitaine, noted that *Placenticerus bidorsatum*, index of the lowest Campanian ammonite zone recognised by De Grossouvre was rare in Aquitaine (12 specimens known), and had not been collected since the nineteenth century. The species is otherwise known only from Touraine and the Corbières in France, northern Spain, Germany,

**Table 1. De Grossouvre's 1901 ammonite zonation for the Campanian of Aquitaine**

Upper	Hoplites vari
Lower	Mortoniceras delawarensis Placenticerus bidorsatum

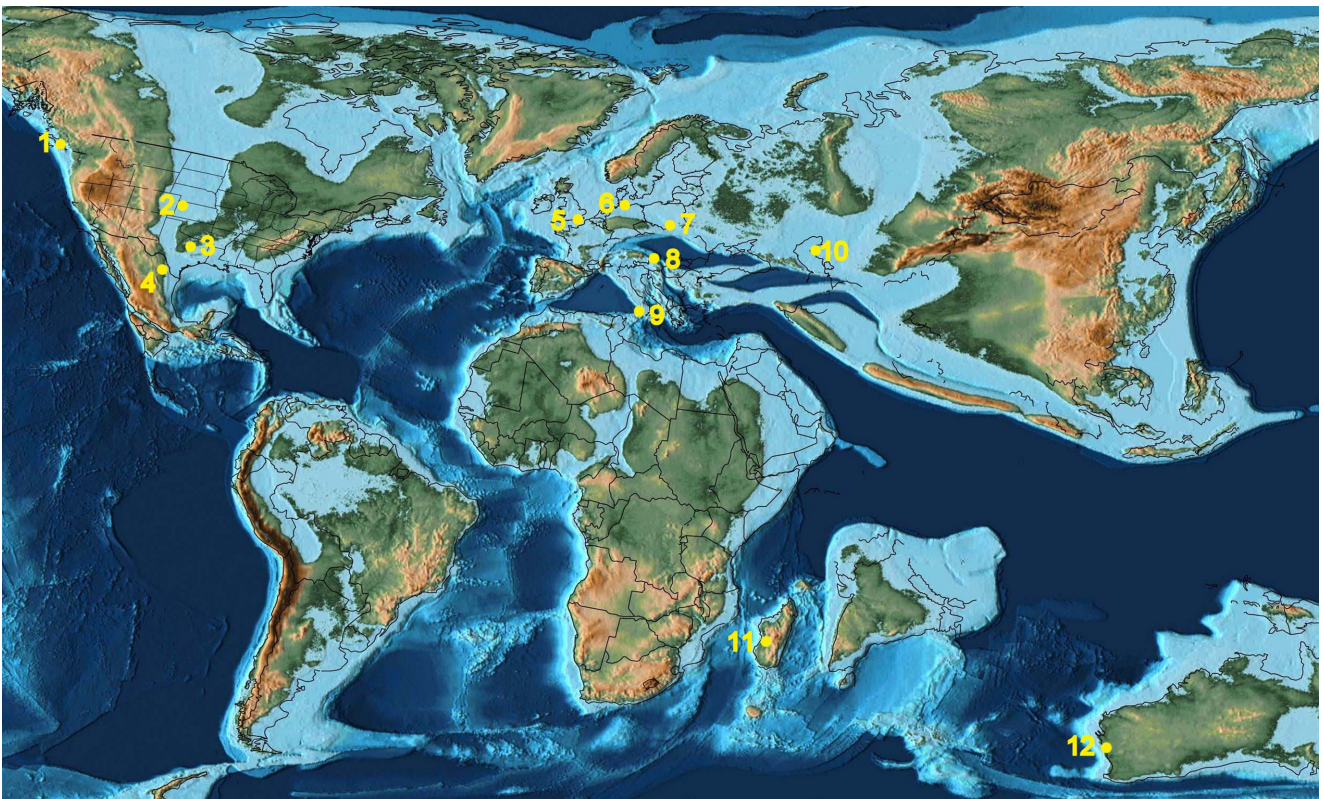


**Figure 1. Map of the Campanian world (Paleomaps, with permission from Dr Chris Scotese) to show important sections mentioned in the text. 1, Vancouver Island, British Columbia, Canada. 2, NW Kansas, USA. 3, Waxahachie, Ellis County, Texas, USA. 4, Tepeyac, Mexico. 5, Seaford Head, Sussex, UK. 6, Lägerdorf, Germany. 7, Biocieniec, Poland. 8, Postalm, Austria. 9, Gubbio, Italy. 10, Mangyschlak, Kazakhstan. 11, Madagascar. 12, Carnarvon Basin, Western Australia.**

and Austria (Kennedy, 1986; Kennedy and Kaplan, 1995) and its approximate co-occurrence with the belemnite *Gonioteuthis granulata quadrata* led to this latter level being adopted as a Campanian boundary marker (Schmid, 1956, 1960; Ernst, 1964). Subsequently, this level was shown to coincide with the highest occurrence of the globally distributed crinoid *Marsupites testudinarius* (Ernst, 1968), which was proposed as a potential boundary marker (Schulz et al., 1984; Birkelund et al., 1984). Although *M. testudinarius* has a global distribution, it is virtually restricted to relatively shallow water chalks and is absent in deeper water and most clastic facies (Gale et al., 2008).

Marks (1984) noted that stratigraphically diagnostic planktonic foraminifera of the *Dicarinella* lineage are absent from the Aquitaine sections but suggested that the extinction of *Dicarinella asymetrica* provided a widely identifiable marker for the top of the Santonian in deeper water Tethyan successions. Following the work of Premoli Silva (1977) and Premoli Silva and Sliter (1995), it has been demonstrated that the base of magnetochron C33r is approximately coincident with the highest occurrence of *D. asymetrica* in the Scaglia Rossa at Gubbio, Italy. The Santonian–Campanian boundary at Gubbio, and elsewhere in deep-water Tethyan settings (e.g., Caron, 1985; Robaszynski and Caron, 1995; Premoli Silva and Sliter, 1995; Petrizzo et al., 2011;

Coccioni and Premoli Silva, 2015), in Crimea (Kopaevich et al., 2020), and in the US Gulf Coastal Plain (Puckett, 2005) has been taken at the top of the range of *D. asymetrica*, which is also widely recognised across ocean basins at various Deep Sea Drilling Project (DSDP), Ocean Drilling Program (ODP) and Integrated Ocean Discovery Project (IODP) sites (e.g., Petrizzo, 2000; Petrizzo et al., 2011; Ando et al., 2013; Miniati et al., 2020).

In the United States Western Interior and Gulf Coast regions, ammonites have been used to define the base of the Campanian. In Texas, the base of the Campanian was placed at the base of the *Submortonicerias tequesquitense* Zone by Young (1963), in the Dessau Member of the Austin Chalk. Gale et al. (2008, 2020a) provided a detailed record of occurrences of *Marsupites* and *Uintacrinus* in Texas and demonstrated that the extinction of *M. testudinarius* lay close to the top of the Austin Chalk and was thus significantly younger than the first occurrence of *S. tequesquitense*. In the Western Interior, Cobban (1969) took the base of the Campanian at the base of the zone of *Scaphites leei* III; *Marsupites testudinarius* occurs in association with *S. leei* II in the underlying *Desmoscaphites bassleri* Zone (Cobban, 1995).

The Pacific Basin comprised two-thirds of the Late Cretaceous world, and Santonian–Campanian boundary intervals are known from

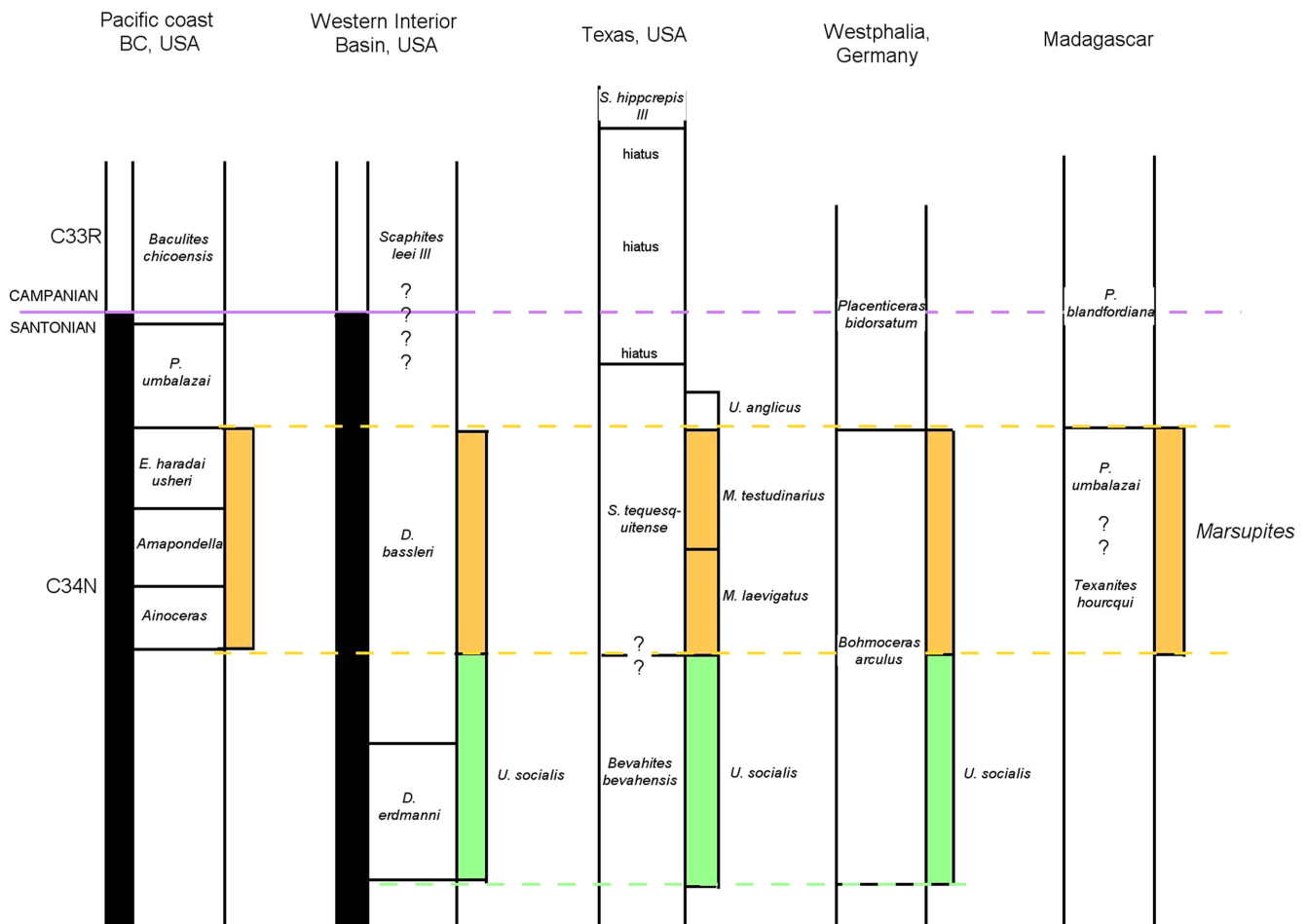


**Figure 2.** Correlation of regional ammonite zonation using magnetostratigraphy and distributions of crinoids *Uintacrinus* and *Marsupites*, to illustrate the problems of provincialism of the ammonite record, and the use of *Marsupites* in correlation. Pacific Realm data from Verosub et al. (1989), Ward et al. (2012), Haggart and Graham (2017). Western Interior Basin from Cobban (1995) and Kita et al. (2017). Texas from Young (1963), Gale et al. (2008, 2020b). Germany from Kaplan et al. (2005). Madagascar from Walaszczyk et al. (2014).

a number of regions therein, including the Pacific coast of United States and Canada, as well as Japan. Unfortunately, extensive regional endemicity of ammonite and inoceramid faunas in this region complicates interregional correlation of numerous Cretaceous boundaries, including the Santonian–Campanian. In California, Matsumoto (1960) placed the boundary just below the first occurrence of *Submortonicerias chicoense* and *Baculites chicoensis*, a placement subsequently followed by Haggart (1984), Verosub et al. (1989), and Ward et al. (2012). In Pacific coastal Canada, Jeletzky (1970) placed the boundary at the first occurrence of the Pacific–endemic ammonite *Eupachydiscus haradai*, but Ward (1978) subsequently identified *Submortonicerias chicoense* at this level, providing a more significant interregional tie. In the Japanese Islands, Matsumoto (1959) placed the boundary at the occurrence of the ammonites '*Neopachydiscus naumanni* and *Desmophyllites diphyllodes* and the inoceramid *Inoceramus orientalis*, all, unfortunately, restricted to the North Pacific Province (Matsumoto, 1959; Haggart and Ward, 1989). Toshimitsu et al. (1998) subsequently placed the boundary at the first occurrence of the somewhat rare *Submortonicerias* cf. *condamyi*, as well as the first occurrence of *Globotruncana arca*, identifying taxa useful for interregional correlation. Identification of the base of magnetochron 33r in the California succession allowed Ward et al. (1983) to confidently place the Santonian–Campanian boundary there and more recently, Haggart and Graham (2017) have recognized the benthic crinoid *Marsupites testudinarius* in the western British Columbia succession, providing a valuable means of correlation (Gale et al., 1995).

The 1995 Brussels Second International Symposium on Cretaceous Stage Boundaries agreed that a number of criteria should be taken into account in defining the Campanian stage boundary and establishing a GSSP (Hancock and Gale, 1996, p. 107). The following motion, put to those present was accepted without dissent:

“1. The definition of the base of the Campanian stage should be compatible with the classic definition by de Grossouvre (1901), that is the lowest level with *Placenticerias bidorsatum*.

2. This corresponds to the extinction level of *Marsupites testudinarius* (Schlotheim) which we recommend provisionally as the boundary marker for the base of the Campanian stage.

3. This datum–level should be linked to:

(a) extinctions in the planktonic foraminiferal group of *Dicarinella concavata*;

(b) nannofossil data, including the lineage of *Broinsonia parca* (note: *Aspidolithus parvus parvus* of other authors and herein);

(c) directly or indirectly to the C33r–C34n paleomagnetic boundary.

4. We invite reports on correlation of these events from members of the working group.”

It was further agreed that “should the crinoid standard eventually be adopted, there were candidate boundary stratotypes in Texas and southern England. Accordingly, reports should be prepared on the sections in England at Seaford Head, Sussex (and possibly Foreness Point, Kent)... and in north–central Texas at the Waxahachie dam–spillway.”

Detailed accounts of the micropalaeontology of the Seaford Head section were published by Hampton et al. (2007), and Gale (2018) described the distribution of the crinoids; the results are discussed further below (see below). The locality has not provided a reliable palaeomagnetic record and lacks diagnostic planktonic foraminifera.

The section at the Waxahachie dam spillway, Ellis County, was pro-

posed as a candidate GSSP by Gale et al. (2008), who provided a detailed account of the biostratigraphy (calcareous nannofossils, planktonic foraminifera, crinoids, inoceramid bivalves, ammonites) of the section. However, the absence of a palaeomagnetic record, the incomplete ranges of key planktonic foraminifera and the presence of a major erosional disconformity between the Austin Chalk and overlying Ozan (Taylor) Formation (Gale et al., 2020a) 2.7 m above the proposed GSSP marker (extinction of *Marsupites testudinarius*) render the locality inappropriate as a GSSP. Important biostratigraphical records from the Waxahachie section are provided (Fig. 3). The Bocieniec locality near Warsaw in southern Poland was proposed by Dubicka et al. (2017) as a potential GSSP candidate, and we here propose it as an auxiliary section (see below). However, the succession is very thin and there is a hiatus close to the level of the proposed boundary.

## Boundary Markers

Previous studies have proposed several viable options for definition of the base of the Campanian; namely, the extinction of the benthic crinoid *M. testudinarius* (only recorded from shallower water chalks and clastics, worldwide); the top of the Cretaceous Long Normal magnetozone C34n (global), the approximately coincident extinction of the planktonic foraminiferan *Dicarinella asymetrica* (deeper water, lower latitude, ocean basins), and the appearance of the calcareous nannofossil *Aspidolithus parvus parvus* (ocean basins to shallow water chalks, global event). Because magnetic reversals are global, and potentially identifiable in all palaeoenvironments, we selected the base of Chron C33r as the now confirmed primary marker. This helps especially in correlation to non–marine continental successions such as those in North America (e.g., Albright and Titus, 2016) and China (e.g., He et al., 2012).

Although the base of polarity Chron C33r has not been identified widely outside the oceanic seafloor, laterally extensive and high–resolution correlation of Santonian–Campanian boundary strata is possible using carbon isotope stratigraphy and development of evolutionary subspecies in the *Aspidolithus parvus* (Stradner, 1963) coccolith lineage (syn. *Broinsonia parca* of Bukry, 1969; see Miniati et al., 2020 and Nannotax3, <https://www.mikrotax.org/Nannotax3/>). A succession of species and subspecies of the family Arkhangelskiellaceae and particularly of the coccolith genus *Aspidolithus* have been described from the Gubbio section (Gardin et al., 2001; Miniati et al., 2020), including the FO of *Arkhangelskiella cymbiformis* (Vekshina, 1959) and the first occurrence (FO) and first common occurrence (FCO) of successive subspecies of *Aspidolithus parvus* (*A. p. expansus*, *A. p. parvus*, *A. p. constrictus*). Some of these events can be identified widely; for example, Kita et al. (2017) recognised the *A. p. parvus* and *A. p. constrictus* levels in the northern part of the Western Interior Basin, USA.

A double positive excursion in bulk carbonate  $\delta^{13}\text{C}$ , the Santonian–Campanian Boundary Event (SCBE), was originally described from southern UK chalks (Jarvis et al., 2006), coincident with the upper part of the range of *M. testudinarius* and immediately succeeding its extinction level. This event is now demonstrated to fall beneath the base of the Campanian and is therefore re–named as the Late Santonian Event (LSE–Fig. 4). The isotope excursion can also be identified in chalks in Yorkshire, north–east England (Deville de Periere et al., 2019), in the Paris Basin (Chenot et al., 2016; Pearce et al., 2022), at Lägerdorf

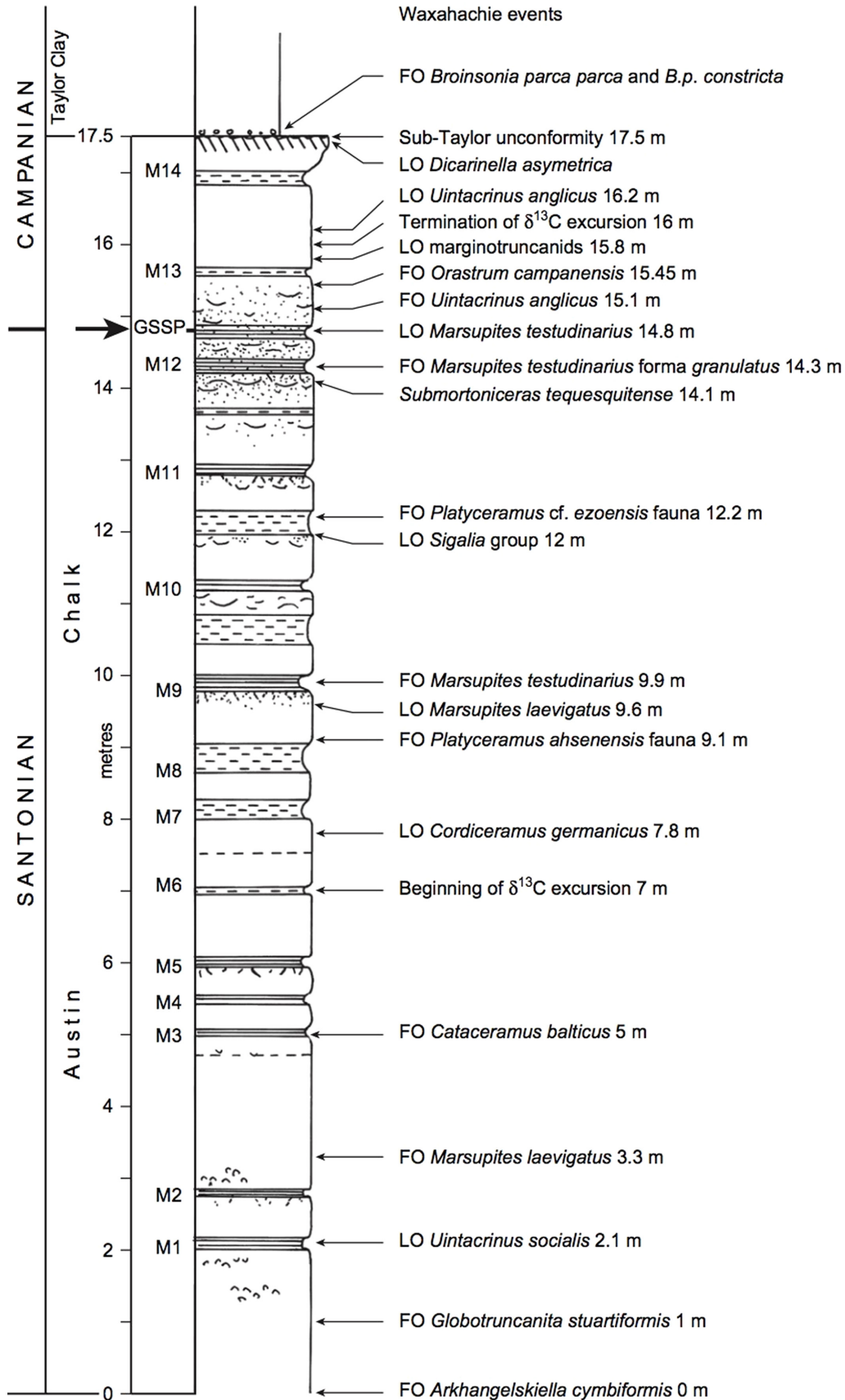
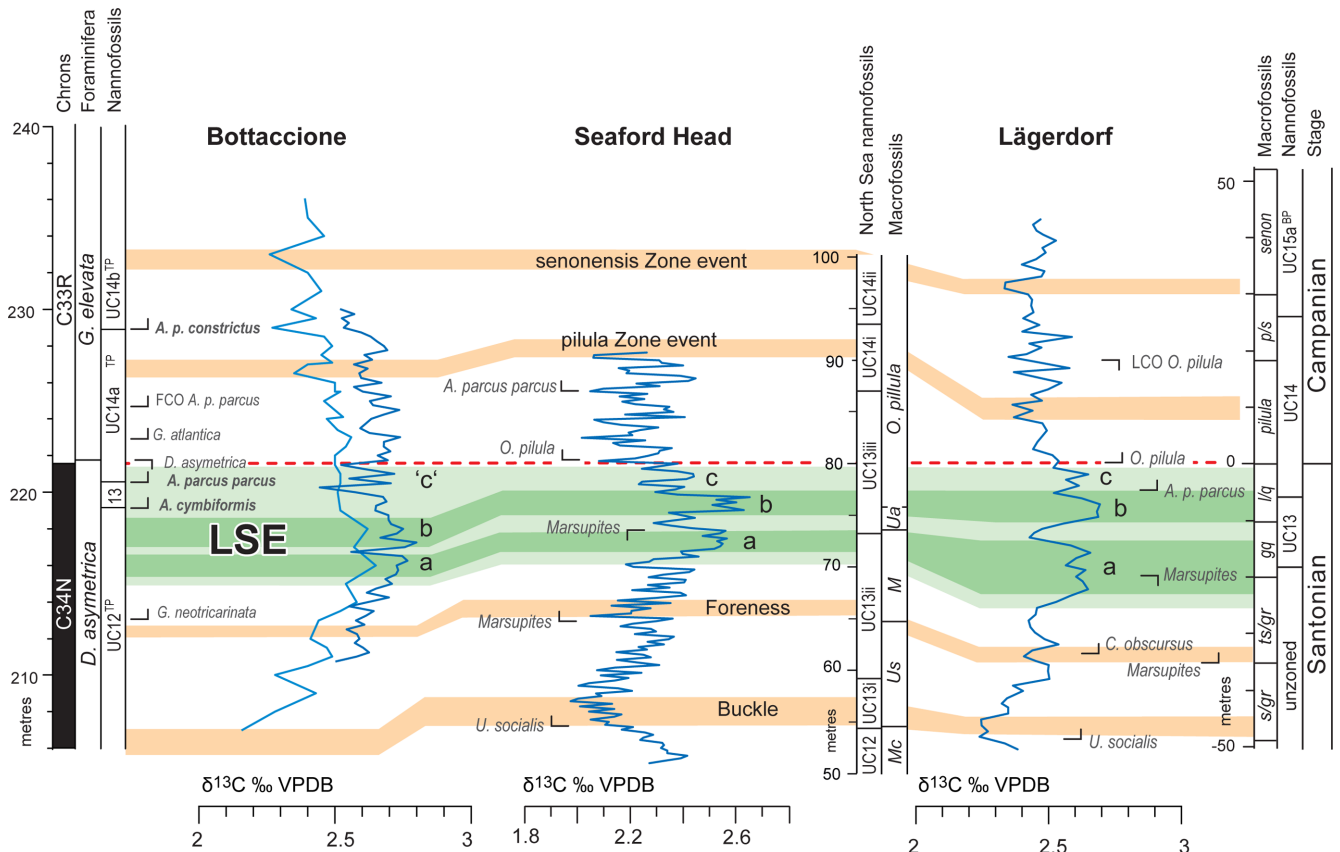


Figure 3. Biostratigraphic markers in the Waxahachie dam spillway, proposed as a potential Campanian GSSP, after Gale et al. (2008, fig. 24.) Note the co-occurrences of inoceramids and crinoids and the abrupt termination of the range of *Dicarinella asymetrica* at the sub-Taylor (=Ozan) unconformity. See also Gale et al. 2020b for further details.



**Figure 4.** Correlation between the Tethyan pelagic carbonate succession at the Bottaccione section (Gubbio, Umbria, Italy) and Boreal chalk successions at Seaford Head (UK) and Lägerdorf (northern Germany), showing correlations based on carbon isotopes, calcareous nannofossils and planktonic foraminifera. Note that the Late Santonian carbon isotope event (LSE) (including peaks a–c), supported by calcareous nannofossils, provides a means of high-resolution correlation between the successions. Modified from Thibault et al. (2016 fig. 4). FCO = first common occurrence; LCO = last common occurrence.

in northern Germany (Voigt et al., 2010), in marls at Bocieniec, Poland (Dubicka et al., 2017), and, critically, in the Global Stratotype section in the Scaglia Rossa in the Bottaccione Gorge at Gubbio, Umbria–Marche Basin, Italy (Fig. 4; see Thibault et al., 2016). It has also been identified in the United States Western Interior Basin (Joo and Sage-man, 2014; Kita et al., 2017) and in Japan (Takashima et al., 2019).

## Bottaccione Gorge, Gubbio, Umbria Marche, Italy: the Global Boundary Stratotype Section for the Base of the Campanian Stage

### The Upper Santonian–Lower Campanian Bottaccione Section (Gubbio, central Italy)

The investigated portion of the Bottaccione section that includes the Global Stratotype Section and Point (GSSP) for the base of the Campanian Stage, is located 1.4 km NNE of the town of Gubbio (central Italy). It is continuously well-exposed with a strike of 140° and a dip of 50°NE along the Regional Road 298 “Eugubina” that crosses the Bottaccione Gorge (Fig. 5), where a continuous magneto–biochronologic record characterizes the Early Cretaceous–Paleogene pelagic carbonates of the Umbria–Marche Apennines (Coccioni and Premoli

Silva, 2015, and references therein; Coccioni et al., 2016, and references therein) and played a prominent role in the establishment of the standard Late Cretaceous time scale (Gale et al., 2020b).

The upper Santonian–lower Campanian Bottaccione section (Fig. 6; 560 m above sea level; coordinates: 43°21′45.6″N, 12°34′58.2″E), which following the study of Coccioni and Premoli Silva (2015), extends from 210.79 to 233.63 m was logged to define a detailed lithostratigraphy, described at the centimetre scale in the field and marked on the outcrop with light blue paint at 1 m intervals. It is 22.84 m thick and consists of well-bedded, pink to red and white bioturbated limestones with bedding thickness ranging from 6 to 80 cm. Pink to reddish and grey to greenish–grey chert nodules and limestone beds with thickness ranging from 3 to 6 cm occur throughout. As a result, the limestone beds are frequently silicified. In particular, the occurrence of white limestone beds together with grey to greenish–grey chert nodules characterises the 228.94–232.75 m interval.

The upper Santonian–lower Campanian Bottaccione section, which following Alvarez and Montanari (1988) is positioned within the upper part of the stratigraphic member R1 (lower Turonian–lower Campanian) of the Scaglia Rossa Formation, is absolutely devoid of turbidites and substantial internal structural deformation. Only a negligible fault with a displacement of a few decimetres occurs at 221.20 m (Maron and Muttoni, 2021). The displaced strata can be easily reconnected

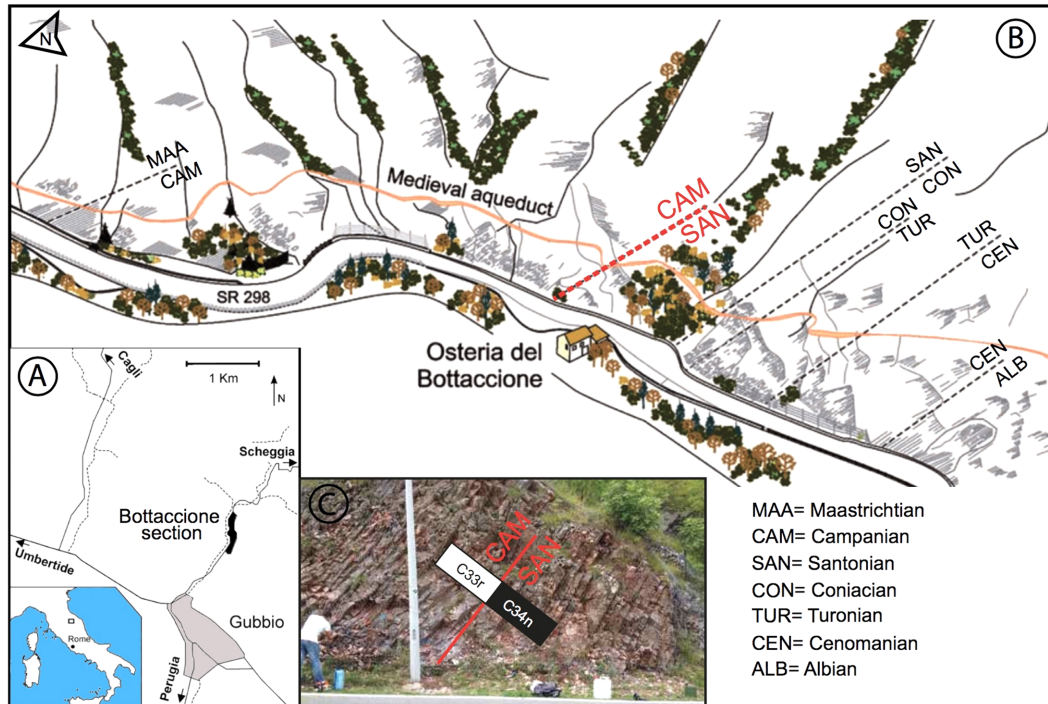


Figure 5. A, Map showing the location of the Bottaccione section at Gubbio, Umbria–Marche Basin, Italy. B, cartoon of the Bottaccione section. C, photograph of the GSSP. After Miniati et al. (2020).

and therefore the stratigraphy is regarded as continuous. Stylolites are common in the thicker beds.

The biogenic pelagic rocks of the upper Santonian–lower Campanian Bottaccione section, which were formed following lithification of nanofossil and planktonic foraminiferal ooze, were deposited at an inferred lower bathyal palaeodepth of 1,000–2,000 m (Frontalini et al., 2016) with a mean accumulation rate of  $\sim 11$  m/myr (Maron and Muttoni, 2021) in a low energy, open marine setting of the central–western Tethys at an estimated palaeolatitude between  $19.5^{\circ}\text{N}$  and  $22.7^{\circ}\text{N}$  (Maron and Muttoni, 2021). Some benthic foraminifera, ostracods, and radiolarians also occur, but have not been documented to date. Macrofossils are conspicuously absent, as expected in deep water sediments. Samples processed from the boundary section have proven barren of palynomorphs.

### Magnetostratigraphy

The base of magnetic polarity Chron C33r, that marks the top of Chron 34n (Cretaceous Long Normal), was indicated by Coccioni and Premoli Silva (2015) as a possible primary criterion for the base of the Campanian Stage, in agreement with Alvarez et al. (1977) and Premoli Silva and Sliter (1995). In the Geologic Time Scale (GTS) 2020, the base of magnetic polarity Chron C33r is used as provisional base for the Campanian Stage at 83.65 Ma (Gale et al., 2020b). A reliable and robust magnetostratigraphic reassessment of the upper Santonian–lower Campanian Bottaccione section has been provided by Maron and Muttoni (2021), who analysed a total of 112 samples for palaeomagnetism (Fig. 7) and 12 for rock magnetism experiments using isothermal remanent magnetization (IRM). The samples were thermally demagnetized up to  $675^{\circ}\text{C}$  (in steps of  $50$ – $25^{\circ}\text{C}$ ) and then

analyzed with a 2G Enterprises DC–SQUID cryogenic magnetometer. Also, the S–Ratio ( $-\text{IRM}_{-0.3\text{T}}/\text{SIRM}_{1.0\text{T}}$ ) and the HIRM [ $(\text{IRM}_{-0.3\text{T}} + \text{SIRM}_{1.0\text{T}})/2$ ] were calculated for 94 of 112 samples, equally distributed through the section.

The IRM experiments show that the ferromagnetic fraction within the samples is dominated by magnetite, with secondary hematite interpreted as mainly pigmentary (Maron and Muttoni, 2021). This type of hematite, causing the pervasive red colour of the Scaglia Rossa, probably derived from dehydration of goethite (Channell, 1978; Channell et al., 1978, 1982). Hematite becomes sporadic in occurrence in the whitish interval between  $\sim 228.9$  and  $\sim 232.7$  m, where hematite formation/preservation was prevented by more reducing conditions (Channell et al., 1982). These variations in hematite content are well displayed by both the S–Ratio and HIRM curves (Fig. 7C; Maron and Muttoni, 2021).

Thermal demagnetization of NRM revealed an initial ‘A’ component, oriented north with positive inclination, isolated from room temperature up to  $150^{\circ}\text{C}$ , and observed in all the 112 samples analysed. The mean direction of the ‘A’ component in *in situ* coordinates is in agreement with the direction of the present–day magnetic field, suggesting a viscous origin for this component. A secondary ‘B’ component, isolated up to  $\sim 300^{\circ}\text{C}$  in 105 samples and antipodal to the ‘A’ component (in *in situ* coordinates), resembles the secondary component recognized by Channell et al. (1982) in the Scaglia Rossa of Gubbio. Channell et al. (1982) interpreted this component as a chemical overprint (CRM) acquired during exhumation and weathering, or as a “hard” viscous component (e.g., Dunlop and Stirling, 1977) acquired during a recent magnetochron of reversed polarity (Channell et al., 1982). The characteristic component (ChRM) has been isolated in 111 of 112 samples between  $\sim 300$  and  $\sim 575^{\circ}\text{C}$  (sometimes up

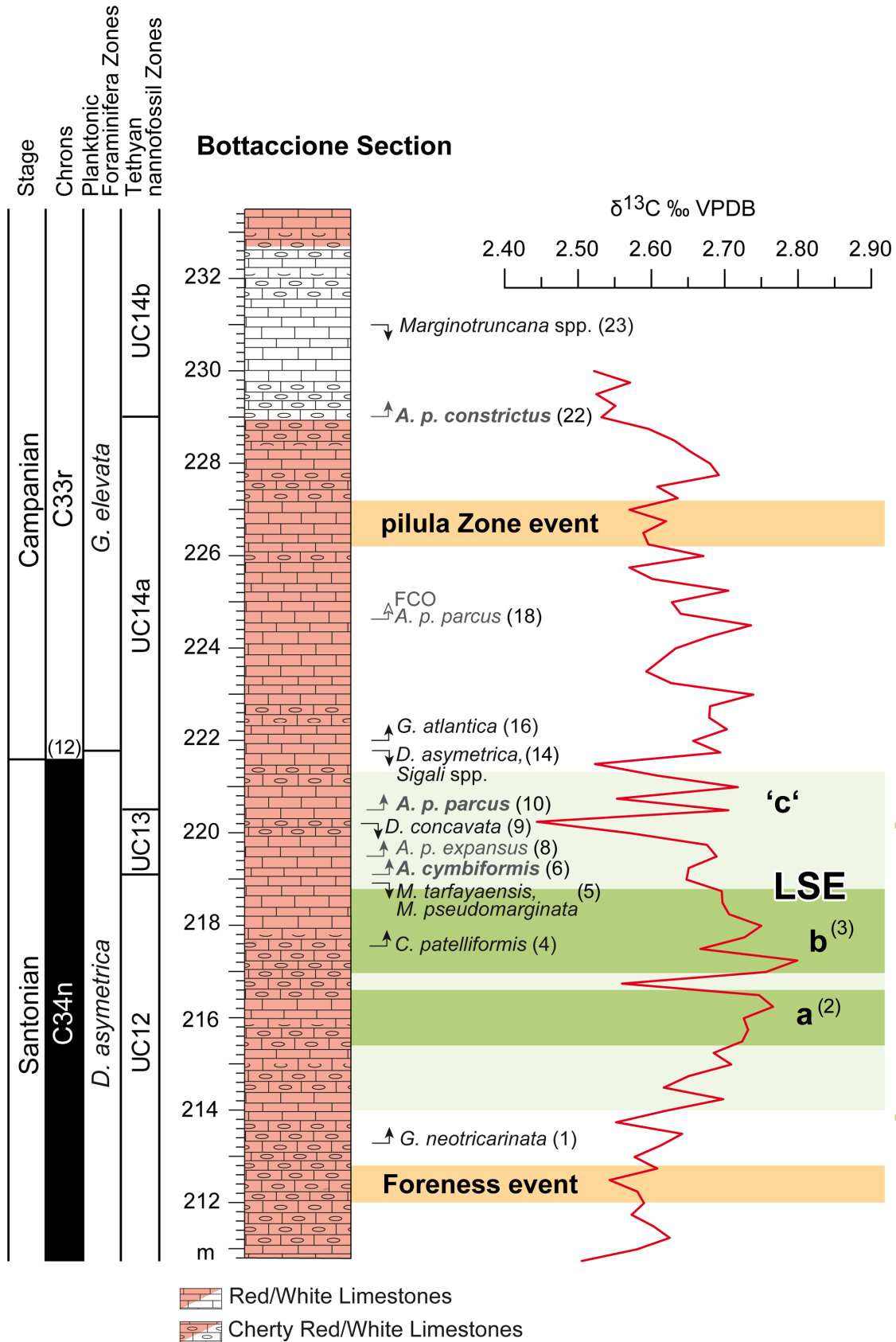


**Figure 6.** Litho- and magnetostratigraphy of the Bottaccione proposed GSSP section (see Fig. 5 for location), after Maron and Muttoni (2021); calcareous microplankton after Miniati et al. (2020), and carbon isotopes after Sabatino et al. (2018) with the auxiliary markers of the Late Santonian Event (LSE) LSE-a and LSE-b after Thibault et al. (2016). The total extent of the LSE carbon isotope excursion is revised to achieve consistency in correlation and includes LSE-c (see text for further explanation). The numbers refer to boundary and auxiliary markers explained in the text.

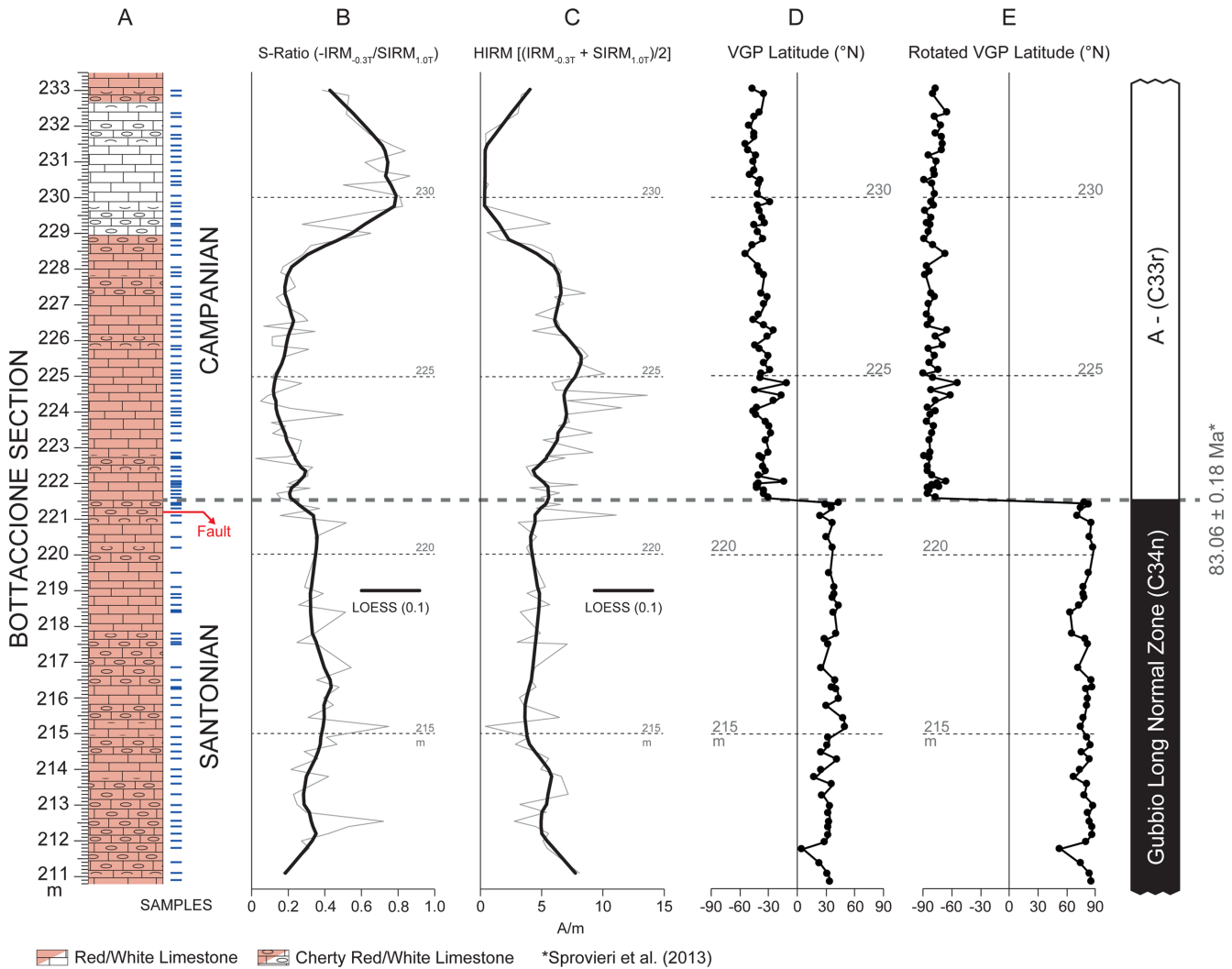


**Figure 7. Rock magnetic properties and magnetostratigraphy of Scaglia Rossa at the Bottaccione section. From left to right: A) lithostratigraphy, B) *S*-Ratio, C) HIRM, D) VGP latitudes, and E) rotated VGP latitudes. *S*-Ratio and HIRM curves show a decrease in hematite and a relative increase in magnetite between ~228.9 m and ~232.7 m, where layers become whitish in color. Magnetostratigraphy derived from rotated VGP latitudes show a normal polarity zone identified as the top of C34n, followed by a reverse polarity zone identified as the lower C33r.**

to ~625°C), showing antipodal distribution in both *in situ* and tilt-corrected coordinates. The mean direction of the ChRM component non corrected for sedimentary inclination flattening (Dec. = 306.0°E, INC = 28.9°,  $k = 32.8$ ,  $95 = 2.4^\circ$ ,  $n = 111$ ; Maron and Muttoni, 2021) is similar to the mean direction calculated for the Cretaceous Scaglia Rossa of Gubbio by Lowrie and Alvarez (1977a, b) and Channell et al. (1978). The Virtual Geomagnetic Pole (VGP) latitudes obtained from each ChRM component (Fig. 7D) were restored to palaeo-coordinates (see Maron and Muttoni, 2021 for details) and used to interpret the magnetostratigraphy, identifying a lower normal polarity zone overlain by a reverse polarity zone (Fig. 7E). Maron and Muttoni (2021) interpret the normal and reverse polarity intervals respectively as the uppermost “Gubbio Long Normal Zone” (GLNZ) and the A-magnetozone of Lowrie and Alvarez (1977a), corresponding to the top of C34n and base of C33r Chrons. The C34n–C33r polarity reversal boundary is placed at  $221.525 \pm 0.075$  m in the Bottaccione section (Maron and Muttoni, 2021) and assigned a nominal age of  $83.06 \pm 0.18$  Ma based on the astrochronological tuning of the Bottaccione  $\delta^{13}\text{C}_{\text{carb}}$  data of

Sprovieri et al. (2013).

The palaeomagnetic pole derived from the ChRM component mean direction (non corrected for sedimentary flattening) falls at Lat.: 36.5°N, Long: 268.5°E,  $A_{95} = 1.5^\circ$ , and is rotated counter-clockwise by  $39.5 \pm 3.3^\circ$  (Maron and Muttoni, 2021) relative to the Africa–Adria reference pole of Muttoni et al. (2013). The pole rotation is interpreted as reflecting the rotation of the central Apennines relative to parautochthonous Adria (e.g., Lowrie and Alvarez, 1977a, b; Roggenthen and Napoleone, 1977; Channell et al., 1978; Maron and Muttoni, 2021). The palaeolatitude, corrected for sedimentary inclination flattening using the E/I method of Tauxe and Kent (2004), places the Bottaccione area at 21.1°N ( $\pm 1.6^\circ$ ) in substantial agreement with the palaeolatitude predicted at Gubbio by the Late Cretaceous Adria–Africa mean palaeopole of Muttoni et al. (2013).

### Biostratigraphy

The biostratigraphy of calcareous plankton across the Santonian–

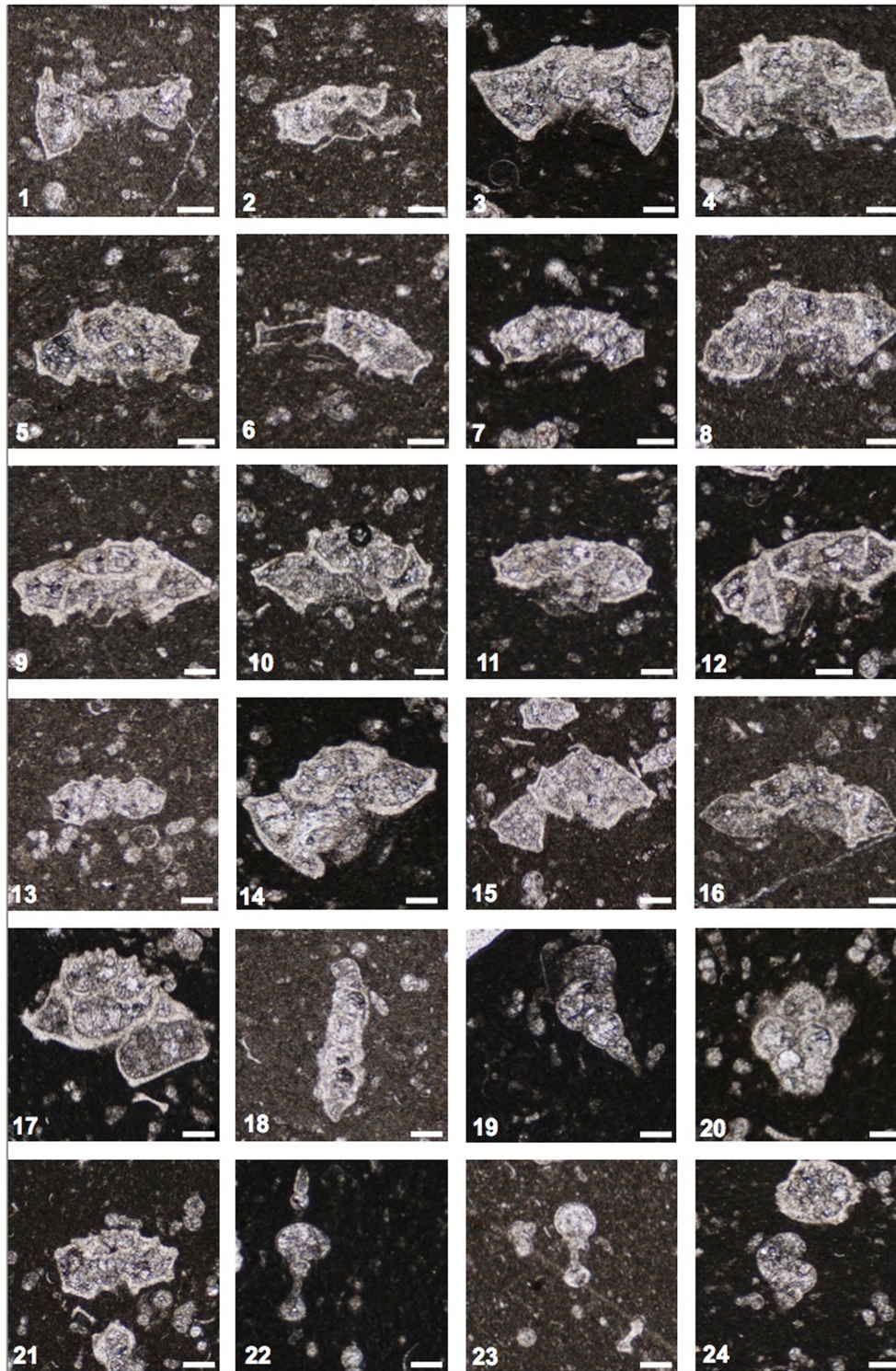
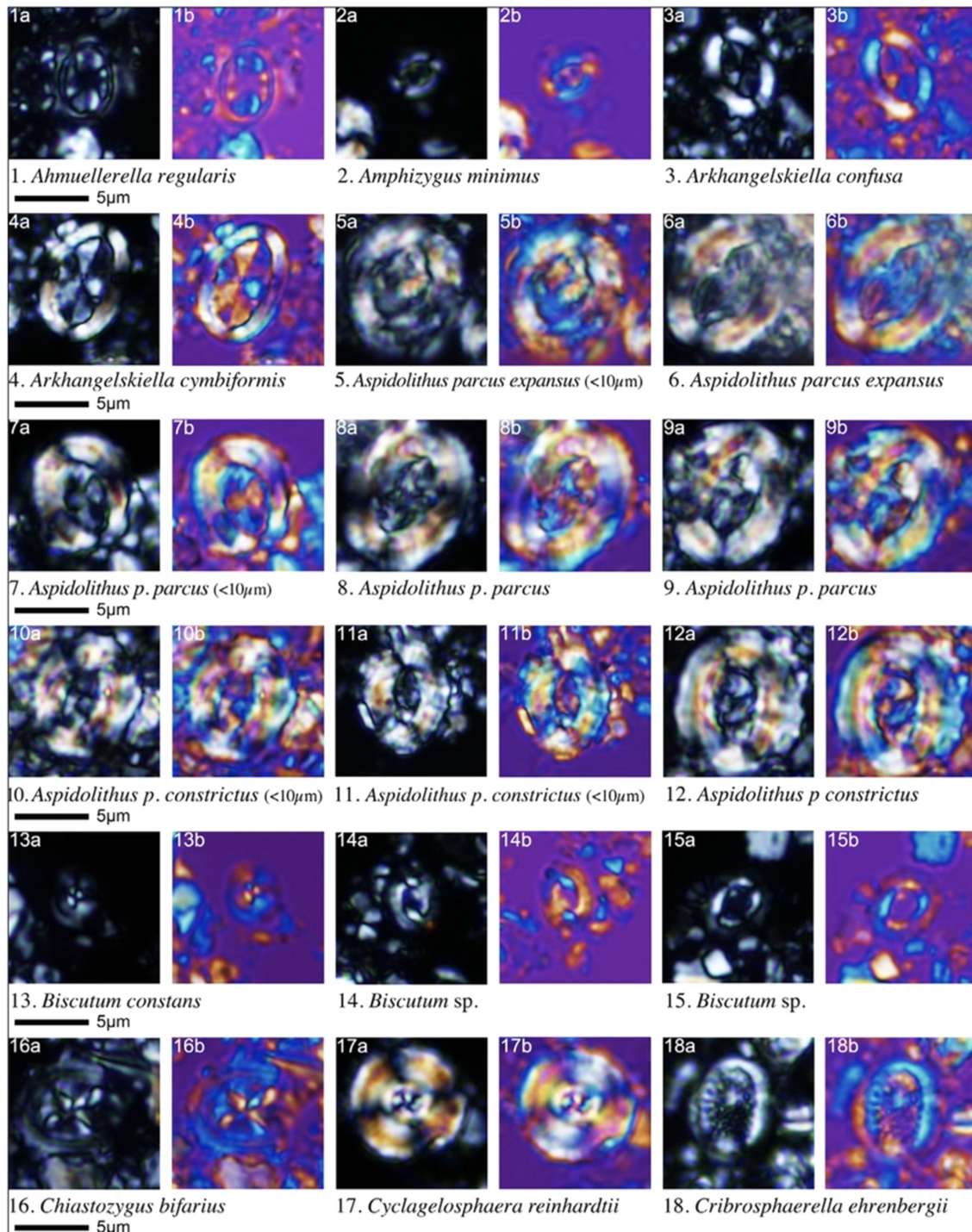


Figure 8. Selected planktonic foraminifera species from the Bottaccione section (after Miniati et al., 2020, Plate 3). Scale bars = 100  $\mu$ m. 1) *Dicarinella asymetrica*, sample 221.72 m. 2) *Globotruncana linneiana*, sample 212.20 m. 3) *Globotruncanita elevata*, sample 224.60 m. 4) *Contusotruncana fornicata*, sample 221.71 m. 5) *Globotruncana arca*, sample 223.92 m. 6) *Marginotruncana coronata*, sample 212.20 m. 7) *Marginotruncana pseudolinneiana*, sample 224.60 m. 8) *Marginotruncana undulata*, sample 225.75 m. 9) *Marginotruncana sinuosa*, sample 218.92 m. 10) *Marginotruncana schneegansi*, sample 217.55 m. 11) *Marginotruncana pseudomarginata*, sample 218.40 m. 12) *Globotruncana neotricarinata*, sample 221.71 m. 13) *Globotruncana bulloides*, sample 222.05 m. 14) *Globotruncanita stuartiformis*, sample 220.25 m. 15) *Contusotruncana patelliformis*, sample 221.71 m. 16) *Globotruncana orientalis*, sample 221.21 m. 17) *Globotruncanita atlantica*, sample 222.05 m. 18) *Sigalia* sp., sample 221.71 m. 19) *Pseudotextularia nuttalli*, sample 229.75 m. 20) *Ventilabrella eggeri*, sample 214.30 m. 21) *Globotruncana hilli*, sample 224.60 m. 22) *Planohedbergella* (= *Globigerinelloides*) *prairiehillensis*, sample 231.76. 23) *Laeviella* (= *Globigerinelloides*) *bollii*, sample 213.30 m. 24) *Laeviheterohelix pulchra*, sample 232.33 m. The generic assignments of the planispiral planktonic foraminifera previously assigned to *Globigerinelloides* follow revision by Huber et al. (2022).

Campanian boundary interval of the Bottaccione section was directly calibrated with polarity magnetozones by Premoli Silva (1977), Premoli Silva and Sliter (1995), Gardin et al. (2001), Tremolada (2002), Petrizzo et al. (2011), Coccioni and Premoli Silva (2015) and Miniati

et al. (2020), with an increasing resolution over time that provides a reliable and robust identification of several primary and secondary biohorizons. The base of polarity Chron C33r at 221.525 m, the marker candidate for the Santonian–Campanian boundary, falls in the lowermost



**Figure 9.** Selected calcareous nannofossil species from the Bottaccione section (after Miniati et al., 2020, Plate 1). For each taxon (a) cross-polarized light; (b) quartz lamina. 1) *Ahmuellerella regularis*, sample 213.8 m. 2) *Amphizygus minimus*, sample 219.75 m. 3) *Arkhangelskiella confusa*, sample 219.5 m. 4) *Arkhangelskiella cymbiformis*, sample 221.4 m. 5) *Aspidolithus parvus expansus* var. “small”, sample 220.5 m. 6) *Aspidolithus parvus expansus*, sample 227.5 m. 7) *Aspidolithus parvus parvus* var. “small”, sample 229 m. 8) *Aspidolithus parvus parvus*, sample 232.33 m. 9) *Aspidolithus parvus parvus*, sample 233 m. 10) *Aspidolithus parvus constrictus* var. “small”, sample 230.6 m. 11) *Aspidolithus parvus constrictus* var. “small”, sample 232.85 m. 12) *Aspidolithus parvus constrictus*, sample 230.6 m. 13) *Biscutum constans*, sample 220.9 m. 14) *Biscutum* sp., sample 212.40 m. 15) *Biscutum* sp., sample 220.2 m. 16) *Chiastozygus bifarius*, sample 218.4 m. 17) *Cyclagelosphaera reinhardtii*, sample 221.4 m. 18) *Cribrosphaerella ehrenbergii*, sample 221.9 m.

part of the calcareous nannofossil CC18 zone of Sissingh (1977), NC18 zone of Roth (1978), NC18\* zone of Bralower et al. (1995) and UC14a<sup>TP</sup> zone of Burnett (1988) and in the topmost part of the planktonic foraminiferal *Dicarinella asymetrica* zone of Premoli Silva and Sliter (1995), Coccioni and Premoli Silva (2015), and Miniati et al. (2020). More specifically, the base of Chron C33r lies between the first occurrence (FO) of the calcareous nannofossil *Aspidolithus parvus parvus* at the 220.50 m level, previously recorded as the FO of “small” *A. parvus parvus* at meter level 220.50 by Gardin et al. (2001) and as the FO of *A. parvus parvus* at 220.00 m by Tremolada (2002), and the last occurrence (LO) of *D. asymetrica* at 221.72 m, previously documented at 221.40 m by Coccioni and Premoli Silva (2015). These biohorizons are reliable secondary markers for the base of Chron C33r. Selected planktonic foraminifera and calcareous nannofossils occurring in the Bottaccione section are illustrated in Figs. 8 and 9.

### Carbon Isotope Stratigraphy

The double-peaked positive  $\delta^{13}\text{C}$  excursion, originally described from English chalks, is a prominent feature in the chalk successions of north-west Europe and was named the Santonian–Campanian Boundary Event (SCBE) by Jarvis et al. (2006). Its proper identification at Gubbio was achieved by Thibault et al. (2016, fig. 8) using the combined evidence of low- and high-resolution  $\delta^{13}\text{C}$  curves from both sides of the Bottaccione Gorge. However, the characteristic double peak of the SCBE, is less distinct at Bottaccione than elsewhere and thus more difficult to define with high accuracy (Fig. 4). The event has been identified in the Bottaccione section as a single carbon isotope event by Sabatino et al. (2018) and Maron and Muttoni (2021) and is further interpreted as representing a minimum in a 405 kyr-long eccentricity cycle (Sprovieri et al., 2013; Thibault et al., 2016).

The stratigraphical extent of the SCBE differs at Bottaccione between the single event definition (213.8–220.2 m, Sabatino et al., 2018; Maron and Muttoni, 2021) and the double-peak definition (215.4–218.8 m, Thibault et al., 2016). Furthermore, the base of the Campanian, the base of Chron C33r, places the stratigraphic range of the SCBE completely in the uppermost Santonian (upper UC12 and UC13, upper *D. asymetrica* Zone). To provide a uniform definition, the SCBE is renamed here as Late Santonian Event (LSE) and its stratigraphic range is revised to achieve consistency in correlation and improve its potential as subsidiary marker for the Santonian–Campanian boundary.

The LSE at Bottaccione extends from 214.0 m to 221.3 m and includes the subsidiary features LSE–a, LSE–b and LSE–c (Fig. 6). LSE–a and LSE–b are the lower and upper SCBE–peak of Thibault et al. (2016). LSE–a and LSE–b serve as auxiliary boundary markers (2) and (3) of the GSSP. The base of the LSE is equivalent to the definition of Sabatino et al. (2018), and the top is extended close to the base of the Campanian to include the subsidiary peak LSE–c (Fig. 6). The LSE–c peak is, although of subsidiary nature, well-developed in chalk sections. At the Bottaccione section, LSE–c is less distinctive, as a result of which it cannot be precisely limited and labelled here with ‘c’. However, the combined evidence of both sides of the Bottaccione Gorge show LSE–c as a distinct positive peak immediately beneath the boundary (Thibault et al., 2016, fig. 8). Altogether, the positive carbon isotope excursion of the LSE may represent a 405-kyr cycle with the subsidiary events LSE–a to LSE–c corresponding to 100-kyr

cyclicality (Thibault et al., 2016). This interpretation is also supported by the 405 kyr orbital calibration of the Bottaccione carbon isotope record whereby the wrongly correlated ‘Horseshoe Bay’ event identified at Gubbio just prior the magnetochron reversal, and which can now be recognized as the LSE, corresponds to a single 405 kyr cycle (Sprovieri et al., 2013, figs. 2 and 4). Thereby, LSE–b is the peak with the highest magnitude reflecting the highest amplitude of eccentricity modulated precession. This interpretation is however challenged by the demonstration by Laurin et al. (2015) of a strong 1.07 Myr cycle pacing the Late Cretaceous carbon isotope record, probably associated with the ~1.2 Myr s4–s3 term that is the largest modulation term of the obliquity (see Laskar, 2020). In the latter interpretation, the ‘SCBE’ here renamed as the LSE, corresponds to one of those ~1.1 Myr cycles, in which case LSE–a, LSE–b and LSE–c would rather represent three g2–g5 405 kyr eccentricity cycles.

### Accessibility and Protection

#### Access

The section is accessible thanks to the Regional Road 298 “Eugubina”, which allows easy access to the outcrop in front of a free parking lot. Free access to the section is guaranteed.

#### Permanent protection

The area around the section is designated for tourism and as a wilderness, with no planning for any kind of urban development. Local institutions (the town of Gubbio, the Province of Perugia in the Umbrian Region, the University of Urbino and the Osservatorio Pianeta Terra of Corinaldo) are willing to cooperate. We have a letter from the mayor of Gubbio supporting the protection of the GSSP.

### The Boundary Level: Primary and Auxiliary Markers

(oldest)

(1) First occurrence of the planktonic foraminiferan *Globotruncana neotricarinata* (213.30 m). This species is cosmopolitan in marine settings at thermocline depth with occurrences in all biogeographic realms.

(2) Carbon isotope peak LSE–a (215.4 to 216.6 m). This event, and the succeeding one, have been identified globally.

(3) Carbon isotope peak LSE–b (217.0 to 218.8 m). The LSE–b peak forms the maximum of the LSE carbon isotope excursion.

(4) First occurrence of the planktonic foraminiferan *Contusotruncana patelliformis* (217.55 m). This species occurs in marine settings at mixed layer to thermocline depth at low to mid-latitudes in the Tethyan realm, Western Interior Seaway, and in the Atlantic, Pacific and Indian Oceans.

(5) Last occurrence of the planktonic foraminiferan *Marginotruncana tarfayaensis*, *Marginotruncana pseudomarginata*, *Muricohedbergella flandrini* (218.92 m). *Marginotruncana tarfayaensis* occurs in marine settings at thermocline depth at low to mid-latitudes in the Tethyan realm, and in the Atlantic, Pacific, and Indian Oceans. *Marginotruncana pseudomarginata* and *M. flandrini* are cosmopolitan species with occurrences at mixed layer to thermocline depth in all biogeographic realms.

(6) First occurrence of the coccolith *Arkhangelskiella cymbiformis* (base of zone UC13) (219.10 m).

(7) First occurrence of the planktonic foraminiferan *Hendersonites carinatus* (219.33 m). This species occurs in marine settings at lower mixed layer depth at low to mid-latitudes in the Tethyan realm, Western Interior Seaway, and in the Atlantic, Pacific, and Indian Oceans.

(8) First occurrence of the coccolith *Aspidolithus parvus expansus* (middle zone UC13) (219.5 m).

(9) Last occurrence of the planktonic foraminiferan *Dicarinella concavata* (220.2 m). This species occurs in marine settings at mixed layer to thermocline depth at low to mid-latitudes in the Tethyan realm, Western Interior Seaway, and in the Atlantic, Pacific, and Indian Oceans.

(10) First occurrence of the coccolith *Aspidolithus parvus parvus* (base of zone UC14) (220.5 m).

(11) First occurrence of the planktonic foraminiferan *Pseudoguembelina costellifera* (221.45 m). This species occurs in marine settings at mixed layer depth at low latitudes in the Tethyan realm, Western Interior Seaway, and in the Atlantic, Pacific, and western Indian Ocean. It is rare in mid-latitude deep sea sites in the south Indian Ocean.

(12) Primary marker, magnetic reversal Chron 33r (221.53 m). Globally recognised reversal, base of C–sequence in oceanic settings.

(13) Last occurrence of the planktonic foraminiferan *Marginotruncana schneegansi* (221.6 m). This species occurs in marine settings at thermocline depth at low to mid-latitudes in the Tethyan realm, Western Interior Seaway, and in the Atlantic, Pacific and Indian Ocean.

(14) Last occurrences of the planktonic foraminiferan *Dicarinella asymetrica* and *Sigalia* spp. (221.72 m) (base of *Globotruncanita elevata* Zone). *Dicarinella asymetrica* occurs in marine settings at mixed layer to thermocline depth at low to mid-latitudes in the Tethyan realm, Western Interior Seaway, and in the Atlantic, Pacific and Indian Oceans. *Sigalia* spp. occur at lower mixed layer depth at low latitudes in the Tethyan realm, in the North Atlantic and in the western Indian Ocean.

(15) First occurrence of the planktonic foraminiferan *Globotruncana hilli* (221.72 m). This species is cosmopolitan in marine settings at thermocline depth with occurrences in all biogeographic realms.

(16) First occurrence of the planktonic foraminiferan *Globotruncanita atlantica* (222.05 m). This species occurs in marine settings at thermocline depth at low latitude in the Tethyan realm, Western Interior Seaway, and in the North Atlantic, western Indian and central Pacific Ocean.

(17) First occurrence of the planktonic foraminiferan *Globotruncana orientalis* (222.21 m). This species is cosmopolitan in marine settings at thermocline depth with occurrences in all biogeographic realms.

(18) First common occurrence of the coccolith *Aspidolithus parvus parvus* (224.60 m) (base of zone UC14a<sup>TP</sup>).

(19) Last occurrence of the planktonic foraminiferan *Marginotruncana undulata* (225.75 m). This species occurs in marine settings at thermocline depth at low latitudes in the Tethyan realm and western Indian Ocean and is rare in mid-latitude deep sea sites in the south Indian Ocean.

(20) First occurrence of the planktonic foraminiferan *Pseudoguembelina costulata* (227.0 m). This species occurs in marine settings at mixed layer depth at low to mid-latitudes in the Tethyan realm, Western Interior Seaway, and in the Atlantic, Pacific and Indian Ocean.

(21) Last occurrence of the planktonic foraminiferan *Marginotruncana*

*cana sinuosa* (227.50 m). This species is cosmopolitan in marine settings at mixed layer to thermocline depths with occurrences in all biogeographic realms.

(22) First occurrence of the coccolith *Aspidolithus parvus constrictus* (229 m) (base of zone UC14b<sup>TP</sup>)

(23) Last occurrence of the planktonic foraminiferan *Marginotruncana* spp. (230.98 m). This genus is cosmopolitan in marine settings at mixed layer to thermocline depth with occurrences in all palaeobiogeographic realms.

(youngest)

## Auxiliary Sections

### Seaford Head, Sussex, England, UK

The sea cliff section in the English Channel at Seaford Head, east of Seaford in Sussex, UK (Figs. 10–13; 50°45′47.25″N, 0°0.6′41.11″E) provides a continuously exposed succession in white chalk facies across the Santonian–Campanian boundary. An early biostratigraphical (zonal macrofossil) description was given by Rowe (1902); Mortimore (1986) and Mortimore et al. (2001) provided a detailed lithological profile and some macrofossil distribution data (echinoids, crinoids). Hampton et al. (2007, fig. 8) included distribution data for selected nannofossils and benthic foraminiferan. Planktonic foraminifera are rare, but Hampton et al. (2007) record a major incursion of double keeled taxa at the level of the Brighton Marl (66–68 m in Figs. 11 and 12). Jenkyns et al. (1994) provided an oxygen– and carbon isotope curve for this section, and Thibault et al. (2016) published high-resolution carbon and oxygen isotope curves, and an orbitally tuned timescale based on these data. Gale (2018) described microcrinoid occurrences in the uppermost Santonian and lowest Campanian parts of the succession. Jarvis et al. (2022) provided detailed palynological data and a high-resolution carbon isotope curve (Fig. 13). Although proposed as a potential GSSP (Hampton et al., 2007), the absence of important planktonic foraminifera and reliable magnetostratigraphy preclude its use. However, it provides an excellent carbon–isotope curve which permits correlation of the crinoid zones to the Bottaccione GSSP section, and palynological data from the stage boundary interval at Seaford Head (Fig. 13) from Jarvis et al. (2022).

The section can be accessed only on low spring tides, from the promenade east of Seaford (50°45′50.70″N, 0°0.6′33.07″E). Care should be taken, as the shore is slippery and cliff-falls are common. The Santonian–Campanian boundary interval is exposed 160–200 m southeast of the promenade. The succession here is in the Newhaven Chalk Formation and comprises soft, white pelagic chalks containing thin marls and numerous layers of nodular flint. A detailed lithostratigraphical nomenclature for the marl and flint layers was provided by Mortimore (1986) and is shown in Figs. 11 and 12. Key markers are the Buckle Marl, the Exceat Flint, the Brighton and Friar's Bay Marls, which extend across the northern part of the Anglo–Paris Basin (Gale, 2018).

Macrofossil subdivision of this section is based primarily upon the distribution of four successive species of stemless benthonic crinoid (*Uintacrinus socialis*, *Marsupites laevigatus*, *M. testudinarius*, *U. anglicus*) which are of worldwide distribution in chalk facies (Gale et al., 2008; see below). These are overlain by an assemblage zone characterised by an echinoid, *Offaster pilula*, within which successive horizons

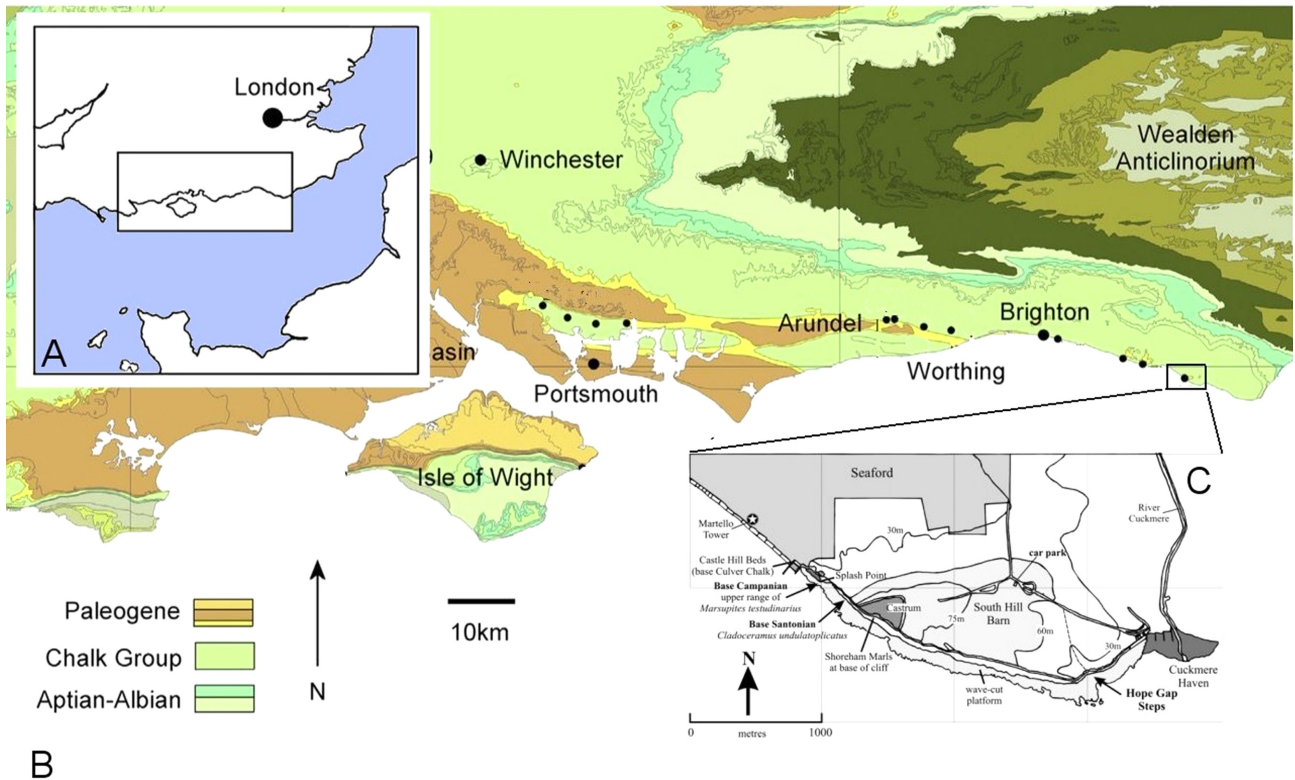


**Figure 10.** Map showing the location of the Seaford Head section, Sussex, U.K. **A**, southern England, to show area in **B**. **B**, geological map of southern English coast to show location of **C**. **C**, detailed map of Seaford and Seaford Head. After Hampton et al. (2007) and Gale (2018).

are recognised using shape variants of the echinoid *Echinocorys scutata* (Brydone, 1914; Mortimore, 1986; Gale, 2018). Microcrinoid zones (Gale, 2018, 2019) extend from SaR4–6 to CaR1, 2; the Santonian–Campanian boundary falls within the upper part of CaR1 (Fig. 12). Nanofossil data (Hampton et al., 2007) include the first occurrence of the coccolith *Aspidolithus parvus parvus*, between the Rottingdean Pair and Rottingdean Triple Marls (9 m above the Late Santonian carbon isotope event–LSE), which possibly correlates with the FCO of the subspecies in the Bottaccione section (Fig. 6) (Miniati et al., 2020).

A new palynological study of 40 samples (average ~1 m spacing) from Seaford Head was completed for this work, spanning the interval from the Buckle Flint (basal upper Santonian, *U. socialis* Zone) to the Old Nore Marl in the lower Campanian *O. pilula* Zone (Fig. 13; Jarvis et al., 2022). The floras are overwhelmingly dominated by organic walled dinoflagellate cysts (~90% of the total) with a moderate species richness of 30 to 64 taxa (average 43), although algae (particularly the prasinophyte *Leiosphaeridia*) are well represented in the Santonian. A conspicuous influx of fungal hyphae and insect remains associated with the Late Santonian CIE may be significant as a similar event is observed at Boceniec (see below).

The dinoflagellate component is represented by a mixture of the marginal marine *Circulodinium–Heterosphaeridium* (C–H; see Pearce et al., 2003) assemblage, and the more distal *Spiniferites–Palaeohystrichophora* (S–P) assemblage (Pearce et al., 2003; Prince et al., 2008; Pearce et al., 2009; Jarvis et al., 2021), with a ratio of ~2:1. Absolute abundances (palynomorphs per gram, ppg) are relatively low and range from 90–1,400 ppg (Fig. 12). The average value of ~300 ppg is con-

sistent with the type C–H assemblage recovered from the Chalk of Berkshire, southern England by Pearce et al. (2003).

Some stratigraphic markers are missing at Seaford Head, presumably due to the relatively marginal setting. Regionally significant events are briefly discussed below, in stratigraphic order from the lowest upwards, which effectively constrain the Santonian–Campanian boundary. Results are compared to other macrofossil-calibrated, high-resolution studies with  $\delta^{13}\text{C}$  data: eastern England (Trunch borehole, Norfolk), southern England (Foreness Point and White Ness sections, Isle of Thanet, Kent; Whitecliff, Isle of Wight), France (Poigny 701 borehole, Seine-et-Marne), and Poland (Boceniec, this paper, see below).

(oldest)

(1) The first occurrence of *Cordosphaeridium catherineae* at Seaford Head is observed at 57 m in the low *U. socialis* Zone, at the top of the Buckle CIE (Fig. 12). Pearce et al. (2020) recorded the first occurrence of the species slightly higher in the upper Santonian (high *U. socialis* Zone) at the base of the Hawks Brow CIE in the type material from the Trunch borehole. More recent work on the Poigny 701 borehole (Pearce et al., 2022) confirms the first occurrence in the (low) *U. socialis* Zone immediately above the Buckle CIE (although due to the wide sampling interval, the event may occur closer to, or within, the Buckle CIE).

(2) First occurrence of *Odontochitina porifera*. Pearce et al. (2020) reported a first occurrence (a likely First Appearance Datum) of *O. porifera* in the lower Santonian as a near globally synchronous event, while noting that a delayed first occurrence in the upper Santonian is

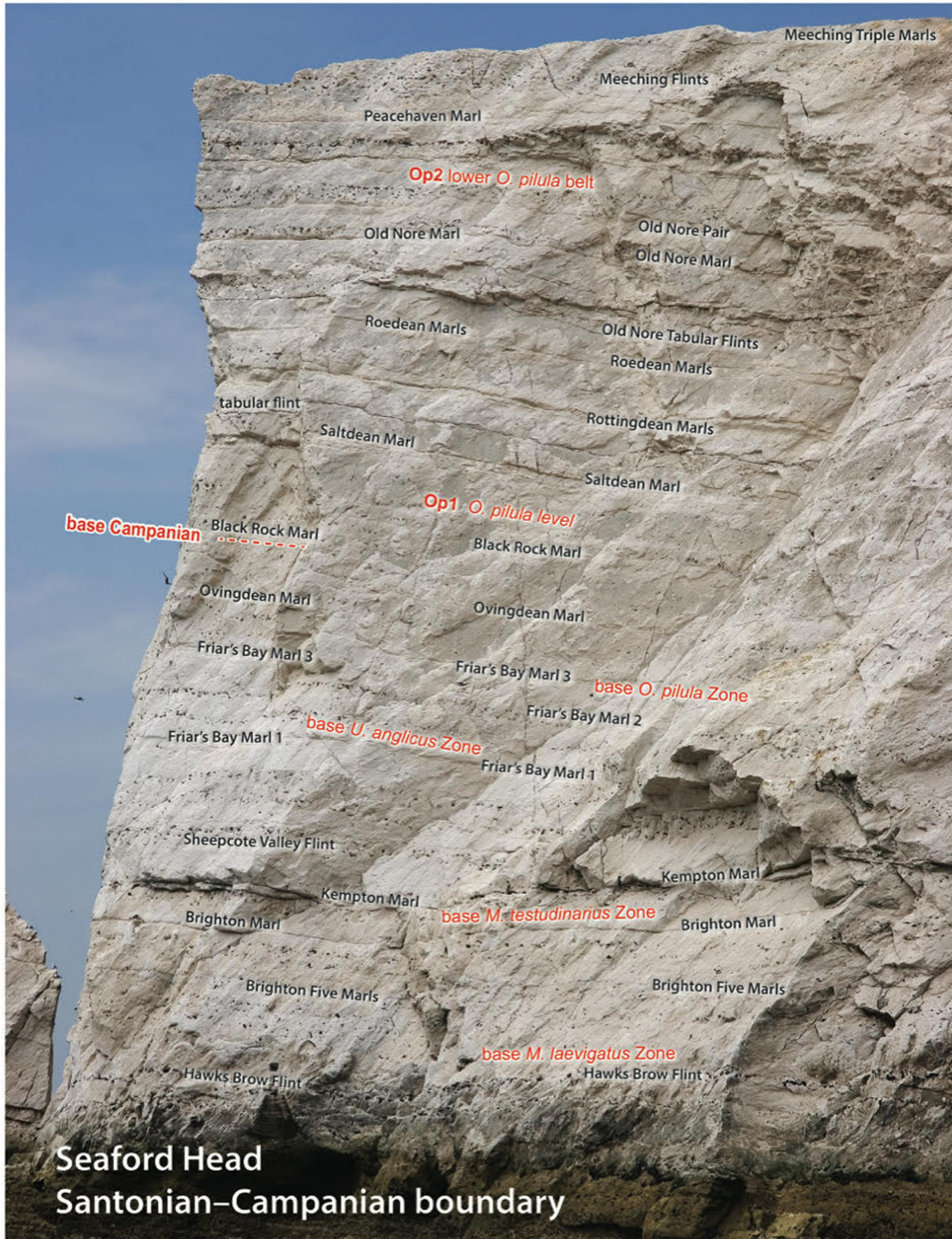


Figure 11. Photograph of Santonian–Campanian chalk succession at Seaford Head, Sussex, UK, looking north-westwards. Modified after Jarvis et al. (2022, fig. 2).

typical in NW Europe. This delayed first occurrence occurs consistently between the Buckle and Hawks Brow CIEs (i.e., in the *U. socialis* Zone) at Bocieniec (see Section 3.2), Trunch (Pearce et al., 2020), Whitecliff (Prince et al., 1999), and White Ness (Prince et al., 2008). At Seaford Head, the lowest occurrence of *O. porifera* occurs at 61 m (*U. socialis* Zone), also below the Hawks Brow CIE, consistent with

other records.

(3) The lowest occurrence of *Dimidium striatum*. As discussed by Pearce et al. (2020), the lowest occurrence of *D. striatum* recorded by Prince et al. (1999) from Culver Cliff (Whitecliff) is tentatively taken to represent the First Appearance Datum of the species and occurs between the Horseshoe Bay and Buckle CIEs. At Seaford Head, the

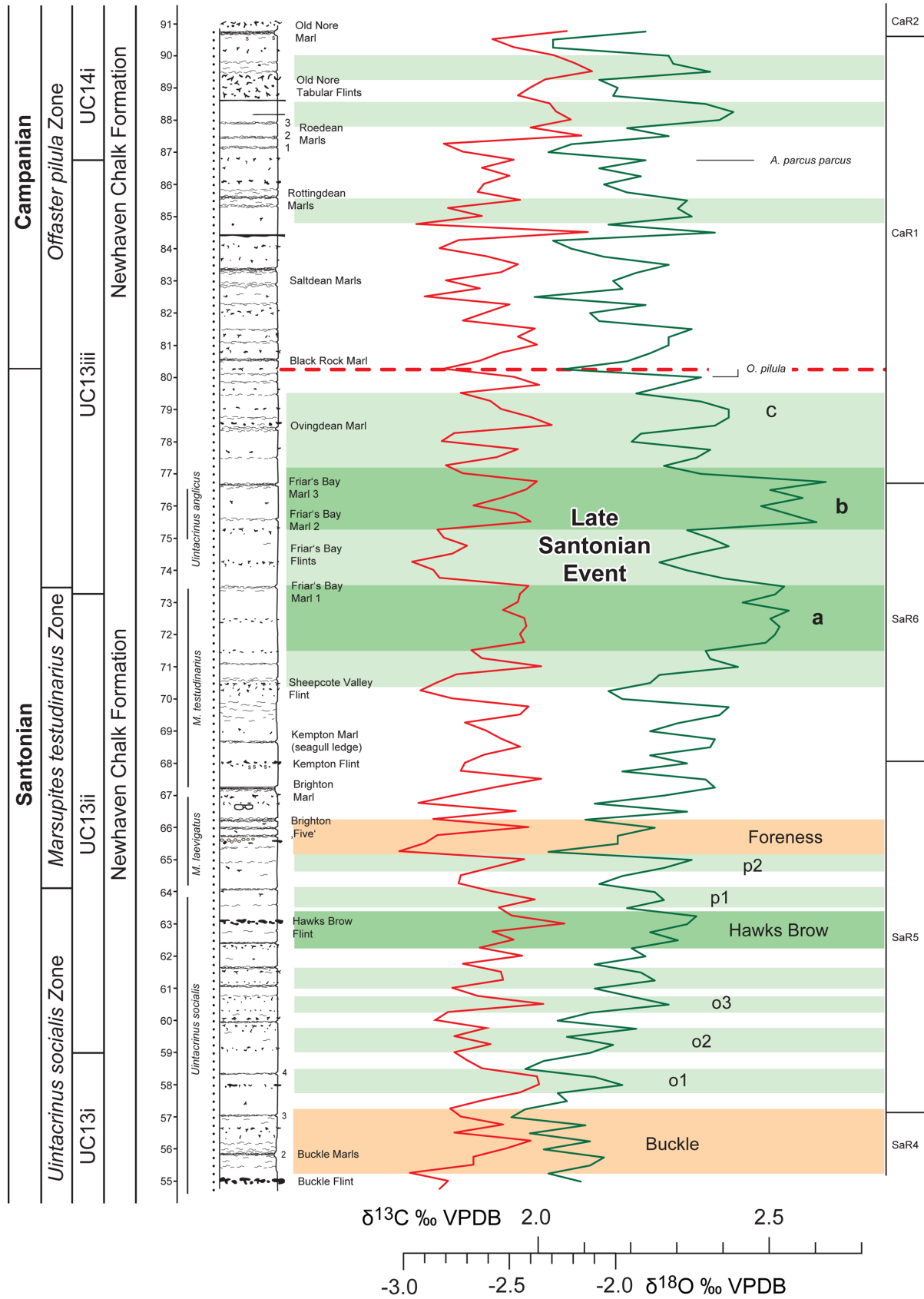


Figure 12. The succession at Seaford Head, Sussex, UK, modified after Thibault et al. (2016). The dotted red line immediately beneath the Blackrock Marl marks the inferred base of the Campanian, based on correlation of the carbon isotope record with the proposed GSSP. Minor carbon isotope excursions are labelled as o1– o3 and p1, 2, Buckle, Hawks Brow and Foreness. The columns on the right shows the microcrinoid zones (SaR4–6 to CaR1, 2, after Gale 2018, 2019) and the North Sea nannofossil zonation (Thibault et al. 2016). Lithostratigraphical terminology after Mortimore (1986).

event occurs stratigraphically higher between the Hawks Brow and Foreness CIEs, but it is still a useful marker for a position no lower than middle Santonian.

(4) Lowest occurrence of *Rhynchodiniopsis saliorum*. According to Pearce et al. (2020), the First Appearance Datum of *R. saliorum* occurs within Hawks Brow CIE in the *U. socialis* Zone in southern England. At Seaford Head, the lowest occurrence of *R. saliorum* occurs above

the Foreness CIE in the *M. testudinarius* Zone. Although this level is slightly higher than the FAD, it is apparently synchronous at Trunch (Pearce et al., 2020) and Poigny (Pearce et al., 2022) and is consistent as a marker for the upper Santonian.

(5) The recognition of a conspicuous absence or minimum relative abundance for *Surculosphaeridium longifurcatum* within the late Santonian is emerging from multiple sections across Europe. At Seaford

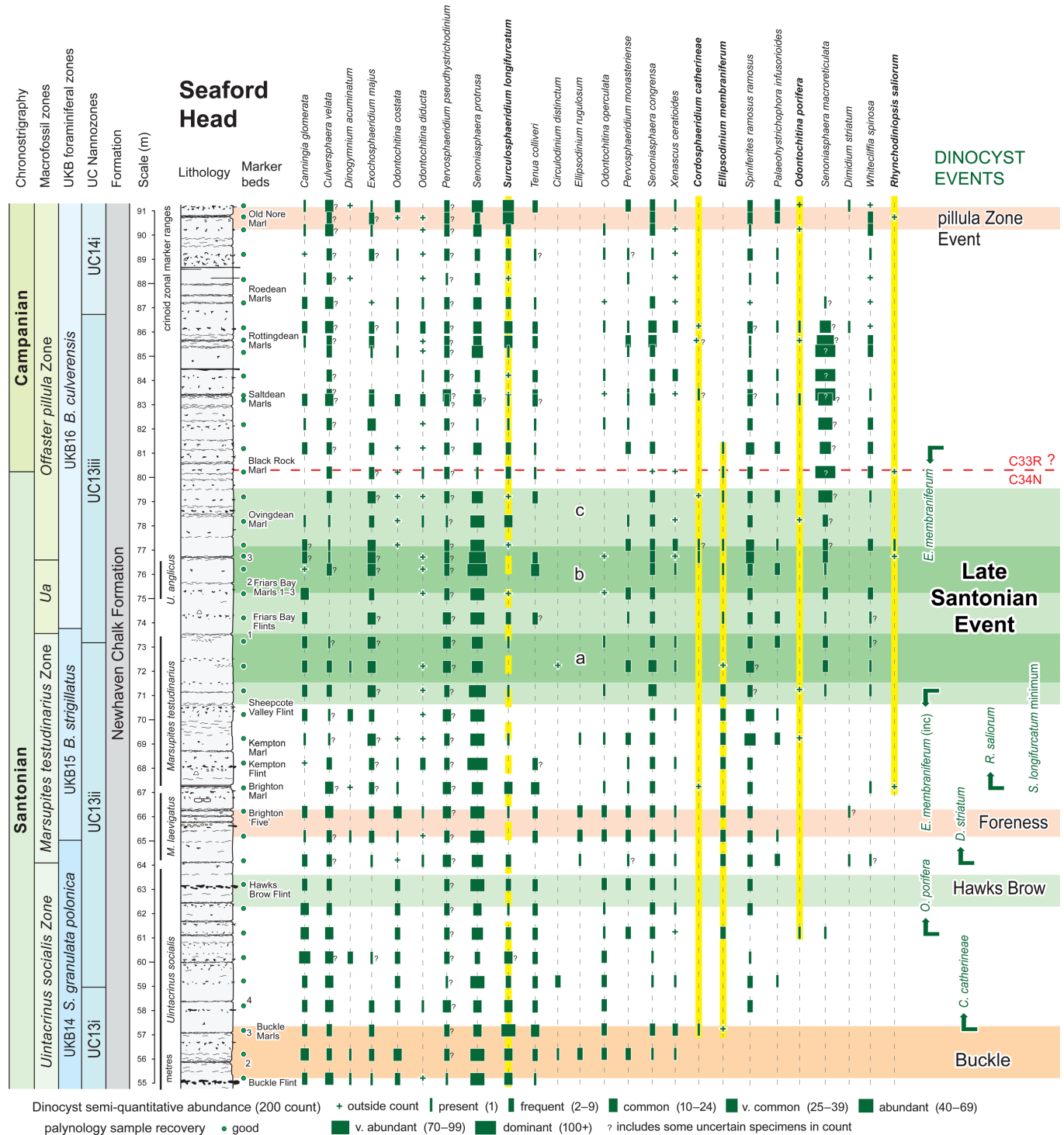


Figure 13. Ranges of selected organic walled dinoflagellate cysts and significant dinocyst events at Seaford Head, Sussex, U.K. See Fig. 12 for additional stratigraphical details. After Jarvis et al. 2022, fig. 5.

Head (Fig. 12), Poigny (Pearce et al., 2022), Trunch (Pearce et al., 2020, suppl. table 2) and Whitecliff (Prince et al., 1999), *S. longifurcatum* is poorly represented from below the Hawks Brow CIE upwards to above the Late Santonian CIE b. In all cases the stratigraphic mid-point of this poor recovery interval lies below the Late Santonian CIE within the *M. testudinarius* Zone. Interestingly, at Bocieniec, where the species is particularly common, a clear minimum in relative abundance occurs at the same stratigraphic level.

(6) The last occurrence of *Ellipsodinium* spp. appears to be a particularly significant, albeit currently local marker for the Santonian–Campanian boundary in NW Europe (Pearce et al., 2022). The last occurrence of *E. membraniferum* at Seaford Head occurs at 81 m, in the basal *O. pilula* Zone, above the Late Santonian Event, and ~1 m above the inferred position of the C34n–C33r boundary (Fig. 12). At Poigny (Pearce et al., 2022), and Trunch (Pearce et al., 2020, suppl. table 2) the last occurrence of *Ellipsodinium* spp. occurs slightly lower, but consistently within the Late Santonian Event. In the type material at Whitecliff, the last occurrence of *Ellipsodinium membraniferum* occurs in the lower *O. pilula* Zone (Prince pers. comm), which according to Jarvis et al. (2006, fig.11), presumably lies a few metres above the Late Santonian Event. Interestingly, in sites from southern England where *Ellipsodinium* is particularly well represented (Seaford Head; Whitecliff, Prince et al. pers comm.; Foreness, Prince et al., 2008), a last common occurrence event is also recognised in the high *M. testudinarius* Zone, below the Late Santonian Event.

(youngest)

The Seaford Head section has provided a high-resolution carbon isotope stratigraphy based upon analysis of closely spaced bulk chalk samples (Thibault et al., 2016; Jarvis et al., 2022). Important features of potential global significance are, successively:

(oldest)

The Buckle Event (Jarvis et al., 2006), a 0.5 per mil symmetrical trough in the lower and middle *U. socialis* Zone.

The Hawks Brow Event, a 0.4 per mil positive peak which is present in the uppermost *U. socialis* Zone.

The Foreness Event, (sensu Thibault et al., 2016) is a short 0.3 per mil trough in the *M. laevigatus* Zone.

The Late Santonian Event, a double peak with amplitudes of approximately 0.4 per mil, of which the lower maximum (peak a) is close to the top of the *M. testudinarius* Zone and the higher maximum (peak b) is coincident with the range of *U. anglicus*. A minor peak (c) is present above.

The *O. pilula* Zone Event, a 0.5 per mil trough is situated at the level of the Old Nore Marl (Fig. 11).

(youngest)

The magnetostratigraphy of the Seaford section given by Barchi (1995) and Montgomery et al. (1998) has been shown to be unreliable (Hampton et al., 2007; Thibault et al., 2016). Thus, the main importance of the Seaford Head section is the relationship between features of the high-resolution carbon isotope curve and successive crinoid zones, which permits these to be correlated into successions in which the crinoids are absent (Fig. 4). The base of the Campanian falls between the higher peak of the Late Santonian Event and the first occurrence of common *Aspidolithus parvus parvus*, a level immediately underly-

ing the Blackrock Marl at 80.2 m (Figs. 11 and 12).

### Bocieniec, Kraków, Poland

An old quarry in the village of Laski Dworski, 25 km north of Krakow (Fig. 14; 50°16'21.21"N, 19°56'1.09"W) exposes 5.5 m of Upper Cretaceous sediments, unconformably overlying Jurassic limestones (Dubicka et al., 2017). The succession (Fig. 15) comprises a thin basal glauconitic marl, overlain by 4.9 m of monotonous grey marls, and capped by 0.6 m of siliceous "opoka" chalk. The succession is thin, but has provided important data on magnetostratigraphy, biostratigraphy (nannofossils, planktonic and benthic foraminifera, crinoids), and a detailed carbon isotope curve, all summarised in Fig. 15, and the results of a recent palynological study (Jarvis et al., 2022) are presented here (Fig. 16). The magnetostratigraphy demonstrates that Chron 34n extends up into the range of *Marsupites*, and that the highest metre is reversed, with an intervening zone of uncertain polarity. The last occurrence of *D. asymetrica* lies 20 cm above the last occurrence level of *Marsupites testudinarius*. The carbon isotope curve shows the negative Foreness Event in the *M. laevigatus* Zone, and a single well developed 0.5 per mil peak of the Late Santonian Event. This was interpreted by Dubicka et al. (2017) as the higher of the double peaks of the LSE, but the coincidence of the main peak with the last occurrence of *M. testudinarius* indicates that it is the lower of the pair (peak a, Fig. 15). Moreover, *Uintacrinus anglicus* is absent, suggesting a minor hiatus around the 4.4 m level, and, in our interpretation, there is a minor hiatus around the 4.3 m level as a result of which the upper part of the LSE (peak b) and the *U. anglicus* Zone are missing. The last occurrence of *D. asymetrica* is recorded at 4.38 m. However, the level of this latter bioevent includes a wide uncertainty, relying on only 3 discontinuous occurrences of the taxon within the lower 4.4 m of the section (Fig. 15). The base of the Campanian at Bocieniec is thus taken at ca. 4.45 m where Dubicka et al. (2017) positioned the base of Chron 33r,



Figure 14. Map to show location of Bocieniec, Poland. After Dubicka et al. (2017).

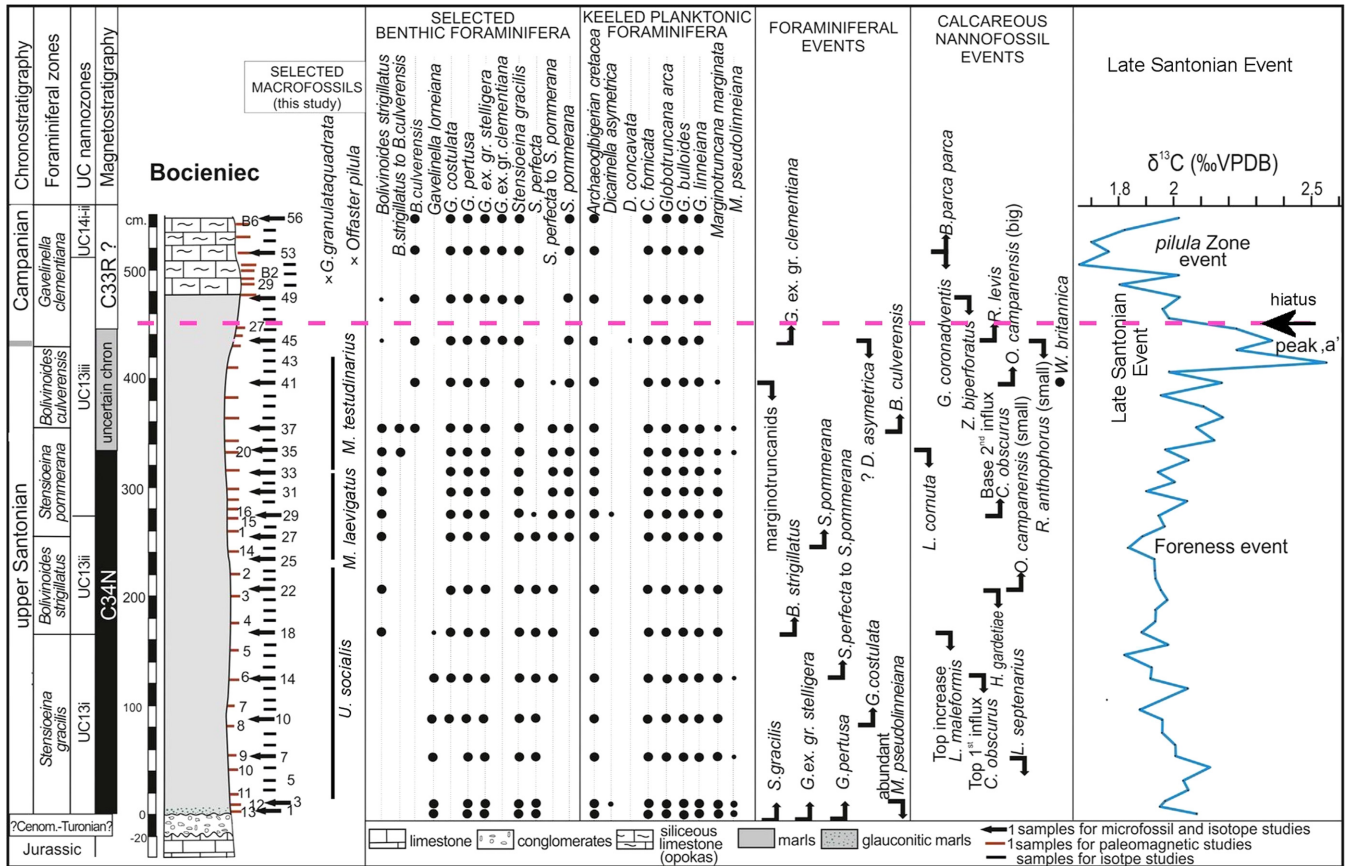


Figure 15. The succession at Bocieniec, near Krakow, Poland, modified after Dubicka et al. (2017). The base of the Campanian is taken at the base of Chron C33r, at 4.5 m. Crinoid distributions as observed by ASG.

within the upper part of *Stensioeina pommerana* Zone, slightly below the FO of true *Bolivinoidea culverensis* (for benthic foraminifera zonation see Walaszczyk et al., 2016).

The palynology of 21 samples from Bocieniec (0.03 to 5.5 m, average spacing of 0.27 m) were studied by Jarvis et al. (2022; Fig. 16). Two samples at 0.03 and 5.28 m had extremely poor recovery with assemblages composed mostly of spores and pollen; these are excluded from further discussion due to statistical unreliability. The floras are overwhelmingly dominated by organic walled dinoflagellate cysts (67–97% of the total) and species richness systematically declines up section from over 70 to 11 taxa in the uppermost sample. As at Seaford Head, a mixture of the C–H and S–P assemblages are observed, but in contrast, the latter dominates at Bocieniec (comprising mostly *Palaeohystrichophora infusorioides*) for most of the section (0.1–4.48 m). From 4.63–5.48 m, the dominant C–H assemblage is characterised by *Sentusidinium* spp., *Circulodinium distinctum* and *Surculosphaeridium longifurcatum*. This switch in assemblages coincides with an up section increase in the relative proportion of spores and pollen from 3.83 m, and fungal and insect remains from 4.08 m. All these observations are consistent with a significant shoaling through time.

Several stratigraphic markers occur through the section and are described below;

(oldest)

(1) The first occurrence of *Senoniasphaera protrusa*. As discussed by Pearce et al. (2020) *S. protrusa* is essentially restricted to the

Northern Hemisphere and has a probable First Appearance Datum in the middle Santonian. The lowest occurrence has been recorded at the Barrois Sponge Bed at White Ness (southern England, Prince et al., 2008), below the Horseshoe Bay CIE in the middle Santonian. At Bocieniec, the event occurs at 0.1 m, well below the Foreness CIE, and therefore, suggests an age no older than middle Santonian.

(2) The first occurrence of *Dimidium striatum*. According to Pearce et al. (2020) the FAD of *D. striatum* occurs at Whitecliff (southern England, Prince et al., 1999, below the Exceat Flint), between the Horseshoe Bay and Buckle CIE's. At Bocieniec, the event is questionable at 0.1 m and confident at 0.54 m, well below the Foreness CIE, suggesting an age no older than middle Santonian.

(3) The first occurrence of *Cordosphaeridium catherineae*. As discussed above (Section 3.1.), the lowest occurrence of *Cordosphaeridium catherineae* is recorded in the low *U. socialis* Zone, at the top of the Buckle CIE (Fig. 13) at Seaford Head, and immediately above the Buckle CIE at Poigny (Pearce et al., 2022). These observations extend the first occurrence of the species in the type material (Pearce, 2010) where it occurs in the Hawks Brow CIE. At Bocieniec, the first occurrence of *C. catherineae* is at 0.88 m, within the *U. socialis* Zone, providing additional evidence for a late Santonian age.

(4) The LO of *Odontochitina porifera*. A first occurrence of *O. porifera* occurs consistently between the Buckle and Hawks Brow CIEs (as at Seaford Head) in NW Europe (see below). At Bocieniec, the first occurrence is at 1.56 m and is supporting evidence for a late

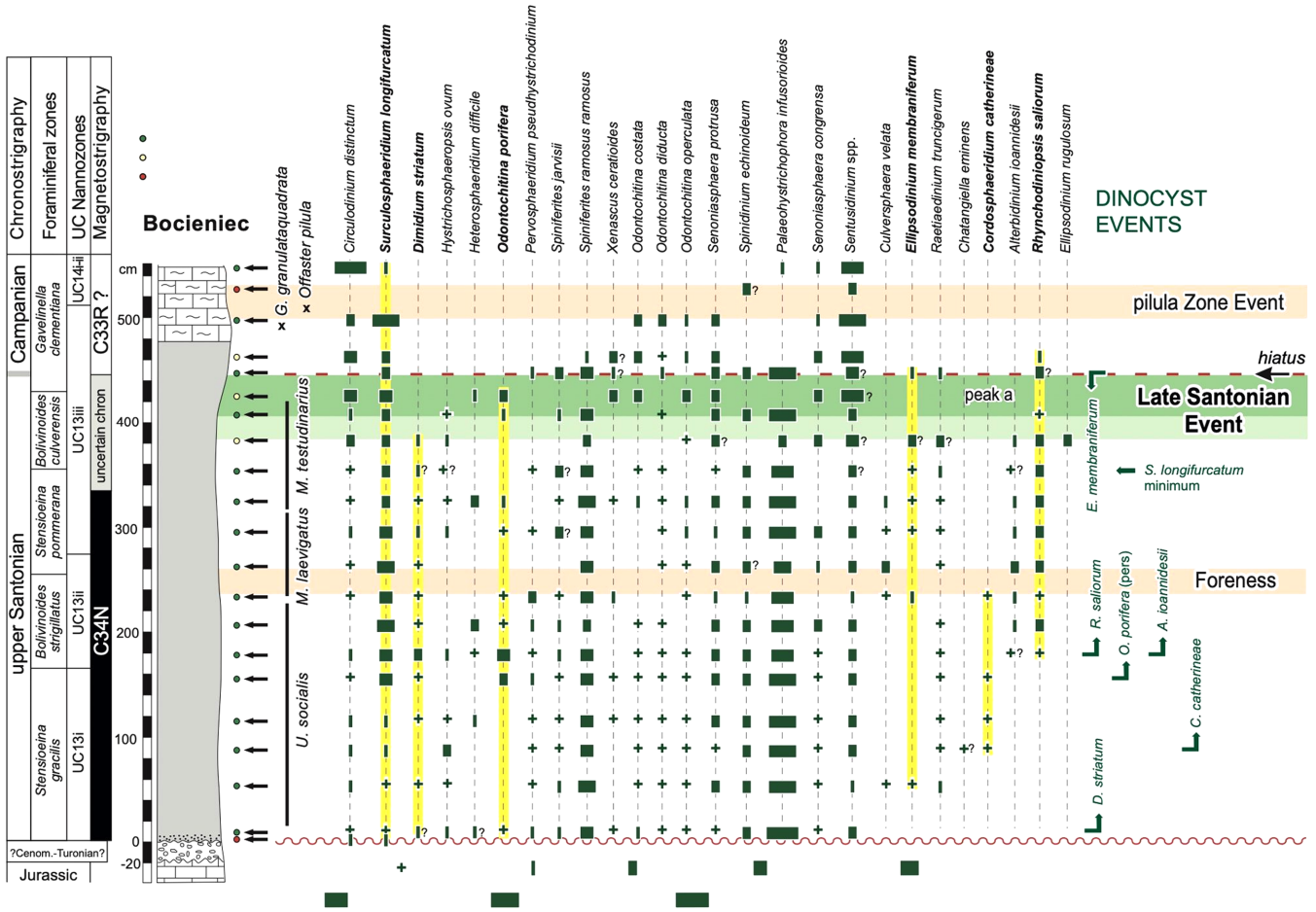


Figure 16. Ranges of selected organic walled dinoflagellate cysts and significant dinocyst events at Bocieniec, Poland, after Jarvis et al. 2022 fig.10. See Fig. 15 for additional stratigraphical details.

Santonian age.

(5) The first occurrence of *Rhynchodiniopsis saliorum*. The FAD of *R. saliorum* occurs within Hawks Brow CIE in the *U. socialis* Zone in southern England. At Bocieniec, the event occurs at 1.79 m within the range of *U. socialis*, and is therefore, a consistent feature of the upper Santonian.

(6) The poor recovery of *Surculosphaeridium longifurcatum* in the upper Santonian appears to be a consistent feature in many high-resolution studies from France and southern England (see Seaford Head, above). Similarly, at Bocieniec, where the species is unusually abundant, a clear minimum in relative numbers occurs at 3.54 m, below the Late Santonian CIE within the *M. testudinarius* Zone. This ‘event’ requires testing but may be stratigraphically significant.

(7) The first occurrence of rare *Heterosphaeridium difficile*. According to Pearce et al. (2020), the last occurrence of *H. difficile* lies in the upper Santonian (mid-*U. socialis* Zone), below the Hawks Brow CIE. The event has subsequently been raised to within the Late Santonian CIE at Poigny (Pearce et al., 2022), and is synchronous at Bocieniec where it was recorded at 4.26 m.

(8) The last occurrence of *Ellipsodinium* spp. This appears to closely approximate the Santonian–Campanian boundary in France, and eastern and southern England (see Seaford Head, above). At Bocieniec, the last occurrence of *E. membraniferum* is recorded at 4.48 m, 3 cm above

the proposed position of the Santonian–Campanian boundary. These results are encouraging, but the geographical extent of the event requires further testing.

(youngest)

Bocieniec is an important section which demonstrates the correspondence of crinoid zones, planktonic foraminifera, calcareous nanofossils, dinoflagellate cysts and magnetostratigraphy across the boundary. However, it is a very thin succession which contains at least one minor hiatus.

**Postalm, Austria**

The Santonian–Campanian boundary interval of the Postalm section within the Gosau Group of the Northern Calcareous Alps of Austria (Figs. 17 and 18) was proposed as a Campanian reference section for the northwestern Tethys (Wolfring et al., 2018, 2020). Including nearby complementary sections like Schattau and Sandkalkbank (Wagreich et al., 2010), the stratigraphy for this time interval in the Gosau Basin is based on palaeomagnetic and stable isotope data, planktonic foraminifera and calcareous nannoplankton biostratigraphy, and strontium isotope stratigraphy, together with published upper Santonian ammonite (e.g., *Placenticeras paraplanum*, *Boehmoceras arculus*, *Placenticeras maherndli*, *Texasia dentatocarinata*; Summesberger, 1985; Wagreich,

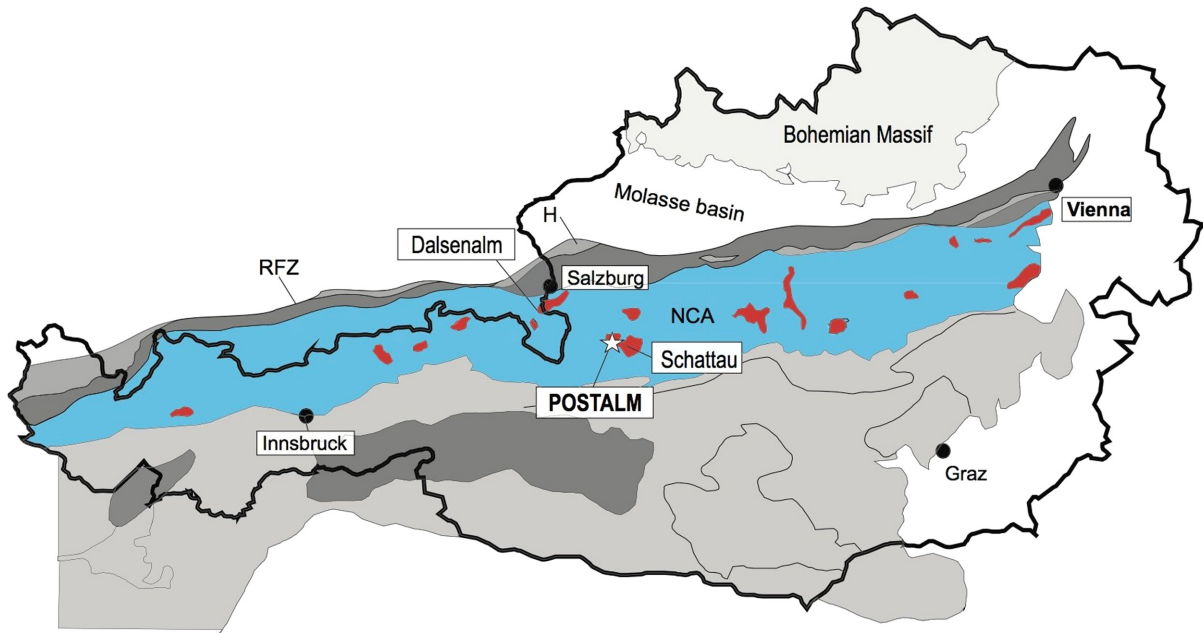


Figure 17. Map to show position of Postalm, Austria, after Wolfgring et al. (2018).

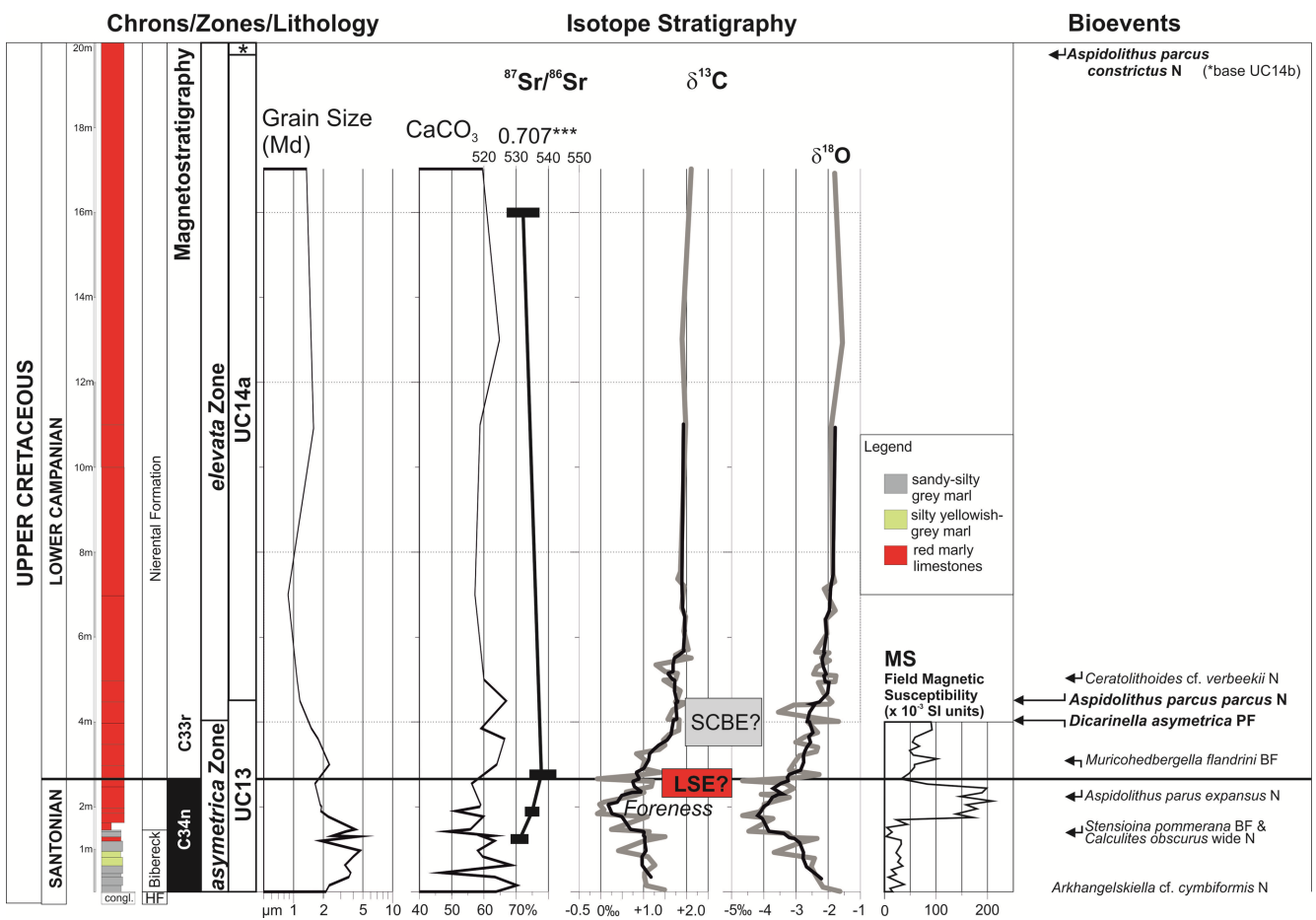


Figure 18. The succession at Postalm, Austria, after Wolfgring et al. 2018. Note the minor extension of the range of *D. asymetrica* into the basal part of Chron C33r. The oxygen and carbon isotope records appear to be compromised partly by diagenesis.

2010), crinoid (single horizon occurrence of *Marsupites laevigatus*; Wagreich et al., 2010) and inoceramid data (*Cordiceramus muelleri*

*muelleri*, *Sphenoceras* ex gr. *pachti/cardissoides*; Wagreich et al., 2010; Summesberger et al., 2017).

The 20 m thick interval of the Postalm section studied (Fig. 18) shows a deepening trend from upper Santonian conglomerates and sandstones, uppermost Santonian grey neritic marls to pelagic upper bathyal red marly limestones of mainly early Campanian age. Sediment accumulation rates of 19–23 mm/kyr were calculated for the fine-grained parts of the Postalm section (Wolfgring et al., 2018, 2020).

Palaeomagnetic data allow recognition of the top of the Long Cretaceous Normal Polarity–Chron 34n and the following reversal Chron C33r in the lower part of the red marly limestones (Fig. 18). This sharp reversal occurs within a 15 cm–thick interval with the first reversed sample at 2.81 m above the top of the conglomerate bed. A 1 m–thick interval of high magnetic susceptibility is present at the top of Chron C34n.

Biostratigraphic events have been correlated to the magnetostratigraphic primary marker. Eight nannofossil and four foraminifera events occur in the Gosau Group successions around the Postalm section (Wolfgring et al., 2018). The closest consistent event above the magnetostratigraphic boundary is the last occurrence of *D. asymetrica* which occurs at 4.08 m, c. 50–60 kyr after the reversal, and overlaps with the range of *Globotruncanita elevata*, defining the *D. asymetrica* Zone below and the *G. elevata* Zone above this bioevent. The first occurrence of large *Aspidolithus parvus parvus* (defined by a length above 9 µm), occurs at 4.47 m, c. 80 ka younger than the base of Chron C33r, marking the base of standard nannofossil zones CC18a (Sissingh, 1977) and UC14 (Burnett, 1998). Below this, the first occurrence of

the benthic foraminiferan *Stensioina pommerana*, (1.32 m) the last occurrence of the planktonic foraminiferan *Muricohedbergella flandrini* (3.45 m) and the first consistent occurrence of the nannofossil *Calculites obscurus* with widely separated sutures (1.30 m) may provide additional bioevents close to the boundary.

The base of the Campanian corresponds to a Sr isotope value of 0.707534 (±0.000005, mean of four analyses around the boundary interval). Although the carbon isotope signal seems to be somehow distorted due to diagenesis in this Alpine section, a constant rise can be seen in the upper Santonian, but no clearly defined Late Santonian Event can be recognized due to a plateau of high δ<sup>13</sup>C above the base of C33r. A negative oxygen isotope excursion just below the base of the Campanian and a positive magnetic susceptibility excursion may provide further means of correlation, corresponding to a short sea-level high in the late Santonian followed by a distinct lowstand around the Santonian–Campanian boundary. Cyclostratigraphy using spectral analyses (REDFIT) of the carbon isotope values and magnetic susceptibility from the lower 7.5 m part of the section shows significant frequencies in the precession band and a faint signal that may correspond to 120 kyr eccentricity (Wolfgring et al., 2018).

**Smoky Hill, Kansas, USA**

The Santonian–Campanian succession in the Western Interior Basin of

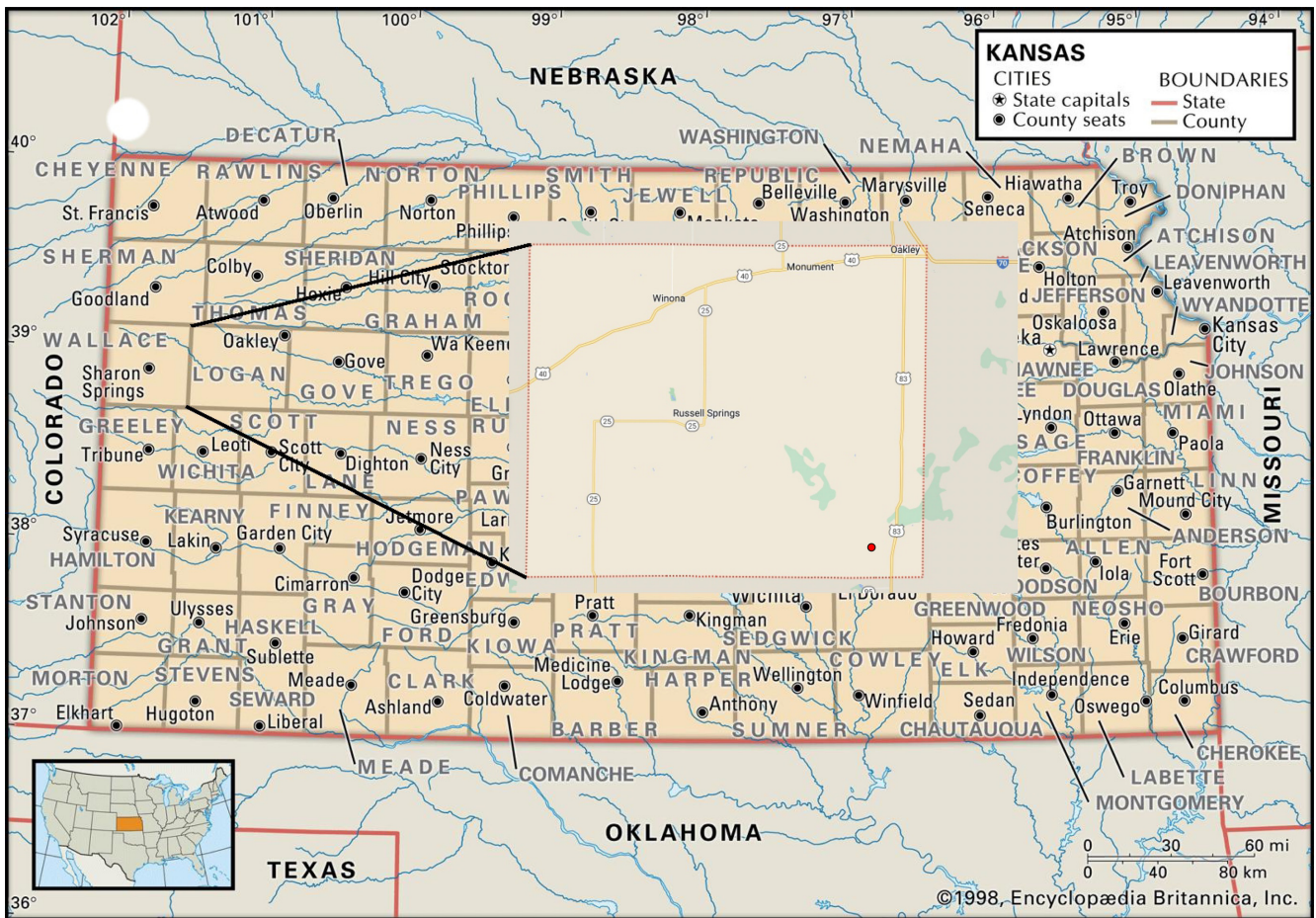


Figure 19. Map to show position of key counties in northern Kansas, and the location of the auxiliary boundary section 24 in Logan County (red dot).

the USA has been documented by Cobban (1952, 1969), Scott and Cobban (1964) and Cobban et al. (2006). The stratigraphy, sedimentology and palaeoecology of the Smoky Hill Chalk Member of the Niobrara Formation of Kansas was described by Hattin (1982), who provided detailed logs. We select locality 24 of Hattin (1982, p. 25) as an auxiliary reference section (Figs. 19 and 20), described by Hattin as “Bluff on east side of Ladder Creek in SW1/4, Sec. 30, T15S, R32W, Logan County, Kansas”. Kita et al. (2017) studied a composite section of the Smoky Hill Member of the Niobrara Formation across Logan, Gove and Trego counties in north Kansas, including locality 24, where the base of Chron 33r was recorded at the 174 m level (Fig. 20). The succession is developed in rhythmically bedded marly chalks. Magnetostratigraphic information (Paul Montgomery, unpublished data) showed that the boundary between Chrons 34n and 33r falls at 174 m in the profile (Fig. 20).

Kita et al. (2017) provided a detailed nannofossil record for the section, showing, importantly, that *Aspidolithus parvus parvus* first occurs at 166.3 m and *A. parvus constrictus* at 193.15 m. They inferred that the base of the *Scaphites leei* III ammonite zone corresponds with the reversal, from data derived from the Aristocrat Angus 12–8 core in northern Colorado (Joo and Sageman, 2014), but this assignment was made by inference; no ammonites have been recovered from the core. Hattin (1982) did not find ammonites diagnostic of the *Desmoscaphites bassleri* Zone nor the succeeding *S. leei* III Zone anywhere in Kansas.

There is some doubt about the precise relationships between ammonite zones and *Marsupites* occurrences in the Western Interior Basin. Cobban (1995) recorded *Marsupites* from only two localities in the United States Western Interior. The key record of *Marsupites* is that of Keefer and Troyer (1956, 1964, p. 88) in the upper part (the Sandy Member) of the Cody Shale west of Thermopolis in Fremont County, Wyoming,

associated with *Desmoscaphites bassleri*, *Scaphites leei* II of Cobban, 1969, and *Mancosiceras mancosense*. The *Marsupites* is described (Cobban, 1995, p. C50) as being a species characterised by “dominantly smooth calyx plates, like those of *M. milleri* Mantell”. *Marsupites milleri* is a synonym of *M. testudinarius* (Gale, in Gale et al., 2008, p. 143), and if Cobban’s comparison is correct, then the last occurrence of *Scaphites leei* II could be either within or above the range of *M. testudinarius*.

### Tepeyac Section, Coahuila, Mexico

The section is located ca. 5 km south of the small village Tepeyac, about 40 km north of Piedras Negras and 15 km SSW of Jiménez, Coahuila (28°54'45"N, 100°44'29"W). It is situated in the bed of the intermittent Arroyo Blanco, a tributary to the Rio Grande, and close to the mouth of the Arroyo Tecolote (Fig. 21). The locality probably corresponds to the original site of Böse (1928), Renz (1936) and Young (1963). It was recently redescribed by Ifrim and Stinnesbeck (2021) and Ifrim et al. (2021) and exposes 28.9 m of rhythmically bedded grey to light yellow-coloured layers of limestone, and intercalated units of marl. The beds dip at about 3° to the east and are well exposed over tens to hundreds of metres along the dry river bed, allowing for a detailed search for fossils over hundreds of square metres up to the level of bed 69 (Fig. 22).

The terrain around the outcrop of the Tepeyac section is in private property. The outcrop itself is in a river bed, which in Mexico is state property. The owner has always been open to giving access for the scientific study of the section; access can be arranged through the Museo del Desierto in Saltillo. This museum is the state museum of Natural History in Coahuila. The region has been safe for fieldwork since 2015.

The ammonite assemblage documented from Tepeyac consists of about 220 specimens and permits identification of a succession of zones originally identified in the Gulf Coast states of the USA and from the Atlantic seaboard. These include;

(oldest)

#### (1) The *Plesiotexanites shiloensis* Interval Zone

The base of this zone is defined by the first occurrence of the index species. At Tepeyac, this species first occurs in bed 12, but layers below this level are little exposed and the fossil record is scarce. We therefore suggest that the first occurrence of *Plesiotexanites shiloensis* may even extend below the base of the Tepeyac section. Species co-occurring with *Plesiotexanites shiloensis* are *Parapuzosia* (*P.*) *leptophylla*, *Pseudoschloenbachia* (*P.*) *mexicana*, *Texanites lonsdalei*; *Menuites stephensoni* has its FO in this zone.

#### (2) The *Menabites* (*Delawarella*) *tequesquitense* Interval Zone

The base of this zone is defined by the first occurrence of the index species in bed 25 at 10.7 m of the Tepeyac section. The zone is 5.3 m thick. Co-occurring species are *Amapondella amapondense*, *Plesiotexanites shiloensis*, *Pseudoschloenbachia* (*Pseudoschloenbachia*) *mexicana*, *Menuites stephensoni*, and *Texanites lonsdalei*. *Bevahites bevahensis*, *Menabites* (*Delawarella*) *mariscalense*, *Menabites* (*Delawarella*) *vamuxemi* and *Parapuzosia* (*Parapuzosia*) *seppenradensis* have their first occurrences within this zone. The index is an endemic species. In spite of this, *Menabites* (*Delawarella*) *tequesquitense* is chosen as the index here because it occurs in several beds, whereas *B. bevahensis*, the other potential zonal marker, is scarce and only found in bed 33, at 14.5 m of

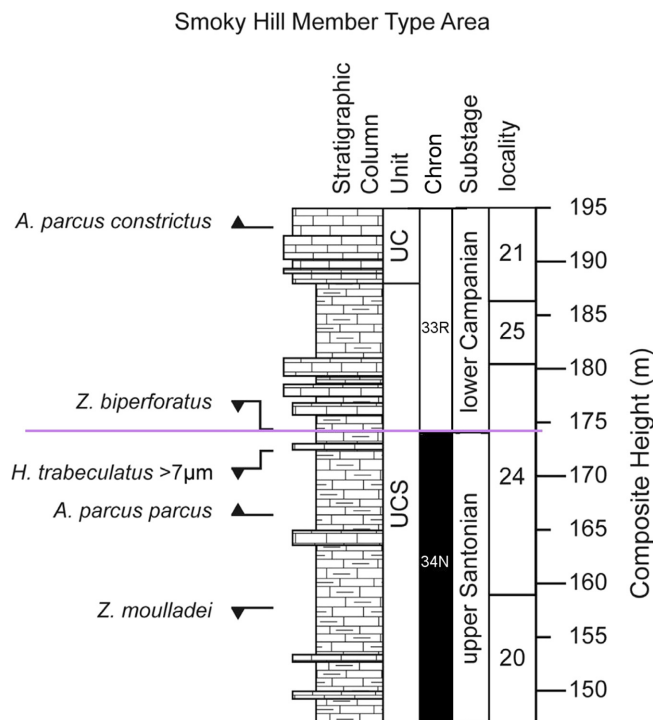


Figure 20. Composite succession in the Smoky Hill Chalk Member of the Niobrara Formation in northern Kansas, after Kita et al. (2017). Stratigraphical log and locality numbers after Hattin (1982).

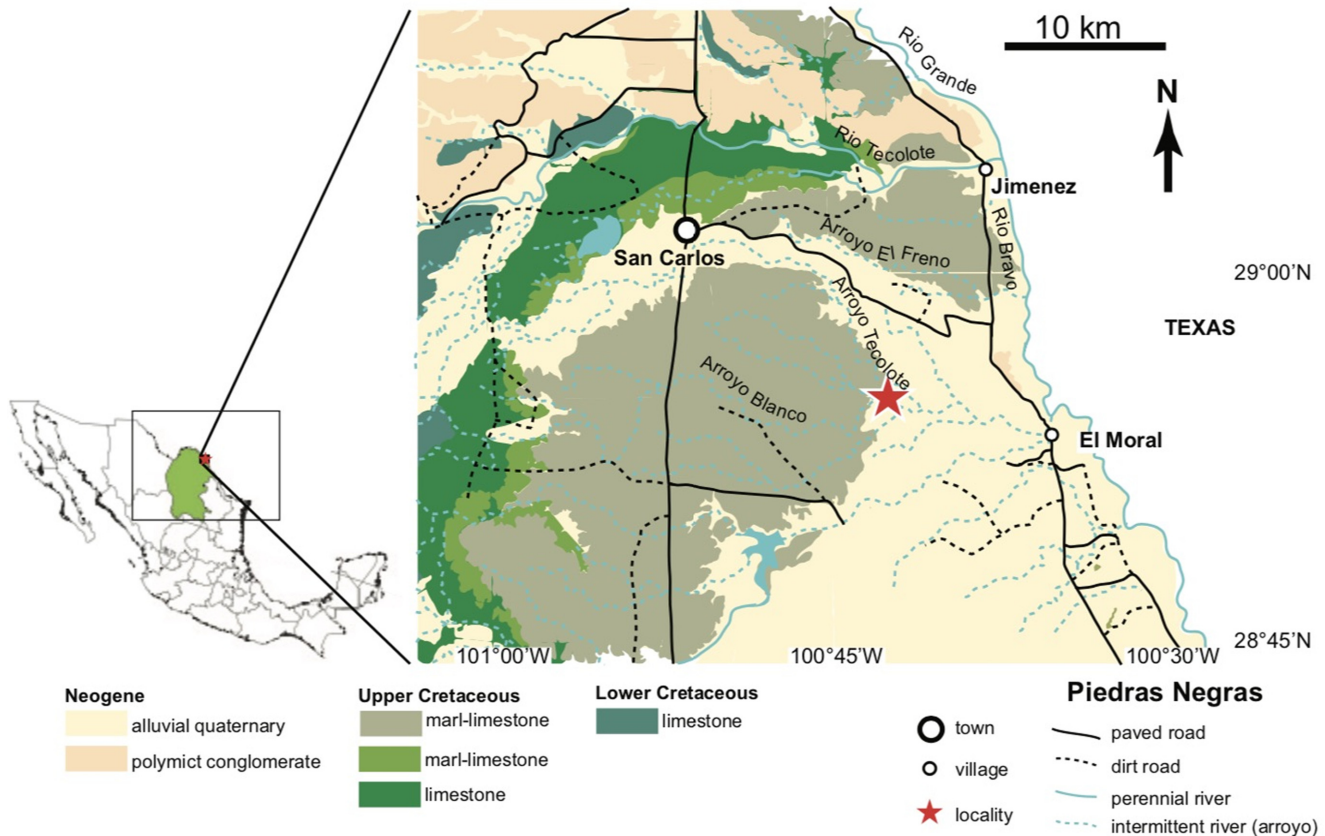


Figure 21. Map to show position of the Tepeyac section, Mexico, after Ifrim and Stinnesbeck (2021).

the section.

### (3) The *Menabites (Delawarella) delawarensis* Interval Zone

The base of this zone is defined by the first occurrence of the index species in bed 35 at 16.0 m of the section. The zone is 6.6 m thick. *Amapondella amapondense*, *Bevahites costatus coahuilaensis*, *Menabites (Delawarella) tequesquitense*, *Menuites stephensoni*, *Plesiotexantans shiloensis*, *Texanites lonsdalei* and the index species have their last occurrences in this zone, while *Parapuzosia (Parapuzosia) seppenradensis*, *Pseudoschloenbachia (Pseudoschloenbachia) mexicana*, *Menabites (Delawarella) mariscalense* and *Menabites (Delawarella) vanuxemi* range throughout the zone, and *Glyptoxoceras texanum*, *Baculites haresi*, *Menabites (Bererella) walnutensis*, *Menabites (Delawarella) danei*, *Pachydiscus (P.) duelmensis* and *Menuites sp.* have their first occurrences. This zone may correspond to the full range of the index fossil, but it is defined as an interval zone.

### (4) The *Baculites taylorensis* Interval Zone

The base of this zone is defined by the first occurrence of the index species in bed 64, at the 22.6 m level of the section. The zone is 5.7 m thick at Tepeyac and is truncated by a disconformity. Co-occurring taxa are *Glyptoxoceras texanum*, *Baculites haresi*, *Menabites (Bererella) walnutensis*, *Menabites (Delawarella) danei*, *Menabites (Delawarella) mariscalense*, *Menabites (Delawarella) uddeni*, *Menabites (Delawarella) vandaliense*, *Menabites (Delawarella) vanuxemi*, *Menuites sp.*, *Pachydiscus (P.) duelmensis*, *Parapuzosia (Parapuzosia) seppenradensis*, *Pseudoschloenbachia (Pseudoschloenbachia) mexicana* and *Scaphites hippocrepis III*.

(youngest)

In addition, 213 in situ specimens of inoceramids were recorded from the Tepeyac section, which include twelve species (Fig. 19). The inoceramids in the Tepeyac section provide the most abundant and detailed record of this group known across the Santonian–Campanian boundary and await detailed further study.

The stable carbon isotope curve from the Tepeyac section is suitable for long-distance correlation. The following carbon isotope events were identified:

- The Horseshoe Bay Event (Jarvis et al., 2006), a 0.5 per mil peak and turning point to decreasing values in the stable carbon isotope curve, in bed 6, lower *P. shiloensis* Zone.
- The Buckle Event, a 0.5 per mil symmetrical trough in bed 14, middle *P. shiloensis* Zone.
- The Hawks Brow Event, a 0.4 per mil positive peak which is present around bed 20, upper *P. shiloensis* Zone.
- The Foreness Event, a short 0.3 per mil trough in bed 26, lower *M. (D.) tequesquitense* Zone.
- The Late Santonian Event, a peak with amplitude of approximately 0.4 per mil in upper bed 30, middle *M. (D.) tequesquitense* Zone.
- The Pilula Event, a negative excursion in beds 42, 43.

The carbon-isotope succession demonstrates that the correlated GSSP marker falls between the Late Santonian Event and the Pilula Event and corresponds approximately with the base of the *Menabites (Delawarella) delawarensis* Zone. The Tepeyac section has not yielded stratigraphically important crinoids, and the original palaeomagnetic signal seems to have been destroyed by diagenesis (Moreno–Bedmar, pers. comm. 2020).

**Tepeyac section TPY**

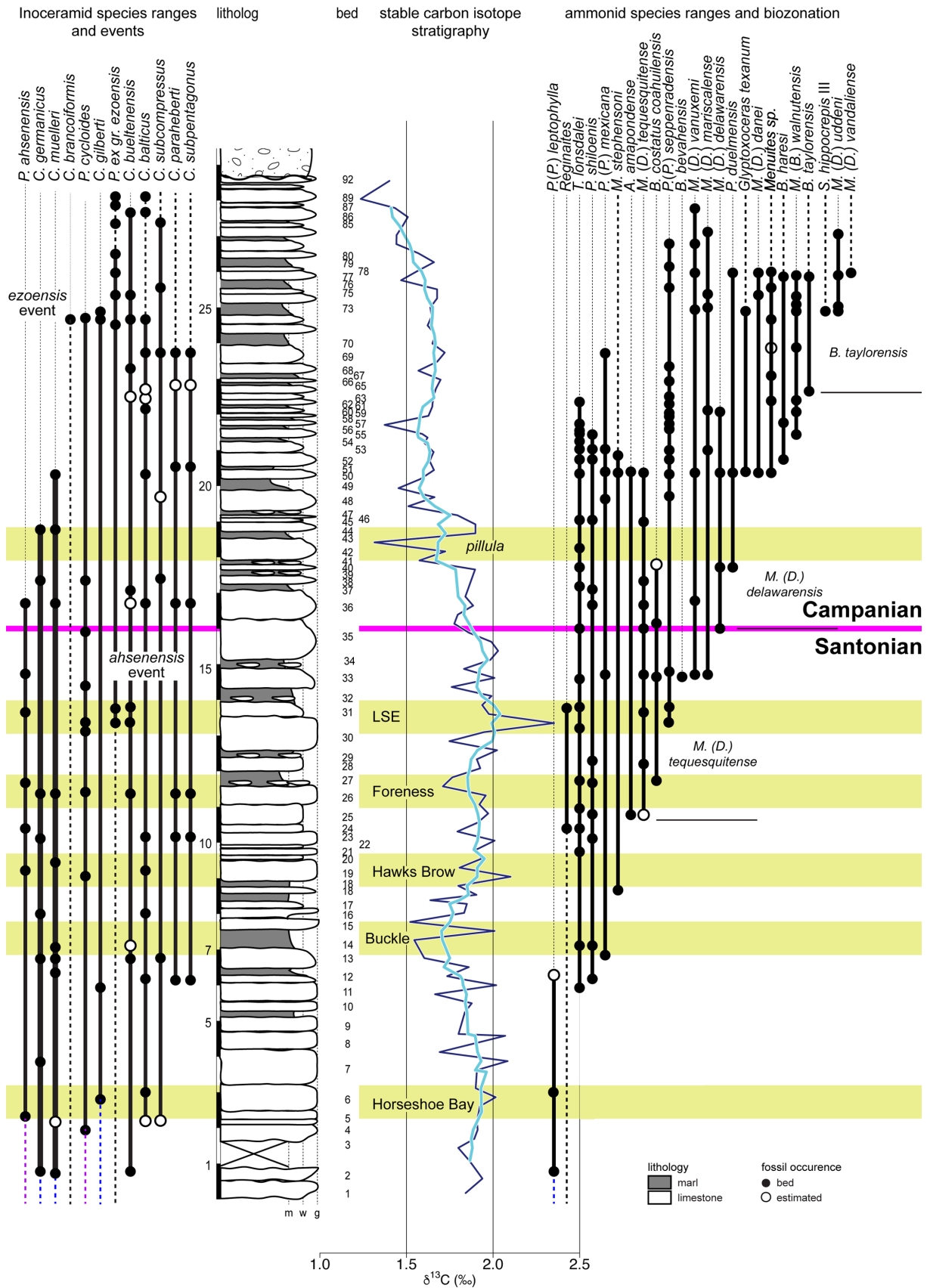


Figure 22. Distribution of inoceramid bivalves, ammonites and carbon–isotope stratigraphy, Tepeyac section in Mexico, after Ifrim and Stinnesbeck (2021). The base of the Campanian is identified from the carbon isotope record and coincides approximately with the base of the *M. (D.) delawarensis* Zone.

## Geochronology

Dates from altered volcanic ash beds (bentonites) in the Western Interior Basin of the USA provide the firmest evidence for the age of the base of the Campanian (Obradovitch, 1993). Sageman et al. (2014) used paired Ar/Ar and U/Pb ages derived from a series of Late Cretaceous bentonites in Montana. However, the key sampled horizon, in the *Desmoscaphtes bassleri* Zone of Montana (Sageman et al., 2014) could not be more precisely horizoned than to within the zone itself. The *D. bassleri* Zone includes the upper part of the range of *Uintacrimus socialis* and the total range of *Marsupites testudinarius* (Cobban, 1995 – see discussion above) and may extend to significantly higher levels. From the tuning of Thibault et al. (2016) the total duration of the *D. bassleri* Zone equivalent represents about 600 kyr. Sageman et al. (2014) provided a date of  $84.14 \pm 0.38$  Ma for the Santonian–Campanian boundary. The top of Chron C34n was identified at the junction of the *D. bassleri* Zone and overlying *Scaphites leei* III Zone (Kita et al. 2017), but the supporting evidence is not clear, as noted above. Wang et al. (2016), studying a lacustrine succession in China, dated a bentonite (using U–Pb CA–ID TIMS) some distance beneath the supposed Chrons C34n–C33r boundary to  $83.27 \pm 0.11$  Ma, and, using sedimentation rates in a cyclic succession, dated the base of the Campanian at  $82.90 \pm 0.18$  Ma. Gale et al. (2020b) placed the boundary at 83.65 Ma, based on a combination of data from radiometric dates, the oceanic magnetostratigraphic record, and orbital tuning. All that can be said with certainty at present is that, according to the present array of proposed radiometric dates and their uncertainties, the boundary must lie between 82.7 and 84.5 Ma.

## Discussion

### Criteria for Correlation of the Santonian–Campanian Boundary Interval

In this section we review recognised and proposed criteria for correlation with the boundary interval, drawing on records from the GSSP and auxiliary sections.

#### Magnetostratigraphy

Chron C33r marks the base of the C–sequence of magnetozones, a fundamental boundary which has been recognised globally in the magnetic anomaly record of oceanic crust, originally calibrated in the South Atlantic (Cande and Kent, 1992, 1995; Ogg, 2020). Correct identification of the C34n–C33r boundary in onshore sedimentary successions has been more limited, but the high-resolution magnetostratigraphy recorded at Gubbio (Alvarez et al., 1977; Maron and Muttoni, 2021) provides an unambiguous record which can be calibrated to the calcareous micro- and nannoplankton and carbon isotope record (Fig. 6). The C34n–C33r boundary has been identified in the auxiliary sections at Postalm in Austria (Wolfring et al., 2018), Bocieniec in Poland (Dubicka et al., 2017), in the Smoky Hill Chalk in northern Kansas (Kita et al., 2017) and in the Aksu–Dere section in the Crimea (Guzhikov, 2021a).

Locally there have been problems with the incorrect identification

of the C34n–C33r boundary, most notably in the English Chalk (Barchi, 1995; Montgomery et al., 1998), which led to a significant misinterpretation of the biostratigraphical age of the reversal as falling within the *U. socialis* Zone of the Santonian (Gale et al., 1995), corrected by Thibault et al. (2016). A parallel situation occurred in the northern part of the Western Interior Basin, where Lerbekmo (1989), Lerbekmo and Braman (2002), Leahy and Lerbekmo (1995) and Lillegraven (1991) identified the C34n–C33r boundary as falling within the “smooth *Baculites* Zone” of Cobban et al. (2006), 5 zones above the *D. bassleri* Zone, and well above the base of the Campanian as now defined. This was corrected by Kita et al. (2017), who reported the chron boundary close to the base of the *Scaphites leei* III ammonite zone within the Upper Chalky Shale (Fig. 20).

#### Carbon isotopes

Carbon isotopes provide a valuable tool in the correlation of successions developed in contrasting facies and faunal realms, sometimes widely separated geographically. The carbon isotope stratigraphy of the investigated interval was first described from the English Chalk by Jenkyns et al. (1994); subsequently, Jarvis et al. (2006) named successive events in the Santonian–Campanian boundary interval:

(oldest)

- Buckle Event; a broad negative excursion within the *U. socialis* Zone.
- Hawks Brow Event; a minor positive peak, at the top of the range of *Uintacrimus socialis*.
- Foreness Event; (sensu Thibault et al., 2016) a minor negative event, coincident with the range of *Marsupites laevigatus*.
- Late Santonian Event, LSE (formerly Santonian–Campanian Boundary Event, SCBE); a double positive peak (a, b), with values reaching 2.4 per mil; the top of the lower peak (a) is coincident with the top of the range of *Marsupites*, the top of the higher peak (b) with the last occurrence of *Uintacrimus anglicus*.

(youngest)

Joo and Sageman (2014) found the LSE (formerly SCBE) in the Western Interior Basin, and it was also reported from Japan (Takashima et al., 2019).

The carbon isotope stratigraphy identified in Santonian–Campanian chalks at Lägerdorf in northern Germany (Voigt et al., 2010) is essentially identical to that in southern England (Fig. 4; Thibault et al., 2016, fig. 3), and the Buckle and all events listed above were also identified at Bottaccione (Thibault et al., 2016, fig. 5), although their amplitude is generally dampened in this Tethyan location as compared to NW European localities. In the lower Campanian, Thibault et al. (2016) defined three additional successive events that correlate between the English and German Chalk and the Bottaccione section in Italy and have also been identified in the North Sea (Perdiou et al., 2016; Eldrett et al., 2020) in the central Paris Basin (Pearce et al., 2022) and in eastern Tethys locations such as Iran (Razmjooei et al., 2018, 2020). These three successive events are in ascending order:

(oldest)

The *pilula* Zone Event, a marked trough that correlates with the Old Nore Marl and the middle of the *Offaster pilula* Zone at Seaford Head and is situated just above the first occurrence of the coccolith *Aspidolithus parvus parvus* in the UK and at Bottaccione and within Chron

33r according to the Italian record.

The *senonensis* Zone Event, a minor shift in carbon isotopes characterised by a small negative excursion followed by a rapid, albeit also minor positive shift, correlates with the level of the Telscombe Marls at Seaford Head and the highest common occurrence of *O. pilula*, as well as the base of the *senonensis* Zone at Lägerdorf, North Germany, while being situated approximately in the middle of Chron C33r at Gubbio.

The *papillosa* Zone Event is a marked positive carbon isotope excursion showing a well-defined local maximum at Gubbio that coincides with the C33n – C33r reversal and correlates to a similar maximum at the base of the *papillosa* Zone at Lägerdorf.

(youngest)

### Planktonic foraminifera

The highest occurrence of the planktonic foraminiferan *Dicarinella asymetrica* marks the top of the *D. asymetrica* Total Range Zone, and the base of the *Globotruncanita elevata* Interval Zone (Miniati et al., 2020) and falls 19.5 cm above the base of Chron C33r at Bottaccione (Figs. 6 and 23). This result differs slightly from previous observations on extinction of species within the *Dicarinella* lineage at Bottaccione, where *D. asymetrica* and *D. concavata* are recorded as disappearing simultaneously 32 cm below the base of Chron C33r (Premoli Silva and Sliter, 1995; Petrizzo et al., 2011; Coccioni and Premoli Silva, 2015). An additional bioevent is the last occurrence of the *Sigalia* lineage that coincides with the last occurrence of *D. asymetrica* and is especially useful at low latitudes in the Gulf of Mexico and in the Tethyan Realm (e.g., Nederbragt, 1991). At Postalm, Austria, the highest occurrence of *D. asymetrica* is at 1.24 m above the base of Chron C33r (Fig. 21; Wolfgring et al., 2018). In Turkey (Wolfgring et al., 2017) the highest *D. asymetrica* occur 2 m beneath the base of Chron 33r. On the Exmouth Plateau, at ODP Site 762C (Petrizzo, 2000) the highest *D. asymetrica* slightly postdate the reversal (Fig. 23; Miniati et al., 2020). Bocieniec, in Poland, is the only locality where both *Marsupites* and *D. asymetrica* are present, and the latter taxon disappears 20 cm above the highest *M. testudinarius* specimen (Fig. 15). In the Crimea sections, the highest record of *D. asymetrica* is approximately 5 m beneath the base of Chron C33r (Guzhikov et al., 2021a, b).

The higher part of the range of *D. concavata*, the ancestral species to *D. asymetrica* (e.g., Petrizzo et al., 2017) is characterized by a decrease in abundance followed by its extinction at 220.20 m in the Bottaccione section. Its extinction level correlates with observations from the Betic Cordillera in southeast Spain (Linares Rodriguez, 1977), in the eastern Indian Ocean (Exmouth Plateau, Petrizzo, 2000) and in the Mangyshlak Peninsula (Kopaevich et al., 2007) and is consistent with the planktonic foraminiferal distributions and biozonation by Postuma (1971). In contrast, *D. concavata* is reported to disappear at the same level as *D. asymetrica* in the US Western Interior (north Texas, Gale et al., 2008) and in the Tethyan record (Tunisia, Robaszynski et al., 2000; Southern Tibet, Wendler et al., 2009). *Globotruncana neotricarinata* appears to provide a reliable bioevent for wide geographic correlation as its first appearance within the *D. asymetrica* Zone in the Bottaccione section at 213.30 m falls at approximately the same stratigraphic level observed in the eastern Indian Ocean (Exmouth Plateau, Petrizzo et al., 2011). Remarkable also is the first occurrence of *Globotruncanita atlantica*, a common species in tropical and subtropical

settings, that falls slightly above the extinction level of *D. asymetrica* in agreement with the record from Tunisia (Kalaat Senan, Robaszynski et al., 2000).

### Benthic foraminifera

The Santonian–Campanian transition is also marked by some stratigraphically important lineages of the benthic foraminiferan genera *Stensioeina*, *Bolivinooides* and *Gavelinella*. While *Stensioeina* and *Gavelinella* are limited to the European epicontinental Upper Cretaceous, from the Atlantic to Kazakhstan (Dubicka and Peryt, 2014 and literature cited therein), *Bolivinooides* is characterized by its worldwide distribution (Dubicka and Peryt, 2016 and literature cited therein) probably owing to the presence of planktonic larvae or propagules (Alve, 1999) or a tythropelagic mode of life (Dubicka and Wierzbowski, 2019).

In the chalk facies of northern Europe, *Bolivinooides strigillatus*, which is the oldest species of the genus, arose in the upper part of the upper Santonian and evolved into *B. culverensis*, a transitional species to *B. decoratus*, within the basal Campanian (i.e., slightly above the last occurrence of the crinoid *Marsupites testudinarius*–Barr, 1966; Hart et al., 1989; Walaszczyk et al., 2016; Dubicka and Peryt, 2016; Dubicka et al., 2017; Fig. 13). It is important to note that in some important stratigraphical papers on the German Cretaceous succession (e.g., Hiltermann, 1952; Koch, 1977; Schönfeld, 1990) *B. culverensis* is not identified within the *B. strigillatus*–*B. decoratus* lineage. This results in significant discrepancies in the stratigraphical position of the bolivinooidid succession within western Europe, and in Germany the position of the last occurrence of *B. strigillatus* is interpreted as occurring higher, in the middle lower Campanian (*senonensis* Zone).

The second benthic foraminiferal event with high potential for recognition of the proximity of the base of the Campanian is a transition within the *Stensioeina perfecta* – *S. pommerana* lineage. The lowest occurrence of true *S. pommerana* occurs slightly below the top of the Santonian in the chalk facies of northern Europe, within the range of *Marsupites testudinarius* and *Bolivinooides strigillatus* (Fig. 15) (Walaszczyk et al., 2016; Dubicka et al., 2017; Schönfeld, 1990). In the Tethyan Postalm section, *S. pommerana* is rather rare, but first occurs about 1.5 m below the base of C33r (Wolfgring et al., 2018).

In the succession of *Gavelinella* species, the last occurrence of the crinoid *Marsupites testudinarius* corresponds with the first occurrence of *Gavelinella costulata* of the *G. amonoides* lineage in western Ukraine (see Dubicka and Peryt, 2014). However, it must be noted that *Gavelinella costulata* evolved from *G. lorneiana* within the upper Santonian and its first occurrence is recorded earlier in the upper Santonian at Bocieniec, Poland, within the range of the crinoid *U. socialis* (Fig. 15). The consistent occurrence of *Gavelinella* ex. gr. *clementiana*, which is the base of the *G. clementiana* Zone (*sensu* Walaszczyk et al., 2016), was considered to be recorded in the lower part of the lower Campanian (upper part of the *Sphenoceramus patootensiformis* inoceramid Zone) in central and eastern Europe (Schönfeld, 1990; Dubicka et al., 2014; Walaszczyk et al., 2016; Dubicka et al., 2017) but this bioevent is actually situated immediately below (<20 cm) the projection of the boundary level at Bocieniec (Fig. 15). Moreover, the event occurs significantly earlier in the Anglo–Paris Basin (Edwards, 1981; Hampton et al., 2007). This is probably because the *G. clementiana* group was especially sensitive to specific ecological requirements and its

migration into central Europe Poland and Ukraine (Walaszczyk et al., 2016) probably represents a delayed response to substantial palaeoenvironmental changes.

According to the projection of the GSSP level at Bocieniec and recorded bioevents in that section (Fig. 15), the successive benthic foraminiferan events are:

(oldest)

- The first occurrence of *Gavelinella costulata* (upper Santonian, within the range of *Uintacrinus socialis*, though a delayed first occurrence has been noted above the top of the range of *Marsupites testudinarius* in Ukraine)
- The first occurrence of *Bolivinooides strigillatus* (upper Santonian, within the range of *U. socialis*)
- The first occurrence of true *S. pommerana* (upper Santonian, within the range of the *Marsupites laevigatus*)
- The first occurrence of *Bolivinooides culverensis* (upper Santonian, within the range of *M. testudinarius*)
- The first consistent occurrence of *Gavelinella* ex. gr. *clementiana* (base of the *G. clementiana* Zone and base of the Campanian, above the range of the crinoid *M. testudinarius*)

(youngest)

### Calcareous nannofossils

Recent work on the *Aspidolithus parvus* lineage at Gubbio (Miniati et al., 2020) has established a detailed succession of subspecies which provide an evolutionary succession through the late Santonian and early Campanian, and with respect to the position of the base of Chron C33r (221.53 m):

(oldest)

- The first occurrence of *A. parvus expansus* ( $\geq 10 \mu\text{m}$ , 219.5 m)
- The first occurrence of *A. parvus expansus* (small,  $< 10 \mu\text{m}$ , 220.2 m)
- The first occurrence of *A. parvus parvus* ( $\geq 10 \mu\text{m}$ , 220.5 m)
- The first occurrence of *A. parvus parvus* (small,  $< 10 \mu\text{m}$ , 221.3 m)
- The first occurrence of common *A. parvus parvus* (224.6 m)
- The first occurrence of *A. parvus constrictus* (229 m)

(youngest)

In addition, the first occurrence of *A. cymbiformis* is recorded at 219.1 m

At Gubbio, the base of Chron 33r thus falls between the first occurrence and the first common occurrence of *A. parvus parvus* (Miniati et al., 2020). However, it is not always possible to separate the FO and the FCO of *A. parvus parvus*, which can leave some doubt as to the significance of the lowest occurrence of the species. Thus, in the Western Interior Basin (Kita et al., 2017; Fig. 20), the FO of *A. parvus parvus* falls within Chron 34n, whereas at Postalm in Austria (Wolfgring et al., 2018; Fig. 18) the FO is 1.66 m above the base of Chron 33r while it is also recorded above that level (though with uncertainty due to a hiatus) at Bocieniec, Poland (Fig. 15). In some localities (Austria, Turkey, Western Interior Basin), the first occurrence of *A. parvus constrictus* provides a useful and consistent marker at a slightly higher level (Miniati et al., 2020; Fig. 20).

In addition to events within the *A. parvus* lineage, other nannofossil bioevents, that have not been recorded at Gubbio, appear to correlate across various ocean basins such as the first occurrence of *Zeughrabdotus biperforatus* recorded in near coincidence with the reversal in the Western Interior basin (Kita et al., 2017), close to the base of Chron

C33r at Bocieniec in Poland (Dubicka et al., 2017), and above the FO of *A. parvus parvus* at Seaford Head, England (Hampton et al., 2007). Although the FO of *Reinhardtites levis* must always be considered with caution due to its gradual evolutionary change from *R. anthophorus* and potential confusion with the latter in poorly preserved material that features overgrown coccoliths (Razmjooei et al., 2018, 2020), this bioevent has been recorded well above the boundary reversal in the Western Interior Basin (6.3 m above base Chron 33r, Kita et al., 2017), in between the FO of *A. parvus parvus* and LO of *Z. biperforatus* at Seaford Head, England, UK (Hampton et al., 2007), and in coincidence with peak a of the LSE at Bocieniec in Poland (Dubicka et al., 2017). The first occurrence of *A. cymbiformis* which defines nannofossil zone UC13 of Burnett (1998) is systematically found well below the boundary level (Hampton et al., 2007; Dubicka et al., 2017; Wolfgring et al., 2018; Miniati et al., 2020).

### Palynology

Valuable syntheses of dinoflagellate cysts ranges through the Cretaceous have been produced by Williams and Bujak (1985), Stover et al. (1996), Costa and Davey (1999) and Williams et al. (2004) and are cited widely in the literature. High resolution studies from NW Europe (e.g., Slimani, 2001; Surlyk et al., 2013; Pearce et al., 2020, 2022; Jarvis et al., 2022) have extended the range of some of these species previously considered significant for the Santonian–Campanian boundary interval. Of the events still considered to occur high in the Santonian (last occurrence of *Scriniodinium campanula*, first occurrence of *Odontochitina porifera*, first occurrence of *Spongodinium delitiense*) only the first occurrence of *O. porifera* was recorded at Bocieniec and Seaford Head (between the Buckle and Hawks Brow CIEs, typical in NW Europe).

Of the events still considered to be markers for the former Santonian – Campanian boundary (now latest Santonian following the now confirmed definition of the boundary): the last occurrence of *Canningia senonica* and the last occurrence of rare *Heterosphaeridium difficile*, only the latter event was recorded at Bocieniec, within the Late Santonian CIE (Fig. 16).

The last occurrence of *Ellipsodinium* spp. may be a good palynological marker for the Santonian–Campanian boundary. Williams and Bujak (1985) and Hardenbol et al. (1998) placed the HO of *Ellipsodinium (rugulosum)* in the mid–Santonian, while Stover et al. (1996) and Costa and Davey (1999) recorded it low in the Santonian. Williams et al. (2004) placed the last occurrence of *Ellipsodinium (rugulosum)* in the lowermost Campanian. Results from France (Pearce et al., 2022), southern and eastern England (Prince et al., 1999, 2008; Pearce et al., 2020) and Bocieniec (Jarvis et al., 2022) show that the last occurrence of *Ellipsodinium (rugulosum or membraniferum)* lies within the Late Santonian CIE, or in the lowermost Campanian.

Finally, Pearce et al. (2020) provided a detailed review of palynological events calibrated by microfossil and  $\delta^{13}\text{C}$  data through the Cenomanian to lower Campanian, with a focus on NW Europe, discussing the spatial and temporal distribution of marker taxa. Many of the species discussed currently were described relatively recently and their distribution requires testing. Incorporating all the available data, the following calibrated sequence of events is considered significant for the Santonian–Campanian boundary.

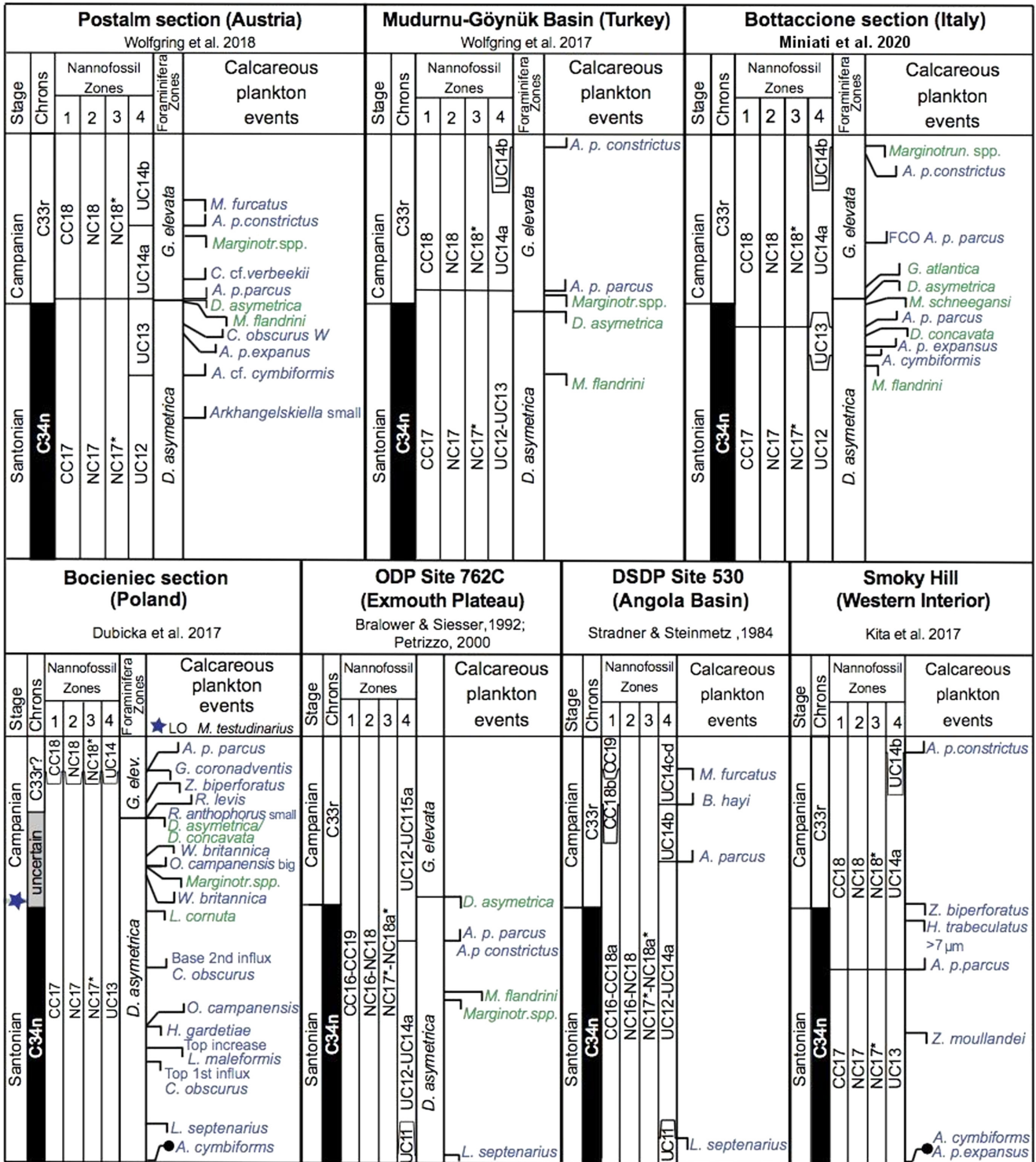


Figure 23. Comparative magnetostratigraphy and calcareous microplankton distribution of localities containing the Santonian–Campanian boundary interval. After Miniati et al. (2020).

(oldest)

- First occurrence of *Dimidium striatum* (between the Horseshoe Bay and Buckle CIEs)
- First occurrence of *Cordosphaeridium catherineae* (top of the Buckle CIE)

[middle–upper Santonian boundary]

- First occurrence of *Odontochitina porifera* (between the Buckle

and Hawks Brow CIEs)

- First occurrence of *Rhynchodiniopsis saliorum* (within the Hawks Brow CIE, occurs high at Seaford Head)
- Last occurrence of rare *Heterosphaeridium difficile* (within the mid–Late Santonian CIE)
- Last common occurrence of *Ellipsodinium* spp. and minimum of *Surculosphaeridium longifurcatum* (below the Late Santonian

Event 'peak a')

[*U. socialis*–*M. testudinarius* zone boundary]

- Last occurrence of *Ellipsodinium* spp. (immediately above the C34n–C33r boundary)

[Santonian–Campanian boundary]

(youngest)

### Crinoids

The stemless benthic (Milsom et al., 1994) crinoid genera *Uintacrinus*

and *Marsupites* are restricted to the late Santonian and occur worldwide but are largely restricted to shallower water chalk facies (Rasmussen, 1961; Gale et al., 2008; Guzhikov et al., 2021b). One species, *M. testudinarius*, is found in sandstones at the level of its acme occurrence, in south-east India, Madagascar, British Columbia, Canada and Mississippi, USA. There are four stratigraphically successive species of the genera (Gale et al., 2008), illustrated in Fig. 24:

(oldest)

- *Uintacrinus socialis* (Utah, Kansas, Texas, USA, UK, France,

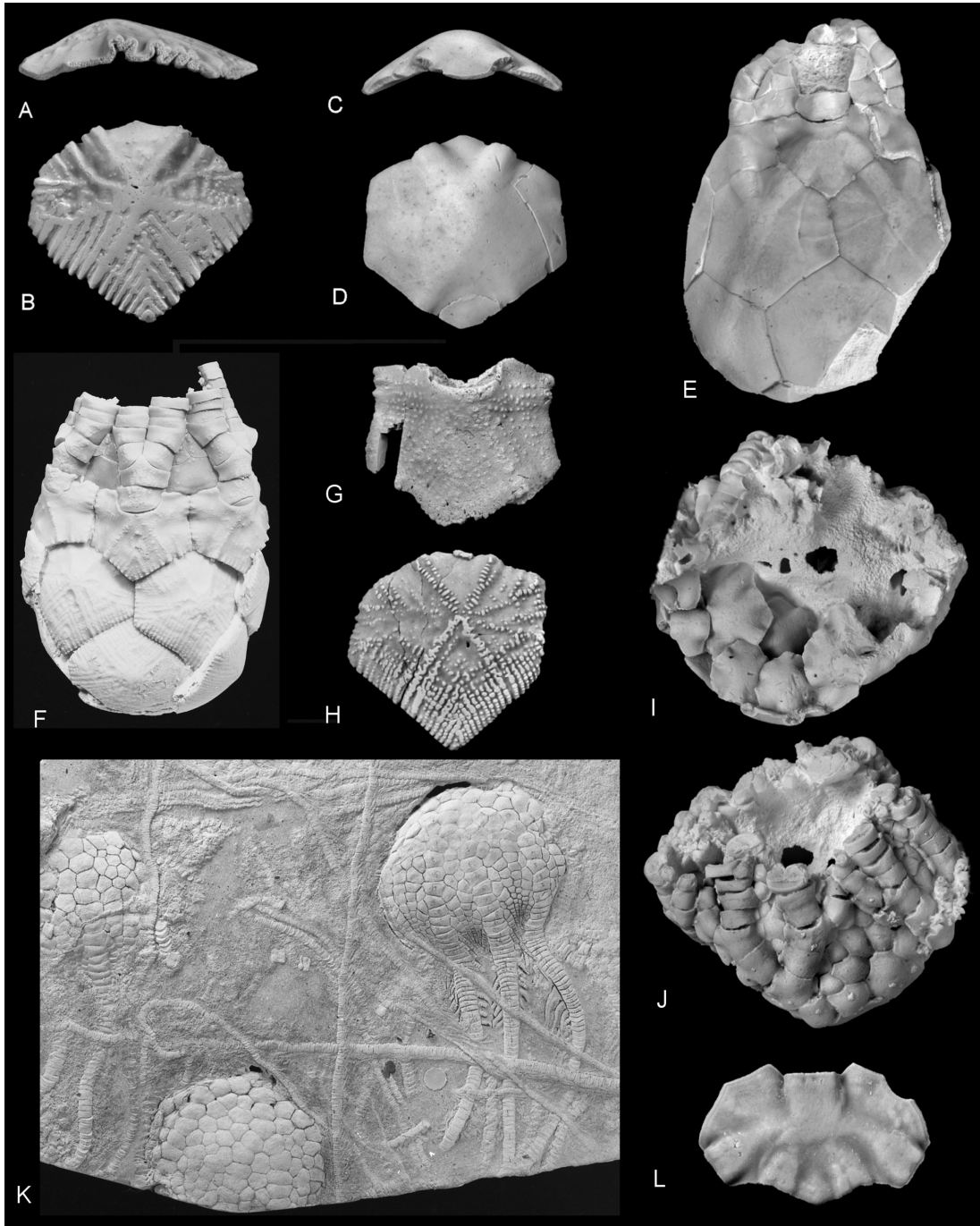


Figure 24. The crinoids *Uintacrinus* and *Marsupites* from the late Santonian. A, B, F–G, *Marsupites testudinarius*. C–E, *Marsupites laevigatus*. K, *Uintacrinus socialis*. J, L, *Uintacrinus anglicus* Rasmussen, 1961. A–D, Margate Chalk, Foreness Point, Thanet, Kent, UK. E, Newhaven Chalk, Sussex, UK, locality unknown. G, H, L, Waxahachie dam spillway, Ellis County, Texas, USA. K, Smoky Hill Chalk, Kansas, USA. I, J, level of Friars Bay Marls 2–3, Newhaven Chalk, Brighton, Sussex, UK.

- Germany, Poland, Kazakhstan, Western Australia)
- *Marsupites laevigatus* (Texas, USA, UK, France, Germany, Poland, Kazakhstan, Western Australia, Crimea)
  - *Marsupites testudinarius* (Texas, Mississippi, Colorado, Montana, USA, Vancouver, Island Canada, UK, France, Germany, Poland, Algeria, Tunisia, Madagascar, Kazakhstan, India, Western Australia, Crimea)
  - *Uintacrinus anglicus* (UK, Kazakhstan, Texas, USA, Western Australia)
- (youngest)

Complete successions with all four species are known from the United Kingdom, Mangyschlak, Kazakhstan, Texas, USA and Toolonga, Western Australia (Gale et al., 1995, 2008). *Uintacrinus socialis* and *M. testudinarius* appear to be the most widespread of the species with the longest ranges; those of the other two taxa are shorter, and they have probably been overlooked in some regions. An estimation of the duration of individual species ranges is made using the orbitally tuned succession at Seaford Head (Thibault et al., 2016). The correlative value of *Uintacrinus* and *Marsupites* is enhanced through their co-occurrence with provincially restricted ammonite faunas (Fig. 2) in the Pacific Realm (Haggart and Graham, 2017), in the Western Interior Basin (Cobban, 1995), Texas (Gale et al., 2008, 2021), Europe (Kaplan and Kennedy, 2005) and Madagascar (Walaczkyk et al., 2014). Additionally, the precise relationships of the crinoids to carbon isotope events is known from Seaford Head (Figs. 11–13), and demonstrates that the Buckle Event falls within the lower part of the range of *U. socialis*, the Foreness Event is in the zone of *M. laevigatus*, the lower LSE carbon isotope peak is coincident with the higher part of the range of *M. testudinarius* and the higher LSE peak approximates

to the range of *U. anglicus*. This information permits correlation between the crinoid zones and the Tethyan deep water succession in the Bottaccione section (Fig. 25). However, the crinoids and distinctive associated carbon isotope excursions all fall *beneath* the GSSP primary marker, the C34n–C33r reversal (Guzhikov et al., 2021a, b) and thus do not help correlation of the boundary itself, although they give some indication of its proximity.

In terms of pelagic microcrinoids, the base of the Campanian as defined herein falls within the middle part of zone CaR1 (Gale, 2018) as defined at Seaford Head (Fig. 12). This interval extends from the LO of *Uintacrinus anglicus* to the FO of *Stellacrinus hughesae* forma *cristatus* Gale, 2018.

### Ammonites

The provincialism of many Santonian and lower Campanian ammonites, and their scarcity in critical localities has been a barrier to global correlation in this interval using the group (Fig. 2 – see also Kennedy, 1984). In North America, there are three distinct faunas, respectively in the Pacific Realm, the Western Interior Seaway and in the Gulf Coast. On Vancouver Island, Canada, in the Pacific province, Haggart and Graham (2017) found *M. testudinarius* immediately beneath the (local) *Pseudoschloenbachia umbulazi* ammonite zone; the base of C33r, and hence of the Campanian, lies at a higher level (Fig. 2; Ward et al., 2012, fig. 13). In the Western Interior Basin, *M. testudinarius* occurs within the *Desmoscaphites bassleri* Zone in association with *Scaphites leei* II (Cobban, 1995; see above), and the base of C33r must fall around or above the contact with the overlying *Scaphites leei* III Zone, although there is some doubt as to its exact position

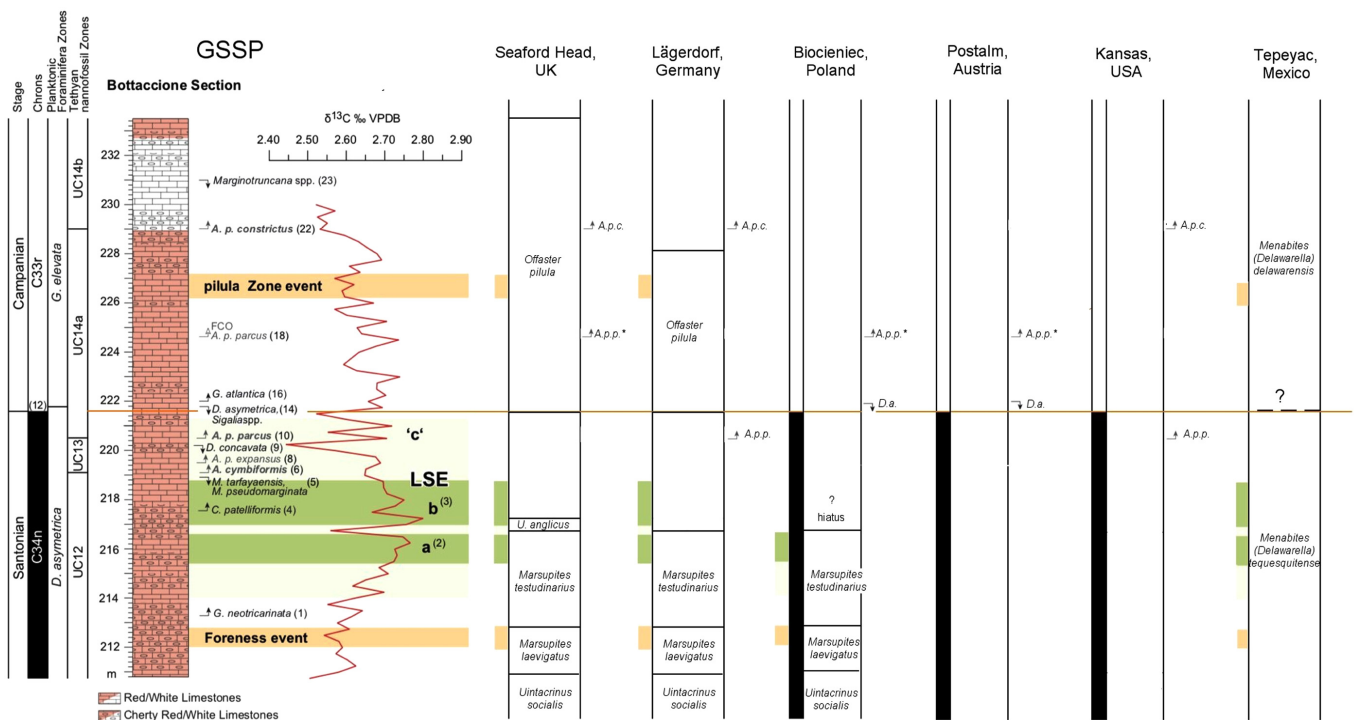


**Figure 25. Summary correlation of the Global boundary Stratotype Section and Point for the base of the Campanian Stage and auxiliary sections, showing how biostratigraphy, magnetostratigraphy and carbon isotope stratigraphy can be used to correlate from the GSSP to auxiliary sections. Localities shown in Fig. 1. Abbreviations: LSE = Late Santonian Event; FCO = first common occurrence; A. p.c. = *Aspidolithus parvus constrictus*; A. p.p. = *Aspidolithus parvus parvus*; D. a. = *Dicarinella asymetrica*.**

(Fig. 2). In Texas, *U. socialis*, *M. testudinarius* and *Uintacrinus anglicus* all occur in the the *Submortonicerias tesquesquitense* Zone (Gale et al., 2008, 2020a). In Wesphalia, Germany, the base of the *Placenticerias bidorsatum* Zone is approximately equivalent to the top of the range of *M. testudinarius* (Fig. 2; Kaplan et al., 2005), and the base of the Campanian must fall within this zone. In Madagascar, *M. testudinarius* occurs in the upper part of the *Pseudoschloenbachia umbulazi* Zone (Walaszczyk et al., 2014), and the base of the Campanian must therefore fall within the overlying *P. blandfordiana* Zone. The difference in the comparative ranges of *P. umbulazi* between Vancouver Island and Madagascar requires investigation.

### *Inoceramid bivalves*

In the Santonian–Campanian boundary interval, inoceramid bivalves are amongst the best–represented marine macrofossil groups world–wide. The structure of the record is, however, only moderately known, both in terms of the stratigraphic distribution of inoceramids and of their biogeographic significance. The Santonian–Campanian boundary interval is the time of highest taxonomic diversity in the Late Cretaceous history of the group (e.g., Tröger, 1976; Voigt, 1995, 1996); however, it is not clear whether this peak represents a record of their genuinely high standing diversity or the cumulative effect of their high evolutionary turnover rates. Undoubtedly, biogeographic differentiation played a role; inoceramids of the Santonian–Campanian boundary interval show a well–documented biogeographical variability, with four biogeographic biochores (biogeographic units after Kauffman, 1973) recognised: the Tethyan–Euramerican marginal area; the northern Euramerican biogeographic region; the East–African Province subprovince; and the North Pacific Province.

A boundary zone exists between the Euramerican Region and the Tethyan Realm (e.g., North American Gulf Coast, southern Europe, Caucasus, Kopet–Dagh). The details of the inoceramid succession in this biochore were studied in detail in the Waxahachie section, SE Texas, USA (Gale et al., 2008) (Fig. 3). There, the Santonian–Campanian boundary as defined by the LO of *Marsupites testudinarius* is not reflected by a single, corresponding inoceramid event with a world–wide expression. However, the inoceramid succession has a well–defined pattern, composed of three successive faunas, which seems to be recorded on a much wider geographic scale, thus potentially having an evolutionary significance, and consequently chronostratigraphic value. In stratigraphic order these three successive faunas are those of *Cordiceramus* ex gr. *muelleri*, *Platyceramus ahsenensis* and *Platyceramus* cf. *ezoensis* (Fig. 3).

The *Cordiceramus muelleri* fauna is dominated by *Cordiceramus germanicus*. It is very probable that the disappearance level or at least the distinct drop in the abundance of this species approximates to the first appearance of *Marsupites testudinarius* and represents its evolutionary last occurrence. Besides a single specimen of *C. germanicus* regarded as of lower Campanian age (Sornay, 1982, pl. 1, fig. 2) from the smectitic facies of the Vaals Formation in northeast Belgium, there are no other convincing records of this species from the lower Campanian (e.g., Seitz, 1961; Tröger, 1989; Lopez, 1992; Tröger and Summesberger, 1994).

The *Platyceramus ahsenensis* fauna is dominated by the eponymous species, with some morphotypes transitional to *Pl. cycloides*. *Platycer-*

*ramus ahsenensis* is a long–ranging species; it first appears in the early Santonian, ranging through the entire stage and possibly into the early Campanian.

The *Platyceramus* cf. *ezoensis* fauna, stratigraphically the highest, spans the Santonian–Campanian boundary itself. It is the most characteristic fauna present in the boundary interval, being represented by huge, flat–lying individuals, dominated by species of *Platyceramus* and rare *C. bueltenensis*. Provisionally, all representatives of the third fauna are referred to *Platyceramus* cf. *ezoensis*, but stratigraphic and evolutionary relationships between them remain poorly known. In Japan, the members of the group are referred to as *P. ezoensis*, *P. vanuxemiformis* (Nagao and Matsumoto, 1940) (originally described as a variety of *P. ezoensis*), and *P. miyahisai* (Noda, 1983). Very close too is *P. colossus* Sornay, 1969 (p. 211, pl. H, fig. 1) from the lower Campanian of Madagascar, characterised by a rhomboid outline. Very similar forms have also been recorded from California under the name of *Inoceramus chicoensis*; this species has recently been reported from Japan (Noda et al., 1996).

Northern areas of the Euramerican Biogeographic region (northern Europe; north–western Siberia; Greenland; northern part of the North American Western Interior): the inoceramids of this biochore are characterised invariably by *Sphenoceramus* faunas; the boundary falls within the range of the *S. patootensiformis*–*S. lundbreckensis* clade (Beyenburg, 1936; Seitz, 1965; McLearn, 1929; Walaszczyk and Cobban, 2006, 2007). Walaszczyk (1992) suggested that a change in ornamentation within this clade around the *Marsupites* extinction level could be a potential boundary marker; both species lost their radial ornament. This, however, still needs confirmation, and even when confirmed, would be limited to the northerly portions of the Euramerican region which is characterised by a regular occurrence of the *Sphenoceramus* fauna. Moving southwards, a clear diachroneity in the distribution of this fauna is observed (Walaszczyk and Cobban, 2006); it is completely absent from the most southerly areas of the Euramerican biogeographic region.

East–African Province–subprovince (South Africa, Madagascar, India): The Santonian–Campanian boundary inoceramid record of the biochore resembles the general pattern of the record from the boundary zone between the northern Tethyan and southern Euramerican Region (see Walaszczyk et al., 2014). The interval is dominated by *Cordiceramus* clade, however, with a distinct presence of members of the *Platyceramus ezoensis* fauna at the boundary itself, which may suggest its widespread, evolutionary occurrence.

North Pacific Province (Japan, Pacific Russia, western margin of North America): The Santonian–Campanian inoceramid boundary record of this province is poorly known. Traditionally the base of the Campanian in Japan was correlated with the base of the ‘*Inoceramus*’ *japonicus* Zone (see Toshimitsu et al., 1995, 1998). Recent correlations based on the carbon isotope curve and additional tephrochronological studies (Takashima et al., 2019 and Kuwabara et al., 2019) support this correlation, although Takashima et al. (2010) suggested that this taxon first appears distinctly higher, and that the base of the Campanian lies somewhere in the upper part of the *Platyceramus amakusensis* Zone. In contrast, some magnetostratigraphic dating in Japan (Toshimitsu and Kikawa, 1997), as well as the recent report of *Marsupites testudinarius* from the Canadian Pacific coast Nanaimo Group and its correlation with the inoceramid succession there (Haggart and Graham, 2017), suggest

that the base of the Campanian in Japan should be placed distinctly higher, at the base of, or even within, the succeeding zone of *Sphenoceras orientalis*–*Sphenoceras schmidtii*. Consequently, the entire ‘*Inoceramus japonicus* Zone of Japan would be of Santonian age.

## Inoceramid Markers of the Santonian–Campanian Boundary

Although the Santonian–Campanian boundary as now defined is not reflected by a single inoceramid event, the boundary interval reveals some inoceramid events that may potentially be of chronostratigraphic importance as secondary boundary markers. Among these are:

(1) The *Platyceras* cf. *ezoensis* acme Zone; first defined in the Waxahachie section (Gale et al., 2008), this zone spans the Santonian–Campanian boundary itself and may represent a good marker of the boundary interval. The regional extent of this zone is still not fully known; further tests are required.

(2) The highest occurrence or distinct drop in abundance of *Cordiceramus germanicus*; this event should point to a level coinciding with the base of the *Marsupites testudinarius* Zone.

(3) The first appearance of *Cataceramus balticus*; this event has often been quoted as being close to the Santonian–Campanian boundary and regarded as its potential inoceramid marker (e.g., Ernst et al., 1979; Schulz et al., 1984). It would seem, however, that the species first appears in the *C. ex gr. muelleri* Zone of the lower upper Santonian (e.g., Europe: Seitz, 1967; Tröger, 1989; Western Interior: Larson et al., 1991; Kauffman et al., 1993, and Hancock and Gale, 1996; Gulf Coast: Gale et al., 2008).

## Summary

The Bottacione Gorge section at Gubbio, Italy, is confirmed as the Global boundary Stratotype Section for the base of the Campanian Stage. Sedimentation in the Santonian–Campanian boundary interval appears to be continuous, supported by evidence from the carbon isotope record and complete calcareous plankton biostratigraphy. The succession comprises deep–water cherty limestones (mudstones and foraminiferal wackestones) which provide a detailed microfaunal record for calcareous nannofossils and planktonic foraminifera and yields an excellent palaeomagnetic record. The high–resolution carbon isotope record, as well as rising strontium isotope values, derived from bulk sediment, provides important additional means of correlation to other regions.

The base of the Campanian Stage is defined by the magnetic polarity reversal from Chron C34n (top of Long Cretaceous Normal Polarity–Chron) to Chron 33r. This has been widely identified in oceanic crust, and in widespread onshore outcrops.

Secondary markers include first and last occurrences of widely distributed planktonic foraminifera and calcareous nannofossils, and positive and negative excursions in the  $\delta^{13}\text{C}$  record. In ascending order, the most important are (Fig. 25):

(oldest)

1) The first occurrence of the widespread planktonic foraminiferan *Globotruncana neotricarinata*

2,3) The Late Santonian Event (LSE), a double (a, b) positive excursion in  $\delta^{13}\text{C}$ , identified globally

4) The first occurrence of the planktonic foraminiferan *Contusotruncana patelliformis*

5) The first occurrences of the planktonic foraminiferan *Marginotruncana tarfayaensis* and *M. pseudomarginata*

6) The first occurrence of the calcareous nannofossil *Arkhangelskiella cymbiformis*

8) The first occurrence of the calcareous nannofossil *Aspidolithus parvus expansus*

9) The last occurrence of the planktonic foraminiferan *Dicarinella concavata*

10) The first occurrence of the calcareous nannofossil *Aspidolithus parvus parvus*

12) The primary marker, base of Chron C33r

14) The last occurrences of the planktonic foraminiferan *Dicarinella asymetrica* and *Sigalia* sp.

16) The first occurrence of the planktonic foraminiferan *Globotruncanita atlantica*

18) The first common occurrence of the calcareous nannofossil *Aspidolithus parvus parvus*

22) The first occurrence of the calcareous nannofossil *Aspidolithus parvus constrictus*

23) The last occurrence of the planktonic foraminiferan *Marginotruncana* spp.

(youngest)

Auxiliary sections are:

Seaford Head, Sussex, UK, which is developed in white chalk facies, and can be correlated to the candidate GSSP section through carbon isotope stratigraphy (Fig. 4–LSE peaks a, b) and the first occurrence of the calcareous nannofossil *Aspidolithus parvus parvus*. This correlation is particularly important because it demonstrates the relative position of the Santonian crinoid zones (*Marsupites*, *Uintacrinus*) to the proposed GSSP, and because the Seaford Head section has been tuned to orbital cyclicity (Thibault et al., 2016) it is thus potentially valuable for securing a more precise age for the Santonian–Campanian boundary. The palynology indicates the site was relatively close to the basin margin and with significantly less surface water fertility than at Bocieniec, and this is the probable reason why a number of stratigraphic markers are absent. The Santonian–Campanian boundary lies between the older first occurrence of *Rhynchodiniopsis saliorum* and first common occurrence of *Ellipsodinium* events and the last occurrence of *Ellipsodinium*.

Biocieniec, near Warsaw, Poland, is a thin development in a marly facies, and provides evidence of the palaeomagnetic reversal at the base of Chron 33r, the last occurrence of the planktonic foraminiferan *Dicarinella asymetrica*, the first occurrence of the calcareous nannofossil *Aspidolithus parvus parvus* and the carbon isotope peak LSE1a. It also yields the crinoids *Uintacrinus* and *Marsupites* which allow precise correlation to the Seaford Head section. The palynology indicates a clear increase in proximity to the shoreline through time at Bocieniec. The surface waters were initially more eutrophic than at Seaford Head (and presumably more distal) but became significantly oligotrophic in the Campanian opoka facies. The Santonian–Campanian boundary lies between the older first occurrence of *Rhynchodiniopsis saliorum*, minimum in *Surculosphaeridium longifurcatum*, and last

occurrence of rare *Heterosphaeridium difficile* events, and the last occurrence of *Ellipsodinium*.

Postalm, Austria, set in the northwestern Tethys, is developed in a rhythmically-bedded, deep-water hemipelagic facies, and provides palaeomagnetic evidence for the base of Chron C33r, the last occurrence of the planktonic foraminiferan *Dicarinella asymetrica*, and the first occurrence of the coccolith *Aspidolithus parvus parvus*.

The Smoky Hill Chalk Member of northern Kansas, USA, is set in the Western Interior Seaway, developed in a marly chalk facies, and has provided correlation to the palaeomagnetic reversal at the base of Chron C33r. It provides a suite of high-resolution calcareous nannofossil datums, including the first occurrences of *Aspidolithus parvus parvus* and *A. p. constrictus*.

The Tepeyac section in northern Coahuila, Mexico, provides a detailed ammonite biostratigraphy through the Santonian–Campanian boundary interval, and a high-resolution carbon–isotope record that permits correlation with the candidate GSSP and other auxiliary sections. It demonstrates that the position of the GSSP primary criterion falls approximately at the base of the *Menabites (Delawarella) delawarensis* Zone of the ammonite zonation developed in the USA Gulf Coast and eastern Atlantic seaboard.

Detailed evidence for the correlation of the GSSP with the auxiliary sections and Lägerdorf, Germany is summarised in Fig. 25. This utilises data from biostratigraphy, carbon isotopes and magnetostratigraphy described in the text.

## Acknowledgements

We would like to thank numerous colleagues for their comments and advice on Cretaceous stratigraphy. We thank the Mayor of Gubbio, Prof Filippo Mario Striati, for his help on conservation of the proposed Bottaccione GSSP and Dave Watkins for location of the Kansas sections. We thank an anonymous referee for invaluable comments. We thank the Voting Members of the International Subcommission on Cretaceous Stratigraphy and of the International Commission on Stratigraphy for comments which helped to improve the final version of the proposal. Jin-Yong Lee, Episodes Editor-in-Chief, is thanked for comments on the final version of the manuscript. We acknowledge financial support by the International Subcommission on Cretaceous Stratigraphy (<http://cretaceous.stratigraphy.org/>).

## References

- Albright III, L.B., and Titus, A.L., 2016, Magnetostratigraphy of Upper Cretaceous strata in the Grand Staircase–Escalante National Monument, southern Utah – the Santonian–Campanian stage boundary, reassessment of C33N/C33R magnetochron boundary, and implications for regional sedimentation patterns within the Sevier foreland basin. *Cretaceous Research*, v. 63, pp. 77–94.
- Alvarez, W., Arthur, M.A., Fischer, A.G., Lowrie, W., Napoleone, G., Premoli Silva, I., and Roggenthen, W.M., 1977, Upper Cretaceous–Paleocene magnetic stratigraphy at Gubbio, Italy: V. Type section for the Late Cretaceous–Paleocene geomagnetic reversal time scale. *Geological Society of America Bulletin*, v. 88, 3, pp. 83–389, doi:10.1130/0016-7606(1977)88<383:UCMSAG>2.0.CO;2
- Alvarez, W., and Montanari, A., 1988, The Scaglia limestone (Late Cretaceous–Oligocene) in the northeastern Apennines carbonate sequence: stratigraphic context and geological significance. In: Premoli Silva, I., Coccioni, R., and Montanari, A. (eds), *The Eocene–Oligocene Boundary in the Marche–Umbria Basin (Italy): Ancona, Italy*. Fratelli Annibaldi, International Union of Geological Sciences Special Publication, International Subcommission on Paleogene Stratigraphy Report, pp. 13–29.
- Alve, A., 1999, Colonization of new habitats by benthic foraminifera: a review. *Earth Science Reviews*, v. 46, pp. 167–185.
- Ando, A., Woodard, S.C., Evans, H.F., Littler, K., Herrmann, S., MacLeod, K.G., Kim, S., Khim, B.-K., Robinson, S.A., and Huber, B.T., 2013, An emerging palaeoceanographic ‘missing link’: multidisciplinary study of rarely recovered parts of deep-sea Santonian–Campanian transition from Shatsky Rise. *Journal of the Geological Society, London*, v. 170, pp. 381–384.
- Arnaud, H., 1878, Parallélisme de la craie supérieur dans le Nord et le Sud–Ouest de la France. *Bulletin de la Société géologique de France*, v. 6, pp. 205–211.
- Barchi, P., 1995, Géochemie et magnetostratigraphie du Campanien de l’Europe nord–ouest. Unpublished doctoral thesis, Université Pierre et Marie Curie (Paris IV).
- Barr, F.T., 1966, The foraminiferal genus *Bolivinooides* from the Upper Cretaceous of the British Isles. *Palaeontology*, v. 9, pp. 34–38.
- Beyenburg, E., 1936, Die Fauna der Halterner Sandfazies im westfälischen Untersenon. *Jahrbuch der Preussischen Geologischen Landesanstalt*, v. 57, pp. 284–322.
- Birkelund, T., Hancock, J. M., Hart, M. B., Rawson, P. F., Remane, J., Robaszynski, F., Schmid, F., and Surlyk, F., 1984, Cretaceous stage boundaries – proposals. *Bulletin of the Geological Society of Denmark*, v. 33, pp. 3–20.
- Böse, E., 1928, Cretaceous ammonites from Texas and northern Mexico. *University of Texas Bulletin* 2748, pp. 143–357.
- Bralower T.J., Leckie R.M., Sliter W.V., and Thierstein H.R., 1995, An integrated Cretaceous microfossil biostratigraphy. In: Berggren, W.A., Kent, D.V., Aubry, M.-P. and Hardenbol, J. (eds.), *Geochronology, Time Scales and Global Stratigraphic Correlation: Society of Economic Paleontologists and Mineralogists, Special Publication*, 54, pp. 65–79.
- Bralower, T.J., and Siesser, W.G., 1992, Cretaceous calcareous nannofossil stratigraphy of ODP Leg 122 Sites 761, 762 and 763, Exmouth and Wombat plateaus, N.W. Australia. In: von Rad, U. and Haq, U. (eds) *Proceedings Ocean Drilling Program Scientific Results*, v. 122, pp. 529–556. Ocean Drilling Program, College Station, Texas.
- Brydone, R.M., 1914, The Zone of *Offaster pilula* in the south English Chalk, Parts I–IV. *Geological Magazine, New Series, Decade VI*, 1, pp. 359–369, 405–411, 449–457, 509–513.
- Bukry, D., 1969, Upper Cretaceous coccoliths from Texas and Europe. *University of Kansas Paleontological Contributions*, Article 51 (Protista 2), pp. 1–79.
- Burnett, J.A. (with contributions from Gallagher, L.T. and Hampton, M.J.), 1988, Upper Cretaceous. In: Bown, P.R. (ed.), *Calcareous Nannofossil Biostratigraphy*. Kluwer Academic Publishing, Dordrecht, The Netherlands, pp. 132–199.
- Cande, S.C., and Kent, D.V., 1992, A new geomagnetic polarity time scale for the Late Cretaceous and Cenozoic. *Journal of Geophysical Research*, v. 97, pp. 13917–13951.
- Cande, S.C., and Kent, D.V., 1995, Revised calibration of the geomagnetic polarity timescale for the Late Cretaceous and Cenozoic. *Journal of Geophysical Research*, v. 100, pp. 6093–6095.
- Caron, M., 1985, Cretaceous planktonic foraminifera. In: Bolli, H.M., Saunders, J.B. and Perch Nielsen, K. (eds.): *Planktonic Stratigraphy*. Cambridge University Press, Cambridge, pp. 17–86.
- Channell, J.E.T., 1978, Dual magnetic polarity measured in a single bed of Cretaceous pelagic limestone from Sicily. *Journal of Geophysics*, v. 44, pp. 613–622.

- Channell, J.E.T., Lowrie, W., Medizza, F., and Alvarez, W., 1978, Palaeomagnetism and tectonics in Umbria, Italy. *Earth and Planetary Science Letters*, v. 39, pp. 199–210.
- Channel J.E.T., Freeman R. Heller F., and Lowrie W., 1982, Timing of diagenetic haematite growth in red pelagic limestones from Gubbio (Italy). *Earth and Planetary Science Letters*, v. 58, pp. 189–201.
- Chenot, E., Pellenard, P., Martinez, M., Deconinck, J.-F., Amiotte-Suchet, P., Thibault, N., Bruneau, L., Cocquerez, T., Laffont, R., Puceat, E., and Robaszynski, F., 2016, Clay mineralogical and geochemical expressions of the “Late Campanian Event” in the Aquitaine and Paris Basins (France): palaeoenvironmental implications. *Palaeogeography, Palaeoclimatology, Palaeoecology*, v. 447, pp. 42–52.
- Cobban, W.A., 1952, Scaphitoid cephalopods of the Colorado Group. United States Geological Survey Professional Paper, 239, 39 pp. (1951 imprint).
- Cobban, W.A., 1969, The Late Cretaceous ammonites *Scaphites leei* Reeside and *Scaphites hippocrepsis* (DeKay) in the Western Interior of the United States. United States Geological Survey Professional Paper, 619, 27p.
- Cobban, W.A., 1995, Occurrences of the free-swimming Upper Cretaceous crinoids *Uintacrinus* and *Marsupites* in the Western Interior of the United States. United States Geological Survey Bulletin, 2113–C, pp. C1–C6.
- Cobban, W.A., Walaszczyk, I., Obradovich, J.D., and McKinney, K.C., 2006, A USGS zonal table for the Upper Cretaceous middle Cenomanian–Maastrichtian of the Western Interior of the United States based on ammonites, inoceramids, and radiometric ages. U.S. Geological Survey Open-File Report, 2006–1250, 45 p.
- Coccioni, R., and Premoli Silva, I., 2015, Revised upper Albian–Maastrichtian planktonic foraminiferal biostratigraphy and magnetostratigraphy of the classical Tethyan Gubbio section (Italy). *Newsletters on Stratigraphy*, v. 48, pp. 47–90, doi:10.1127/nos/2015/0055
- Coccioni, R., Catanzariti, R., Frontalini, F., Galbrun, B., Jovane, L., Montanari, A., Savian, J.F., and Sideri, M., 2016, Integrated magnetostratigraphy, biostratigraphy, and chronostratigraphy of the Paleogene pelagic succession at Gubbio (central Italy). In: Menichetti, M., Coccioni, R., and Montanari, A., eds., *The Stratigraphic Record of Gubbio: Integrated Stratigraphy of the Late Cretaceous–Paleogene Umbria–Marche Pelagic Basin*. Geological Society of America, Special Paper, 524, pp. 139–160, doi:10.1130/2016.2524(10)
- Coquand, H., 1856, Notice sur la formation crétacée du département de la Charente. *Bulletin de la Société géologique de France* (2), v. 14, pp. 55–98.
- Coquand, H., 1857, Position des *Ostrea columba* et *biauriculata* dans le groupe de la craie inférieure. *Bulletin de la Société géologique de France* (2), v. 14, pp. 841–903.
- Coquand, H., 1858, Description physique, géologique, paléontologique et minéralogique du département de la Charente (imprimé sous la direction du Conseil Générale) I. De Doidivers et Cie, Besançon, 542p.
- Coquand, H., 1859, Synopsis des animaux, et des végétaux fossils observés dans la formation crétacé du Sud–Ouest de la France. *Bulletin de la Société géologique de la France* (2), v. 16, 945–1023.
- Coquand, H., 1860, Description physique, géologique, paléontologique et minéralogique du Département de la Charente (imprimé sous les auspices du Conseil Générale) II. Barlatier–Feissat et Demonchy, Marseille, 420p.
- Costa, L.I., and Davey, R.J., 1999, Dinoflagellate cysts of the Cretaceous System, In: Powell, A.J. (Ed.) *A Stratigraphic Index of Dinoflagellate Cysts*. 2nd edition. Kluwer Academic Press, Dordrecht, pp. 99–153.
- Deville Periere, M., Lellenard, P., and Thibault, N., 2019, The Santonian – Campanian Boundary Event (SCBE) in Boreal Basins: new geochemical and mineralogical data from the Northern Chalk Province (East Yorkshire, UK). *Cretaceous Research*, v. 95, pp. 61–76.
- Dubicka, Z., Jurkowska, A., Thibault, N., Razmjooei, M.J., Wójcik, K., Gorzelak, P., and Felisiak, I., 2017, An integrated stratigraphic study (benthic foraminifera, calcareous nannofossils, crinoids, carbon isotopes and magnetic polarities) across the Santonian/Campanian boundary at Bocieniec, southern Poland: a new possible boundary stratotype. *Cretaceous Research*, v. 80, pp. 61–85.
- Dubicka, Z., and Peryt, D., 2014, Classification and evolutionary interpretation of the late Turonian–early Campanian *Gavelinella* and *Stensioeina* (Gavelinellidae, benthic foraminifera) from western Ukraine. *Journal of Foraminiferal Research*, v. 44, pp. 151–176.
- Dubicka, Z., and Peryt, D., 2016, *Bolivinoidea* (benthic foraminifera) from the Upper Cretaceous of Poland and Western Ukraine: taxonomy, evolutionary changes and stratigraphic significance. *Journal of Foraminiferal Research*, v. 46, pp. 75–94.
- Dubicka, Z., and Wierzbowski, H., 2019, Planktic propagules as a potential long–distance dispersal mechanism of Cretaceous serial Rotaliida benthic foraminifera. *Cretaceous Research*, v. 100, pp. 14–23.
- Dunlop D.J., and Stirling J.M., 1977, “Hard” viscous remanent magnetization (VRM) in fine–grained hematite. *Geophysical Research Letters*, v. 4, pp. 163–166.
- Edwards, P.G., 1981, The foraminiferid genus *Gavelinella* in the Senonian of northwestern Europe. *Palaeontology*, v. 24, pp. 391–416.
- Eldrett, J.S., Vieira, M., Gallagher, L., Hampton, M., Blaauw, M., and Swart, P.K., 2020, Late Cretaceous to Palaeogene carbon isotope, calcareous nannofossil and foraminifera stratigraphy of the Chalk Group, central North Sea. *Marine and Petroleum Geology*, v. 124, article 104789, doi:10.1016/j.marpetgeo.2020.104789
- Ernst, G., 1964, Ontogenie, Phylogenie und Stratigraphie der Belemniten-gattung *Gonioteuthis* BAYLE aus dem nordwestdeutschen Santon/Campan. *Fortschritte in der Geologie von Rheinland und Westfalen*, v. 7, pp. 113–174.
- Ernst, G., 1968, Die Oberkreide– Aufschlusse im Raume Braunschweig–Hannover und ihre stratigraphische Gliederung mit Echinodermen und Belemniten. Teil: Die Jungeren Oberkreide (Santon–Maastricht). *Beihfte zu den Berichten der Naturhistorischen Gesellschaft zu Hannover*, v. 5, pp. 235–284.
- Ernst, G., Schmid, F., and Klischies, G., 1979, Multistratigraphische Untersuchungen in der Oberkreide des Raumes Braunschweig–Hannover. In: Wiedmann, J. (Ed.), *Aspekte der Kreide Europas*. IUGS Series, A6, pp. 11–46.
- Gale, A.S., 2018, An integrated microcrinoid zonation for the Lower Campanian chalk of southern England, and its implications for correlation. *Cretaceous Research*, v. 87, 312–357, doi:10.1016/j.cretres.2017.02.002
- Gale, A.S., 2019, Microcrinoids (Echinodermata: Articulata: Roveacrinida) from the Cenomanian– Santonian chalk of the Anglo–Paris Basin: taxonomy and biostratigraphy. *Révue de Paléobiologie*, v. 38, pp. 379–533.
- Gale, A.S., Kennedy, W.J., Montgomery, P., Hancock, J.M., and McArthur, J.M., 1995, Global correlation and definition of the Santonian – Campanian boundary. *Terra Nova*, v. 7, pp. 611–622.
- Gale, A.S., Kennedy, W.J., Lees, J.A., Petrizzo, M.R., and Walaszczyk, I., 2008, An integrated study (inoceramid bivalves, ammonites, calcareous nannofossils, planktonic foraminifera, stable carbon isotopes) of the Waxahachie Dam spillway section, Ellis County, north Texas, a candidate Global boundary Stratotype Section and Point for the base of the Campanian Stage. *Cretaceous Research*, v. 29, pp. 131–167.
- Gale, A.S., Kennedy, W.J., and Walaszczyk, I., 2020a, Correlation of the late Santonian–early Campanian of Texas, USA with the Anglo–Paris Basin and other regions. *Newsletters on Stratigraphy*, v. 54, pp. 433–460, doi:10.1127/nos/2020/0641
- Gale, A.S., Mutterlose, J., and Batenburg, S.F., 2020b, Chapter 27. The Cretaceous Period. In: Gradstein, F.M., Ogg, J.G., Schmitz, M.D., Ogg, G.M., (eds), *Geologic Time Scale 2020*. Elsevier, pp. 1023–1086.
- Gardin, S., Del Panta, F., Monechi, S., and Pozzi, M., 2001, A Tethyan reference record for the Campanian and Maastrichtian stages: the Bottaccione section (central Italy). Review of data and new calcareous nannofossil results. In: Odin, G.S., eds., *The Campanian–Maastrichtian Stage Boundary*. *Developments in Palaeontology and Stratigraphy*, Elsevier, v. 19,

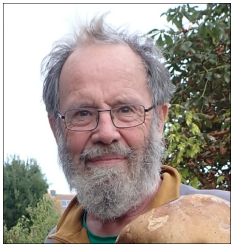
- pp. 745–757.
- Grossouvre, A. de, 1894, Recherches sur la craie supérieure, 2, Paléontologie. Les ammonites de la craie supérieure. Mémoires pour servir à l'explication de la Carte Géologique détaillée de la France. 264 p., 39 pls. (misdated 1893).
- Grossouvre, A. de, 1901, Recherches sur la craie supérieure, part 1, no. 2, Stratigraphie générale. Mémoires pour servir à l'explication la carte géologique détaillée de la France, pp. 561–1013.
- Guzhikov, A.Y., Barbaroshkin, E.Y., Aleksandrova, G.N., Ryabov, I.P., Ustinova, M.A., Kopaevich, L.F., Mirantsev, G.V., Kuznetsov, A.B., Fokin, P.A., and Kosorukov, V.L., 2021a, Bio-, chemo- and magnetostratigraphy of the Santonian–Campanian boundary in the Kudrino and Aksu–Dere sections (SW Crimea): problems of global correlation and selection of the lower boundary stratotype of the Campanian. 2. Magneto- and chemostratigraphy. Discussion. Stratigraphy and Geological Correlation, v. 29, pp. 518–547 [In Russian].
- Guzhikov, A.Y., Barbaroshkin, E.Y., Aleksandrova, G.N., Ryabov, I.P., Ustinova, M.A., Kopaevich, L.F., Mirantsev, G.V., Kuznetsov, A.B., Fokin, P.A. and Kosorukov, V.L., 2021b, New bio-, chemo- and magnetostratigraphy of the Santonian–Campanian boundary in the Kudrino and Aksu–Dere sections (SW Crimea): problems of global correlation and selection of the lower boundary stratotype of the Campanian. 1. Geological framework, sedimentology, biostratigraphy. Stratigraphy and Geological Correlation, v. 29, pp. 450–494 [In Russian].
- Haggart, J.W., 1984, Upper Cretaceous (Santonian–Campanian) ammonite and inoceramid biostratigraphy of the Chico Formation, California. Cretaceous Research, v. 5, pp. 225–241.
- Haggart, J.W., and Graham, R., 2017, The crinoid *Marsupites* in the Upper Cretaceous Nanaimo Group, British Columbia: resolution of the Santonian – Campanian boundary in the North Pacific province. Cretaceous Research, v. 87, pp. 277–295, doi:10.1016/j.cretres.2017.05.029
- Haggart, J.W., and Ward, P.D., 1989, New Nanaimo Group ammonites (Cretaceous, Santonian–Campanian) from British Columbia and Washington State. Journal of Paleontology, v. 63, pp. 218–227.
- Hampton, M.J., Bailey, H.W., Gallagher, L.T., Mortimore, R.N., and Wood, C.J., 2007, The biostratigraphy of Seaford Head, Sussex, southern England; an international reference section for the basal boundaries for the Santonian and Campanian stages in chalk facies. Cretaceous Research, v. 28, pp. 46–60.
- Hancock, J.M., and Gale, A.S., 1996, The Campanian Stage. Bulletin de l'Institut Royal des Sciences Naturelles Belges. Sciences de la Terre, v. 66, pp. 103–109.
- Hardenbol, J., Thierry, J., Farley, M.B., Jacquin, T., De Graciansky, P.-C., and Vail, P.R., 1998, Chart 5 – Cretaceous Biostratigraphy. In: De Graciansky, P.-C., Hardenbol, J., Jacquin, T., and Vail, P.R. (Eds.) Mesozoic and Cenozoic Sequence Stratigraphy of European Basins, SEPM Special Publication.
- Hart, M.B., Bailey, H.W., Crittenden, S., Fletcher, B.N., Price, R.J., and Swiecicki, A., 1989, Cretaceous. In: Jenkins, D.G., and Murray, J.W. (eds.), Stratigraphical Atlas of Fossil Foraminifera, Second Edition: Ellis Horwood Limited, Chichester, pp. 273–371.
- Hattin, D.E., 1982, Stratigraphy and depositional environment of Smoky Hill Chalk Member, Niobrara Chalk (Upper Cretaceous) of the type area, western Kansas. Kansas Geological Survey, Bulletin 225, University of Kansas Publications, 109p.
- He, H., Deng, C., Wang, P., Pan, Y., and Zhu, R., 2012, Toward age determination of the termination of the Cretaceous Normal Superchron. Geochemistry, Geophysics, Geosystems (G<sup>3</sup>), v. 13, Q02002, doi:10.1029/2011GC003901
- Hiltermann H., 1952, Stratigraphische Fragen des Campan und Mastricht unter besonder Berücksichtigung der Mikropaläontologie. Jahrbuch Geologische Landesanst, v. 67, pp. 47–66.
- Huber, B.T., Petrizzo, M.R., and Falzoni, F., 2022, Taxonomy and phylogeny of Albian–Maastrichtian planispiral planktonic foraminifera traditionally assigned to *Globigerinelloides*. Micropaleontology, v. 68, pp. 117–183.
- Ifrim, C., and Stinnesbeck, W., 2021, Ammonoids and their zonation across the Santonian–Campanian boundary in north–eastern Coahuila, Mexico. Palaeontologica Electronica, v. 24, doi:10.26879/1046
- Ifrim, C., Stinnesbeck, W., Gonzalez Gonzalez, A.H., Schorndorf, N., and Gale, A.S., 2021, Ontogeny, evolution and paleogeographic distribution of the world's largest ammonite, *Parapuzosia seppenradensis* (Landois, 1895). PLOS ONE. doi:10.1371/journal.pone.0258510
- Jarvis, I., Gale, A.S., Jenkyns, H.C., and Pearce, M.A., 2006, Secular variation in Late Cretaceous carbon isotopes: a new  $\delta^{13}\text{C}$  reference curve for the Cenomanian–Campanian, 99.6–70.6 myr. Geological Magazine, v. 143, pp. 561–608.
- Jarvis, I., Pearce, M., Püttman, T., Voigt, S., and Walaszczyk, I., 2021, Palynology and calcareous nannofossil biostratigraphy of the Turonian–Coniacian boundary: the proposed boundary stratotype at Salzgitter–Salder, Germany and its correlation in NW Europe. Cretaceous Research, v. 123, pp. 1–32. doi:10.1016/j.cretres.2021.104782
- Jarvis, I., Pearce, M.A., Monkenbusch, J., Jurowska, A., Ullmann, C.V., Dubicka, S., and Thibault, N., 2022, Carbon isotopes, palynology and stratigraphy of the Santonian–Campanian boundary: the GSSP auxiliary sections, Seaford Head (England) and Biocieniec (Poland), and correlation between the Boreal and Tethyan realms. Cretaceous Research. doi:10.1016/j.cretres.2022.105415
- Jeletzky, J.A., 1970, Biochronology. In: Muller, J.E. and Jeletzky, J.A., Geology of the Upper Cretaceous Nanaimo Group, Vancouver Island and Gulf Islands, British Columbia. Geological Survey of Canada, Paper 69–25, pp. 35–58.
- Jenkyns, H.C., Gale, A.S., and Corfield, R., 1994, The stable oxygen and carbon isotope stratigraphy of the English Chalk and the Italian Scaglia. Geological Magazine, v. 13, pp. 1–34.
- Joo, Y.J., and Sageman, B.B., 2014, Cenomanian to Campanian carbon isotope chemostratigraphy from the Western Interior Basin, U.S.A. Journal of Sedimentary Research, v. 84, pp. 529–542.
- Kaplan, U., Kennedy, W.J., and Hiss, M., 2005, Stratigraphie und Ammonitenfaunen des Campan im nordwestlichen und zentralen Munsterland. Geologie und Paläontologie in Westfalen, v. 64, pp. 5–176.
- Kaplan, U., and Kennedy, W.J., 2005, Ammonitenfaunen des höheren Oberconiac und Santon in Westfalen. Geologie und Paläontologie in Westfalen, v. 57, pp. 3–131.
- Kauffman, E.G., 1973, Cretaceous Bivalvia. In: A. Hallam (Ed.), Atlas of Palaeobiogeography. Elsevier Scientific Publishing Company, Amsterdam – London – New York, pp. 353–383.
- Kauffman, E.G., Sageman, B.B., Kirkland, J.I., Elder, W.P., Harries, P.J., and Villamil, T., 1993, Molluscan biostratigraphy of the Cretaceous Western Interior Basin, North America. In: Caldwell, W.G.E., Kauffman, E.G. (Eds.), Evolution of the Western Interior Basin. Geological Association of Canada, Special Paper, 39, pp. 397–434.
- Keefer, W.R., and Troyer, M.L., 1956, Stratigraphy of the Upper Cretaceous and lower Tertiary rocks of the Shotgun Butte area, Fremont County, Wyoming. United States Geological Survey Oil and Gas Investigation Chart OC–56.
- Keefer, W.R., and Troyer, M. L., 1964, Geology of the Shotgun Butte area, Fremont County, Wyoming. United States Geological Survey Bulletin 1157, 123 pp.
- Kennedy, W.J., 1984, Ammonite faunas and the “standard zones” of the Cenomanian to Maastrichtian stages in their type areas, with some proposals for the definition of the stage boundaries by ammonites. Bulletin of the Geological Society of Denmark, v. 33, pp. 147–161.
- Kennedy, W.J., 1986, Campanian and Maastrichtian ammonites from northern Aquitaine, France. Special Papers in Palaeontology, no. 36, Palaeontological Association, London.
- Kennedy, W.J., and Kaplan, U., 1995, *Parapuzosia* (*Parapuzosia*) *seppenradensis* (Landois) und die Ammoniten fauna der Dülmener Schichten, Westfalen. Geologie und Paläontologie in Westfalen, v. 33, 127 pp., 43 pls.

- Kita, Z.A., Watkins, D.K., and Bradman, B.B., 2017, High-resolution calcareous nannofossil biostratigraphy of the Santonian/Campanian stage boundary, Western Interior Basin, U.S.A. *Cretaceous Research*, v. 69, pp. 49–55.
- Koch, W., 1977, *Stratigraphie der Oberkreide in Nordwestdeutschland (Pompeckjsche Scholle). Teil 2. Biostratigraphie in der Oberkreide und Taxonomie von Foraminiferen.* *Geologisches Jahrbuch*, v. 38, pp. 11–123.
- Kopaevich, L.F., Beniamovski, V.N., and Sadekov, Ayu, 2007, Middle Coniacian–Santonian foraminiferal bioevents around the Mangyschlak Peninsula and Russian Platform. *Cretaceous Research*, v. 28, pp. 108–118.
- Kopaevich, L.F., Proshina, P.A., Ryabov, I.P., Ovechkina, M.N., and Grechikhina, N.O., 2020, Santonian–Campanian boundary position in the Alan–Kyr section (Central Crimea): new micropaleontological data. *Moscow University Geology Bulletin*, 75, pp.246–253.
- Laskar, J., 2020, Chapter 4 – Astrochronology. In: Gradstein, F.M., Ogg, J.G., Schmitz, M.D. and Ogg, G.M. (Eds.) *Geologic Time Scale 2020*. Elsevier, pp. 139–158.
- Laurin, J., Meyers, S.R., Ulicný, D., Jarvis, I., and Sageman, B.B., 2015, Axial obliquity control on the greenhouse carbon budget through middle- to high-latitude reservoirs. *Paleoceanography and Paleoclimatology*, v. 30, pp. 133–149.
- Larson, P.A., Morin, R.W., Kauffman, E.G., and Larson, A., 1991, Sequence stratigraphy and cyclicity of lower Austin/upper Eagle Ford outcrops (Turonian–Coniacian), Dallas County, Texas. In: *Field Trip Guidebook, 9*, Dallas Geological Society, Dallas, Texas, 61 pp.
- Leahy, G.D., and Lerbekmo, J.F., 1995, Macrofossil magnetobiostratigraphy for the upper Santonian–lower Campanian interval in the Western Interior of North America: comparisons with European stage boundaries and planktonic foraminiferal zonal boundaries. *Canadian Journal of Earth Sciences*, v. 32, pp. 247–260.
- Lerbekmo, J.F., 1989, The stratigraphic position of the 33–33r (Campanian) polarity chron boundary in southeastern Alberta. *Bulletin of Canadian Petroleum Geology*, v. 37, pp. 43–47.
- Lerbekmo, J.F., and Braman, D.R., 2002, Magnetostratigraphic and biostratigraphic correlation of late Campanian and Maastrichtian marine and continental strata from the Red Deer River Valley to the Cypress Hills, Alberta, Canada. *Canadian Journal of Earth Sciences*, v. 39, pp. 539–557.
- Lillgraven, J.A., 1991, Stratigraphic placement of the Santonian–Campanian boundary (Upper Cretaceous) in the North American Gulf Coastal Plain and Western Interior, with implications for geochronology. *Cretaceous Research*, v. 12, pp. 115–136.
- Linares Rodriguez, D., 1977, *Foraminíferos Plantónicos del Cretácico Superior de las Cordilleras Béticas (Sector central)*. Tesis Doctoral, Departamento de Geología, Universidad de Malaga, Malaga, 410 p.
- Lopez, G., 1992, Paleontología y bioestratigrafía de los inocerámidos (Bivalvia) del Cretácico superior de la Cuenca Navarro–Cántabra y de la Plataforma Norcastellana. Parte IV: Estudio sistemático del subgenero *Cordiceramus* Seitz y bioestratigrafía. *Boletín Geológico y Minero*, v. 103, pp. 873–892.
- Louwe, S., 1992, Dinoflagellate cyst stratigraphy of the Upper Cretaceous of western Belgium. *Bulletin de la Société Belge de Géologie*, v. 101, pp. 255–275.
- Lowrie, W., and Alvarez, W., 1977a, Upper Cretaceous–Paleocene magnetic stratigraphy at Gubbio, Italy III. Upper Cretaceous magnetic stratigraphy. *Geological Society of America Bulletin*, v. 88, pp. 374–377.
- Lowrie W., and Alvarez W., 1977b, Late Cretaceous geomagnetic polarity sequence: detailed rock and palaeomagnetic studies of the Scaglia Rossa limestone at Gubbio, Italy. *Geophysical Journal International*, v. 51, pp. 561–581.
- Marks, P., 1984, Proposals for the recognition of boundaries between Cretaceous stages by means of planktonic foraminiferal stratigraphy. *Bulletin of the Geological Society of Denmark*, v. 33, pp. 163–169.
- Maron, M., and Muttoni, G., 2021, A detailed record of the C34n/C33r magnetozone boundary for the definition of the base of the Campanian Stage at the Bottaccione section (Gubbio, Italy). *Newsletter on Stratigraphy*, v. 54, pp. 107–122, doi: 10.1127/nos/2020/0607
- Matsumoto, T., 1959, Zonation of the Upper Cretaceous in Japan. *Kyushu University, Memoirs of the Faculty of Science, Series D (Geology)*, v. 9, no. 2, pp. 55–93, pls. 6–11.
- Matsumoto, T., 1960, Upper Cretaceous ammonites of California. Part III. With notes on stratigraphy of the Redding area and the Santa Ana Mountains by T. Matsumoto and W. P. Popenoe. *Kyushu University, Memoirs of the Faculty of Science, Series D (Geology), Special Volume II*, 204 p.
- McLearn, F.H., 1929, Cretaceous invertebrates, in Mesozoic paleontology of Blairmore region, Alberta. *National Museum of Canada Bulletin*, 58, pp. 73–79.
- Milson, C., Simms, M., and Gale, A.S., 1994, The taxonomy and palaeobiology of the crinoids *Umtacrinus* and *Marsupites*. *Palaeontology*, v. 37, pp. 595–607.
- Miniati, F., Petrizzo, M.R., Falzoni, F., and Erba, E., 2020, Calcareous plankton biostratigraphy boundary interval in the Bottaccione section (Umbria–Marche Basin, central Italy). *Rivista Italiana di Paleontologia e Stratigrafia*, v. 126, pp. 771–789.
- Montgomery, P., Hailwood, E.A., Gale, A.S., and Burnett, J.A., 1998, The magnetostratigraphy of Coniacian–Campanian chalk sequences in southern England. *Earth and Planetary Science Letters*, v. 156, pp. 209–224.
- Mortimore, R.N., 1986, Stratigraphy of the Upper Cretaceous White Chalk of Sussex. *Proceedings of the Geologists' Association*, v. 97, pp. 97–139.
- Mortimore, R.N., Wood, C.J., and Gallois, R.W., 2001, *British Upper Cretaceous Stratigraphy*, Geological Conservation Review Series, no. 23, Joint Nature Conservation Committee, Peterborough, 558 p.
- Muttoni, G., Dallanave E., and Channell J.E.T., 2013, The drift history of Adria and Africa from 280 Ma to Present, Jurassic true polar wander, and zonal climate control on Tethyan sedimentary facies. *Palaeogeography, Palaeoclimatology, Palaeoecology*, v. 386, pp. 415–435.
- Nagao, T., and Matsumoto, T., 1940, A monograph of the Cretaceous *Inoceramus* of Japan. Part II. *Journal of the Faculty of Science, Hokkaido Imperial University*, v. 6, pp. 1–64.
- Nederbragt, A.J., 1991, Late Cretaceous biostratigraphy and development of Heterohelicidae (planktic foraminifera). *Micropaleontology*, v. 37, 329–360.
- Noda, M., 1983, Some Cretaceous inoceramids (Bivalvia) from the Ominogadai Hills of Matsuyama, Shikoku. In: *Memorial Papers of the Late Prof. Michtoshi Miyahisa*. Earth Scientific Papers Association of Ehime, Matsuyama, 103–117. [In Japanese].
- Noda, M., Ohtsuka, M., Kano, M., and Toshimitsu, S., 1996, The Cretaceous inoceramids from the Mifune and Himenoura groups in Kyushu. *Special Issue of the Geological Society of Oita*, v. 2, pp. 1–63 [in Japanese].
- Obradovich, J.D., 1993, A Cretaceous time scale. In: Caldwell, W.G.E., and Kauffman, E.G. (eds), *Evolution of the Western Interior Basin*. Geological Association of Canada, Special Paper, 39, pp. 379–396.
- Ogg, J.G., 2020, Geomagnetic polarity timescale. In: Gradstein, F.M., Ogg, J.G., Schmitz, M.D., and Ogg, G.M. (eds), *Geologic Time Scale 2020*. Volume 1, 159–193. Elsevier.
- Orbigny, A. d', 1842–1843, *Paléontologie française: Terraine Crétacés. 2. Gastropodes*, 1–224 (1842); 225–456 (1843). Masson, Paris.
- Pearce, M.A., Jarvis, I., Ball, P.J., and Laurin, J., 2020, Palynology of the Cenomanian to lowermost Campanian (Upper Cretaceous) Chalk of the Trunch Borehole (Norfolk, UK) and a new dinoflagellate cyst bioevent stratigraphy for NW Europe. *Review of Palaeobotany and Palynology*, v. 278, pp. 104–188, doi:10.1016/j.revpalbo.2020.104188
- Pearce, M.A., Jarvis, I., Monkenbusch, J., Thibault, N., Ullmann, C.V., and Martinez, M., 2022, Coniacian–Campanian palynology, carbon isotopes and clay mineralogy of the Poigny borehole (Paris Basin) and its correlation in NW Europe. *Comptes Rendus Géoscience, Special*

- Volume in Memory of Jacques Rey, doi:10.5802/crgeos.118
- Pearce, M.A., Jarvis, I., Swan, A.R.H., Murphy, A.M., Tocher, B.A., and Edmunds, W.M., 2003, Integrating palynological and geochemical data in a new approach to palaeoecological studies, Upper Cretaceous of the Banterwick Barn Chalk borehole, Berkshire, UK. *Marine Micro-paleontology*, v. 47, pp. 271–306, doi:10.1016/S0377-8398(02)00132-9
- Pearce, M.A., Jarvis, I., and Tocher, B.A., 2009, The Cenomanian – Turonian boundary event, OAE2 and palaeoenvironmental change in epicontinental seas: new insights from the dinocyst and geochemical records. *Palaeogeography, Palaeoclimatology, Palaeoecology*, v. 280, pp. 207–234, doi:10.1016/j.palaeo.2009.06.012
- Perdiou, A., Thibault, N., Anderskov, K., van Buchem, F., Buijs, G.J.A., and Bjerrum, C.J., 2016, Orbital calibration of the Late Campanian carbon isotope event in the North Sea. *Journal of the Geological Society of London*, v. 173, pp. 504–517, doi:10.1144/jgs2015-120
- Petruzzo, M.R., 2000, Upper Turonian – lower Campanian planktonic foraminifera from southern mid–high latitudes (Exmouth Plateau, N Australia): biostratigraphy and taxonomic notes. *Cretaceous Research*, v. 21, pp. 479–505.
- Petruzzo, M.R., Falzoni, F., and Premoli Silva I., 2011, Identification of the base of the lower–to–middle Campanian *Globotruncana ventricosa* zone: Comments on reliability and global correlations. *Cretaceous Research*, v. 32, pp. 387–405.
- Platel, J.P., 1989, Le Crétacé Supérieur de la plate–forme septentrionale du Bassin d’Aquitaine. *Stratigraphie et Évolution Géodynamique. Documents du Bureau des Recherches Géologiques et Minières*, v. 164, 572 p.
- Postuma, J.A., 1971, *Manual of Planktonic Foraminifera*. Elsevier, Amsterdam, 420 pp.
- Premoli Silva, I., 1977, Upper Cretaceous–Paleocene magnetic stratigraphy at Gubbio. II. Biostratigraphy. *Geological Society of America Bulletin*, v. 88, pp. 371–374, doi: 10.1130/0016-7606(1977)88<371:UCMSAG>2.0.CO;2
- Premoli Silva, I., and Sliter, W.V., 1995, Cretaceous planktonic foraminiferal biostratigraphy and evolutionary trends from the Bottaccione section, Gubbio, Italy. *Palaeontographia Italica*, v. 82, pp. 1–85.
- Prince, I.M., Jarvis, I., and Tocher, B.A., 1999, High–resolution dinoflagellate cyst biostratigraphy of the Santonian–basal Campanian (Upper Cretaceous): new data from Whitecliff, Isle of Wight, England. *Review of Palaeobotany and Palynology*, v. 105, pp. 143–169.
- Prince, I.M., Jarvis, I., Pearce, M.A., and Tocher, B.A., 2008, Dinoflagellate cyst biostratigraphy of the Coniacian–Santonian (Upper Cretaceous): new data from the English Chalk. *Review of Palaeobotany and Palynology*, v.150, pp. 9–96. doi:10.1016/j.revpalbo.2008.01.005
- Puckett, T.M., 2005, Santonian–Maastrichtian planktonic foraminiferal and ostracode biostratigraphy of the northern Gulf Coastal Plain, USA. *Stratigraphy*, v. 2, pp. 117–146.
- Rasmussen, H.W., 1961, A monograph on the Cretaceous Crinoidea. *Biologiske Skrifter fra det Kongelige Danske Videnskaberne Selskab*, v. 12, 428 p.
- Razmjooei, M.J., Thibault, N., Kani, A., Dinarès–Turell, J., Pucéat, E., Shahriari, S., Radmacher, W., Jamali, A.M., Ullmann, C.V., Voigt, S., and Cocquerez, T., 2018, Integrated bio– and carbon–isotope stratigraphy of the Upper Cretaceous Gurpi Formation (Iran): a new reference for the eastern Tethys and its implications for large–scale correlation of stage boundaries. *Cretaceous Research*, v. 91, pp. 312–340.
- Razmjooei, M.J., Thibault, N., Kani, A., Ullmann, C.V., and Jamali, A.M., 2020, Santonian–Maastrichtian carbon–isotope stratigraphy and calcareous nannofossil biostratigraphy of the Zagros Basin: long–range correlation, similarities and differences of carbon–isotope trends at global scale. *Global and Planetary Change*, v. 184, 103075.
- Renz, H.H., 1936, Neue Cephalopoden aus der oberen Kreide von Rio Grande del Norte (Mexico und Texas). *Abhandlungen der Schweizerischen Paläontologischen Gesellschaft*, v. 57, pp. 1–16.
- Robaszynski, F., and Caron, M., 1995, Foraminifères planctoniques du Crétacé: commentaire de la zonation Europe–Méditerranée. *Bulletin de la Société géologique de France*, v. 166, pp. 681–692.
- Robaszynski, F., Gonzalez Donoso, J.M., Linares, D., Amédéo, F., Caron, M., Dupuis, C., Dhondt, A.V., and Gartner, S., 2000, Le Crétacé supérieur de la région de Kalaat Senan, Tunisie centrale. Litho–biostratigraphie intégrée: zones d’ammonites, de foraminifères planctoniques et de nannofossiles du Turonien supérieur au Maastrichtien. *Bulletin des Centres de Recherches–Exploration–Production. Elf–Aquitaine*, v. 22, pp. 359–490.
- Roggenthen, W.M., and Napoleone, G., 1977, Upper Cretaceous–Paleocene magnetic stratigraphy at Gubbio, Italy IV. Upper Maastrichtian–Paleocene magnetic stratigraphy. *Geological Society of America Bulletin*, v. 88, pp. 378–382.
- Roth, P.H., 1978, Cretaceous nannoplankton biostratigraphy and oceanography of the northwestern Atlantic Ocean. In: Benson W.E., Sheridan, R.E. et al. (eds.), *Initial Reports of the Deep Sea Drilling Project: U.S. Government Printing Office, Washington*, v. 44, pp. 663–701.
- Rowe, A.W.E., 1902, The zones of the White Chalk of the English coast. 1, Kent and Sussex. *Proceedings of the Geologists’ Association*, v. 16, pp. 289–368.
- Sabatino, N., Meyers, S.R., Voigt, S., Cocconi, R., and Sprovieri, M., 2018, A new high–resolution carbon–isotope stratigraphy for the Campanian (Bottaccione section): Its implications for global correlation, ocean circulation, and astrochronology. *Palaeogeography, Palaeoclimatology, Palaeoecology*, v. 489, pp. 29–39, doi: 10.1016/j.palaeo.2017.08.026
- Sageman, B.B., Singer, B.S., Meyers, S.R., Walaszczyk, I., Seiwert, S.E., Condon, D.J., Jicha, B.R., Obradovich, J.D., and Sawyer, D.A., 2014, Integrating <sup>40</sup>Ar/<sup>39</sup>Ar, U–Pb, and astronomical clocks in the Cretaceous Niobrara Formation, Western Interior Basin, USA. *Bulletin of the Geological Society of America*, v. 126, pp. 956–973. doi:10.1130/B30929.1
- Schmid, F., 1956, Jetziger Stand der Oberkreide–Biostratigraphie in Nordwestdeutschland: Cephalopoden. *Paläontologische Zeitschrift*, v. 30, pp. 7–10.
- Schmid F., 1960, La définition des limites Santonien–Campanien et de Campanien inférieur–supérieur en France et dans le Nord Ouest de l’Allemagne. *Congrès des Sociétés Savantes, Section des Sciences. Sous–section de Géologie. Colloque sur le Crétacé Supérieur Français. Dijon*, 1959, v. 84, pp. 535–545. Paris.
- Schönfeld, J., 1990, Die Stratigraphie und Ökologie benthischer Foraminiferen im Schreibkreide–Richtprofil von Lägerdorf/Holstein. *Geologisches Jahrbuch, Reihe A*, v. 117, pp. 3–151.
- Schulz, M.-G., Ernst, G., Ernst, H., and Schmid, F., 1984, Coniacian to Maastrichtian stage boundaries in the standard section for the Upper Cretaceous white chalk of NW Germany (Lagerdorf–Kronsmoor–Hemmoo): definitions and proposals. *Bulletin of the Geological Society of Denmark*, v. 33, pp. 203–215.
- Scott, G.R., and Cobban, W.A., 1964, Stratigraphy of the Niobrara Formation at Pueblo, Colorado. *United States Geological Survey Professional Paper*, 454–L, pp. iii+1–30.
- Seitz, O., 1961, Die Inoceramen des Santon von Nordwestdeutschland. I. Teil. Die Untergattungen *Platyceramus*, *Cladoceramus* und *Cordiceramus*. *Beihefte zum Geologischen Jahrbuch*, v. 46, 186 p.
- Seitz, O., 1965, Die Inoceramen des Santon und Unter–Campan von Nordwestdeutschland. II. Teil. Biometrie, Dimorphismus und Stratigraphie der Untergattung *Sphenoceramus* J. Böhm. *Beihefte zum Geologischen Jahrbuch*, v. 69, pp. 1–194.
- Seitz, O., 1967, Die Inoceramen des Santon und Unter–Campan von Nordwestdeutschland. III. Teil. Taxonomie und Stratigraphie der Untergattungen *Endocostea*, *Haenleinia*, *Platyceramus*, *Cladoceramus*, *Selenoceramus* und *Cordiceramus* mit besonderer Berücksichtigung des Parasitismus bei diesen Untergattungen. *Beihefte zum Geologischen Jahrbuch*, v. 75, pp. 1–171.
- Séronie–Vivien, M., 1972, Contribution à l’étude du Sénonien en Aquitaine septentrionale, ses stratotypes: Coniacien, Santonien, Campanien. *Les Stratotypes Française*, 2, 195 p.

- Sissingh, W., 1977, Biostratigraphy of Cretaceous calcareous nannoplankton. *Geologie en Mijnbouw*, v. 56, pp. 37–65.
- Slimani, H., 2001, Les kystes de dinoflagellés du Campanien au Danian dans la région de Maastricht (Belgique, Pays-Bas) et de Turnhout (Belgique): biozonation et corrélation avec d'autres régions en Europe occidentale. *Geologica et Palaeontologia*, v. 35, pp. 161–201.
- Somay, J., 1969, Espèces et sous-espèces sénoniennes nouvelles de la faune d'inocérames de Madagascar. *Annales de Paléontologie (Invertébrés)*, v. 55, pp. 195–222.
- Sornay, J., 1982, Sur la faune d'inocérames de la Smectite de Herve (Campanien) et sur quelques inocérames du Campanien et du Maastrichtien de la Belgique. *Bulletin de l'Institut royal des Sciences naturelles de Belgique, Sciences de la Terre*, v. 54, pp. 1–15.
- Sprovieri, M., Sabatino, N., Pelosi, N., Batenburg, S.J., Coccioni, R., Iavarone, M., and Mazzola, S., 2013, Late Cretaceous orbitally-paced carbon isotope stratigraphy from the Bottaccione Gorge (Italy). *Palaeogeography, Palaeoclimatology, Palaeoecology*, v. 379–380, pp. 81–94.
- Stradner, H., and Steinmetz, J., 1984, Cretaceous calcareous nannofossils from the Angola Basin, Deep Sea Drilling Project Site 530. In: Hay, W. W., Sibuet, J.-C. (eds), *Initial Reports of the Deep Sea Drilling Project*, v. 75, pp. 565–649. U.S. Government Printing Office, Washington.
- Stover, L.E., Brinkhuis, H., Damassa, S.P., de Verteuil, L., Helby, R.J., Monteil, E., Partridge, A.D., Powell, A.J., Riding, J.B., Smelror M., and Williams, G.L., 1996, Mesozoic–Tertiary dinoflagellates, acritarchs and prasinophytes. In: Jansonius, J. and McGregor, D.C. (Eds.) *Palynology: principles and applications*. American Association of Stratigraphic Palynologists Foundation, pp. 641–750.
- Summesberger, H., 1985, Ammonite zonation of the Gosau Group (Upper Cretaceous, Austria). *Annalen des Naturhistorischen Museums Wien*, v. 87, pp. 145–166.
- Summesberger, H., Kennedy, W.J., Wolfgring, E., Wagreich, M., Tröger, K.-A., and Skoumal, P., 2017, Integrated stratigraphy of the upper Santonian (Upper Cretaceous) Hochmoos and Bibereck formations of the Schattaugraben section (Gosau Group; Northern Calcareous Alps, Austria). *Abhandlungen der Geologischen Bundesanstalt*, v. 71, pp. 151–248.
- Surlyk, F., Rasmussen, S.L., Boussaha, M., Schiøler, P., Schovsbo, N.H., Sheldon, E., Stemmerik, L., and Thibault, N., 2013, Upper Campanian–Maastrichtian holostratigraphy of the eastern Danish Basin. *Cretaceous Research* v. 46, pp. 232–256.
- Takashima, R., Nishi, H., Yamanaka, T., Orihashi, Y., Tsujino, Y., Quidelleur, X., Hayashi, K., Sawada, K., Nakamura, H., and Ando, T., 2019, Establishment of Upper Cretaceous bio- and carbon isotope stratigraphy in the northwest Pacific Ocean and radiometric ages around the Albian/Cenomanian, Coniacian/Santonian and Santonian/Campanian boundaries. *Newsletters on Stratigraphy*, v. 52, pp. 342–376, doi:10.1127/nos/2019/0472
- Tauxe L., and Kent D.V., 2004, A simplified statistical model for the geomagnetic field and the detection of shallow bias in paleomagnetic inclinations: was the ancient magnetic field dipolar? In: Channell J.E.T., Kent D.V., Lowrie W. & Meert J.G. (eds.), *Timescales of the paleomagnetic field*. Geophysical Monograph Series, 145, American Geophysical Union, Washington, pp. 101–105.
- Thibault, N., Jarvis, I., Voigt, S., Gale, A. S., Attree, K., and Jenkyns, H.C., 2016, Astronomical calibration and global correlation of the Santonian (Cretaceous) based on the marine carbon isotope record. *Paleoceanography*, v. 31, pp. 847–865, doi:10.1002/2016PA002941
- Toshimitsu, S., and Kikawa, E. 1997, Bio- and magnetostratigraphy of the Santonian–Campanian transition in northwestern Hokkaido, Japan. *Memiors of the Geological Society of Japan*, v. 48, pp. 142–151.
- Toshimitsu, S., Matsumoto, T., Noda, M., Nishida, T., and Maiya, S., 1995, Towards an integrated of mega-, micro- and magneto-stratigraphy of the Upper Cretaceous in Japan. *Journal of the Geological Society of Japan*, v. 101, pp. 19–29.
- Toshimitsu, S., Maiya, S., Inoue, Y., and Takahashi, T., 1998, Integrated megafossil–foraminiferal biostratigraphy of the Santonian to lower Campanian (Upper Cretaceous) succession in northwestern Hokkaido, Japan. *Cretaceous Research*, v. 19, pp. 69–85.
- Tremolada, F., 2002, Aptian to Campanian calcareous nannofossils biostratigraphy from the Bottaccione section, Gubbio, central Italy. *Rivista Italiana di Paleontologia e Stratigrafia*, v. 108, pp. 441–456.
- Tröger, K.-A., 1989, Problems of Upper Cretaceous inoceramid biostratigraphy and paleobiogeography in Europe and Western Asia. In: Wiedemann, J. (ed.), *Cretaceous of the Western Tethys*. E. Schweizerbart, Stuttgart, pp. 911–930.
- Tröger, K.-A., 1976, Evolutionary trends of Upper Cretaceous inoceramids. *Evolutionary Biology* 1976, pp. 193–203.
- Tröger, K.-A., and Summesberger, H., 1994, Coniacian and Santonian inoceramid bivalves from the Gosau-Group (Cretaceous, Austria) and their biostratigraphic and paleobiogeographic significance. *Annalen des Naturhistorischen Museums in Wien*, v. 96A, pp. 161–197.
- Vekshina, V.N., 1959, Coccolithophoridae of the Maastrichtian deposits of the West Siberian lowlands. *Siberian Science Research Institute of Geology Geophysics Mineralogy and Raw Materials*, v. 2, pp. 56–81.
- Verosub, K.L., Haggart, J.W., and Ward, P.D., 1989, Magnetostratigraphy of Upper Cretaceous strata of the Sacramento Valley, California. *Geological Society of America Bulletin*, v. 101, pp. 521–533.
- Voigt, S., 1995, Palaeobiogeography of early Late Cretaceous inoceramids in the context of a new global palaeogeography. *Cretaceous Research*, v. 16, pp. 343–356.
- Voigt, S., 1996, Paläobiogeographie oberkretazischer Inoceramen und Rudisten – ozeanographische und klimatologische Konsequenzen einer neuen Paläogeographie. *Münchener Geowissenschaftliche Abhandlungen, A. Geologie und Paläontologie*, v. 31, pp. 1–101.
- Voigt, S., Friedrich, O., Norris, R.D., and Schönfeld, J., 2010, Campanian – Maastrichtian carbon isotope stratigraphy: shelf–ocean correlation between the European shelf sea and the tropical Pacific Ocean. *Newsletters on Stratigraphy*, v. 44, pp. 57–72.
- Wagreich, M., Summesberger, H., and Kroh, A., 2010, Late Santonian bioevents in the Schattau section, Gosau Group of Austria – implications for the Santonian–Campanian boundary stratigraphy. *Cretaceous Research*, v. 31, 181–191, doi:10.1016/j.cretres.2009.10.003
- Walaszczyk, I., 1992, Turonian through Santonian deposits of the Central Polish Uplands; their facies development, inoceramid paleontology and stratigraphy. *Acta Geologica Polonica*, v. 42, pp. 1–122.
- Walaszczyk, I., and Cobban, W.A., 2006, Paleontology and biostratigraphy of the Middle–Upper Coniacian and Santonian inoceramids of the US Western Interior. *Acta Geologica Polonica*, v. 36, pp. 241–348.
- Walaszczyk, I., and Cobban, W.A., 2007, Inoceramid fauna and biostratigraphy of the upper middle Coniacian–lower middle Santonian of the Pueblo section (SE Colorado, US Western Interior). *Cretaceous Research*, v. 28, pp. 132–142.
- Walaszczyk, I., Dubicka, Z., Olszewska–Nejbert, D., and Remin, Z., 2016, Integrated biostratigraphy of the Santonian through Maastrichtian (Upper Cretaceous) of extra-Carpathian Poland. *Acta Geologica Polonica*, v. 66, pp. 313–350.
- Walaszczyk, I., Kennedy, W.J., Dembiczyk, K., Praszkiel, T., Gale, A.S., Armand, H., Rasoamiaramana, A.H., and Randrianaly, H., 2014, Ammonite and inoceramid biostratigraphy and biogeography of the Cenomanian through basal middle Campanian (Upper Cretaceous) of the Morondava Basin, western Madagascar. *Journal of African Earth Sciences*, v. 89, pp. 79–132.
- Wang, T.T., Ramezani, J., Wang, C.S., Wu, H.C., He, H.Y., and Bowring, S.A., 2016, High-precision U–Pb geochronologic constraints on the Late Cretaceous terrestrial cyclostratigraphy and geomagnetic polarity from the Songliao Basin, northeast China. *Earth and Planetary Science Letters*, v. 446, pp. 37–44.
- Ward, P.D., 1978, Revisions to the stratigraphy and bio-chronology of the Upper Cretaceous Nanaimo Group, British Columbia and Washington State: *Canadian Journal of Earth Sciences*, v. 15, no. 3, p. 405–423, doi:10.1139/e78-045

- Ward, P.D., Haggart, J.W., Mitchell, R., Kirschvink, J., and Tobin, T., 2012, Integration of macrofossil biostratigraphy and magnetostratigraphy for the Pacific coast Upper Cretaceous (Campanian–Maastrichtian) of North America and implications for correlation with the Western Interior and Tethys. *Geological Society of America Bulletin* v. 124, pp. 957–974.
- Ward, P.D., Verosub, K.L., and Haggart, J.W., 1983, Marine magnetic anomaly 33–34 identified in the Upper Cretaceous of the Great Valley sequence in California. *Geology*, v. 10, pp. 90–93.
- Wendler, I., Wendler, J., Grafe, K.-U., Lehmann, J., and Willems, H., 2009, Turonian to Santonian carbon isotope data from the Tethys Himalaya, southern Tibet. *Cretaceous Research*, v. 30, pp. 961–979.
- Wegner, T., 1905, Die Granulaten– Kreide des westlichen Münsterlands. *Zeitschrift der Deutschen Geologischen Gesellschaft*, v. 57, pp. 112–232.
- Williams, G.L., and Bujak, J.P., 1985, Mesozoic and Cenozoic dinoflagellates. In: Bolli, H.M., Saunders, J.B. and Perch–Nielsen, K. (Eds.) *Plankton Stratigraphy*. Cambridge University Press, pp. 847–964.
- Williams, G.L., Brinkhuis, H., Pearce, M.A., Fensome, R.A., and Weegink, J.W., 2004, Southern Ocean and global dinoflagellate cyst events compared: index events for the Late Cretaceous–Neogene. In Exon, N.F., Kennett, J.P., and Malone, M.J. (Eds.), *Proceedings of the Ocean Drilling Program, Scientific Results*, v. 189, pp. 1–98.
- Wolfgring, E., Wagneich, M., Dinares–Turell, J., Yilmaz, I.O., and Bohm, K., 2017, Plankton biostratigraphy and magnetostratigraphy of the Santonian–Campanian boundary interval in the Mudurnu–Gyntik Basin, northwestern Turkey. *Cretaceous Research*, v. 87, pp. 296–311.
- Wolfgring, E., Wagneich, M., Dinares Turell, J., Gier, S., Böhm, K., Sames, B., Spötl, C., and Popp, F., 2018, The Santonian–Campanian boundary and the end of the Long Cretaceous Normal Polarity–Chron: isotope and plankton stratigraphy of a pelagic reference section in the NW Tethys (Austria). *Newsletters on Stratigraphy*, v. 51, pp. 445–476. doi:10.1127/nos/2018/0392
- Wolfgring, E., Wagneich, M., Hohenegger, J., Böhm, K., Dinares Turell, J., Gier, S., Sames, B., Spötl, C., and Jin, S.D., 2020, An integrated multi–proxy study of cyclic pelagic deposits from the north–western Tethys: the Campanian of the Postalm section (Gosau Group, Austria). *Cretaceous Research*, v. 120, 104704. doi:10.1016/j.cretres.2020.104704
- Young, K., 1963, Upper Cretaceous ammonites from the Gulf Coast of the United States. *University of Texas Bulletin* 6304, pp. 1–373.



**Andy Gale** is an Emeritus Professor at the University of Portsmouth and Research Associate at the Natural History Museum, London. His research interests include Cretaceous stratigraphy (biostratigraphy, cyclostratigraphy, carbon isotope stratigraphy) and the phylogeny of echinoderms and cirripedes. He has undertaken fieldwork on Cretaceous rocks in Europe, Asia, Arabia, North America and Africa, with a special interest in the Albian to Maastrichtian interval.



**Maria Rose Petrizzo** is chair of the International Subcommittee on Cretaceous Stratigraphy, and Associate Professor at the Università degli Studi di Milano. She teaches micropalaeontology, stratigraphic palaeontology, sedimentary rocks and geologic maps. Her research interests focus on taxonomy, phylogeny, biostratigraphy, palaeoecology, palaeobiogeography and palaeoceanography of Cretaceous and Paleogene planktonic foraminifera, and has worked extensively on both IODP oceanic core material and onshore sections.



**Seitske Batenberg** is a lecturer at the University de Barcelona. Her PhD, undertaken at the University of Portsmouth, studied the cyclostratigraphy of Maastrichtian rocks in northern Spain and provided the basis for a Milankovitch timescale of the stage. Subsequent postdoctoral positions at the universities of Oxford, Rennes and Frankfurt involved the geochemistry of Cretaceous marine sediments, with a special focus on Cretaceous Greenhouse Climates and Oceanic Anoxic Events.



**Jim Kennedy** is Emeritus Professor of Natural History at the University of Oxford, and Director Emeritus of the Oxford University Museum of Natural History. His publications are focussed on the Cretaceous, ranging from trace fossils to chalk sedimentation and diagenesis, stratigraphy, and ammonite systematics, with studies extending from East Greenland to the Antarctic Peninsula and Northern Ireland to Australia, but particularly the United States Atlantic Seaboard, Gulf Coast, and Western Interior, Europe, North and South Africa.